

Dissertation

submitted to the
Combined Faculties for the Natural Sciences and for Mathematics
of the Ruperto-Carola University of Heidelberg, Germany
for the degree of
Doctor of Natural Sciences

presented by:
Hung-wei Sung
Diploma: Master of Life Science
born in Taipei, Taiwan
Oral examination:

The Role of Zygotic Gene Activation Controlling
the Onset and Coordination of Mid-blastula
Transition

Referees: Prof. Dr. Herbert Steinbeisser
Prof. Dr. Jörg Großhans

To my beloved wife, Hsiang

Contents

Contents	4
Acknowledgements	7
Summary	8
Zusammenfassung	9
Abbreviations	10
1. Introduction	12
1.1. The Midblastula transition	12
1.2. The cell cycle in early development of Drosophila	13
1.3. Degradation of Maternal Transcripts	19
1.4. Zygotic Gene Activation (ZGA)	21
1.5. The coordination of events at MBT	24
Aim of the Studies	25
2. Materials and Methods	26
2.1. Materials	26
2.1.1 Regents.....	26
2.1.2 Radioactivity.....	26
2.1.3 Antibiotics.....	26
2.1.4 Enzymes.....	26
2.1.5 RNA probe for in situ hybridization.....	27
2.1.6 Primary antibodies.....	27
2.1.7 Secondary Antibodies.....	28
2.1.8 Other reagents used in immunostainings.....	28
2.1.9 Buffer.....	29
2.1.10 Media for bacterial culture.....	32
2.1.11 Fly food.....	32
2.1.12 Apple juice plates.....	32
2.1.13 Oligonucleotides.....	33
2.1.14 Plasmids.....	41
2.1.15 EST clones & BAC clones.....	42
2.1.16. Column.....	42
2.1.17. Kits.....	42
2.1.18. Bacterial cell lines.....	42
2.1.19. Fly stocks.....	42
2.1.20. Agarose gel electrophoresis.....	45
2.1.21. Microscopy.....	45
2.1.22. Other materials.....	46

2.1.23. Other Equipments.....	46
2.1.24. Software.....	47
2.2. Methods.....	48
2.2.1. DNA sequencing.....	48
2.2.2. Extraction of Genomic DNA from a single fly.....	48
2.2.3. polymerase chain reaction PCR.....	48
2.2.4. quantitative real time polymerase chain reaction (QPCR).....	49
2.2.5. Molecular Cloning.....	49
2.2.6. Motif predication by MEME program.....	49
2.2.7. Antibody Staining.....	49
2.2.8. Preparation of antisense Dig-labelling RNA probe.....	50
2.2.9. In situ hybridization with alkaline phosphatase.....	50
2.2.10. Isolation and fractionation of nuclei for EMSA.....	51
2.2.11. Prepare the radio-labelled DNA probe.....	52
2.2.12. Electrophoretic Mobility Shift Assay (EMSA).....	53
2.2.13. Western Blotting.....	53
2.2.14. Isolation of total RNA and cDNA synthesis.....	54
2.2.15. Generation of Germline Clones.....	54
2.2.16. The injection of α -amanitin.....	54
2.2.17. Generating Transgenic flies.....	55
2.2.18. Mapping of unknown mutants with duplication and deficiency.....	55
2.2.19. Mapping with Single-Nucleotide Polymorphism (SNP).....	56
3. Results.....	58
3.1. The genomic regulatory elements of <i>frs</i>.....	58
3.1.1. The conservation of the promoter region of <i>frs</i>	58
3.1.2. The <i>frs</i> promoter-driven GFP reporter construct.....	58
3.1.3. The substation constructs.....	62
3.1.4. The -260 to -211bp upstream region is a protein binding motif.....	65
3.2. The Genetic Analysis of <i>RPII215^{X161}</i>.....	67
3.2.1. <i>X161</i> germline clone undergoes only 12 nuclear divisions.....	67
3.2.2. The general mechanism of cell cycle is not disturbed.....	69
3.2.3. <i>X161</i> mutant doesn't affect the ploidy.....	72
3.2.4. The complex interaction between X161 and hyploid.....	72
3.2.5. Partial rescue of the phenotype by zygotic activation.....	73
3.2.6. Cellularization occurs immediately after cell cycle stop.....	74
3.2.7. <i>X161</i> causes premature degradation of <i>cdc25</i> homologs.....	75
3.2.8. <i>X161</i> causes premature expression of zygotic genes.....	76

3.2.9. The <i>X161 frs</i> double mutant could not rescue premature cell cycle pause.....	77
3.2.10. The premature cell cycle pause requires the expression of zygotic genes.....	78
3.2.11. Mapping of <i>X161</i> with Duplication Kit.....	79
3.2.12. Mapping with Single nucleotide polymorphisms and first chromosome cleaning.....	81
3.2.13. <i>X161</i> is a novel allele of RNA polymerase II 215 subunit.....	85
3.2.14. The motif predication of X161 mutation site.....	87
3.2.15. Dynamics of RPII 215 mRNA and protein.....	88
4. Discussions.....	90
4.1. Dissection of <i>frs</i> genomic regulatory module.....	90
4.1.1. The genomic regulatory modules of <i>frs</i> expression.....	90
4.1.2. The TAGteam motif is not required for <i>frs</i> expression.....	92
4.1.3. In situ hybridization as a tool studying temporal expression.....	92
4.1.4. The N/C ratio and number of cleavage cycles.....	93
4.1.5. Outlook for the investigation of <i>frs</i> genomic regulatory elements.....	93
4.2. The Role of RPII215 in controlling onset of MBT.....	94
4.2.1. <i>RPII 215^{X161}</i> is a novel allele of RNA polymerase 215 subunit.....	94
4.2.2. Two models for <i>RPII 215^{X161}</i> phenotype.....	95
4.2.3. The Regulation of onset of Zygotic Gene Activation.....	96
4.2.4. The Coupling of Cell Cycle Pause and Cellularization.....	98
4.2.5. Role of zygotic transcription in timing and coordination of MBT.....	98
5. References.....	100
6. List of Figures and Tables.....	107

Acknowledgements

First, I would like to thank my supervisor Prof. Dr. Jörg Großhans for offering me the opportunity to carry out my doctoral work in his group. He is always willing to answer question, and discuss any ideas openly and enthusiastically.

I would like to thank my first advisor Prof. Dr. Herbert Steinbeisser for offering me support throughout my doctoral work, both scientifically and mentally, and for his suggestions that contributed to this work. I would also like to thank Deutscher Akademischer Austausch Dienst (DAAD) to offer me three years scholarship, and organize all the scientific and cultural events. Through the support of DAAD, I can not only focus on my study, but also understand more about Germany, one of the great and beautiful countries.

I thank all present and past members of the Großhans lab, especially Dr. Christian Wenzl, Dr. Maria Polychronidou, Dr. Shuling Yan and Dr. Takuma Kanasaki. Christian not only for provide many suggestion for my study but also for helping me to settle down as a foreigner. Maira for demonstrating how an efficient and well-organized research is. I would also like to thank our Technician Kristina Hänecke for not only maintaining our fly facility but also helping me to deal with many daily-life problems. I would also like to thank again all members in Großhans lab to provide an intellectual but also cheerful research environment.

I also want to thank my mentor of bachelor and master study. Because of his guidance, I made my first contact with flies and developmental biology. I have learned a lot in his lab. Last but not least, I want to thank my mother and brother for their endless support and for always being there for me.

Finally I want to thank my beloved wife, Hsiang Pan with my whole heart and soul. Without her ceaselessly support and encouragement, I could not finish this work.

Summary

In the early embryos of *Drosophila*, the nuclei proliferate by invariantly 13 synchronous nuclear divisions. After nuclear divisions, the cell cycle stops, the zygotic gene is activated, maternal transcripts are degraded and cellularization starts. The transition is commonly referred to as mid-blastula transition (MBT). Previously, evidences have been showed that the following factors were involved in controlling MBT: (1) the extension of interphases and the cell cycle regulators such as *grapes*. (2) the degradation of maternal RNAs, such as *string* mRNA, and (3) the expression of zygotic mitotic inhibitors, such as *frühstart*. However, the molecular mechanism for controlling number of nuclear divisions remains unclear.

In order to investigate the role of the zygotic gene expression in regulating the onset of MBT, I used two approaches: (1) the dissection of genomic regulatory elements of *frühstart*. (2) the phenotypic analysis of a novel RNA polymerase II allele, *RPII215X¹⁶¹*. Via a reporter assay, we identified two motifs at the *frs* promoter region which prevent the premature expression of *frühstart*. By EMSA, we identified another motif which show protein binding and is required for the strong *frs* expression. By analysis of a novel RNA polymerase II allele, *RPII215^{X161}*, we identified a single nucleotide exchange in the 3'-untranslated region of *RPII215^{X161}*, which led to higher level of protein and transcripts in early embryo. Half of the mutant embryos (independent of the zygotic genotype) undergo only 12 nuclear divisions and start cellularization precociously. In addition, zygotic genes *slam* and *fühstart* are expressed earlier and maternal transcripts of CDC 25 homologs, *string* and *twine* are degraded earlier than normal in all embryos. Our data demonstrated zygotic gene activation play an essential role regulating the timing and coordination of MBT.

Zusammenfassung

Im frühen Embryo vermehren sich die Kerne zunächst durch 13 synchrone Kernteilungen. Nach den Kernteilungen stoppt der Zellzyklus, die zygotische Transkription wird aktiviert, maternale RNAs werden abgebaut und die Zellularisation beginnt. Dieser Übergang wird allgemein als mid-blastula transition (MBT) bezeichnet. Es konnte gezeigt werden, dass (1) die Verlängerung der Interphasen und Regulatoren des Zellzyklus wie z.B. *grapes*, (2) der Abbau maternaler RNAs wie z.B. *string* mRNA und (3) die Expression zygotischer Mitoseinhibitoren wie z.B. *frühstart* an der zeitlichen Koordination des Übergangs beteiligt sind. Trotzdem ist der molekulare Mechanismus zur Kontrolle der Kernteilungszahl immer noch unbekannt.

Um die Rolle der zygotischen Genexpression bei der Regulation des MBT-Starts zu erforschen, wurden zwei Ansätze gewählt: (1) Die Analyse genomischer Regulationselemente von *frühstart*. (2) Die phänotypische Analyse eines neuen RNA Polymerase II Alleles, *RPII215X*¹⁶¹. Mittels Reporterassay wurden zwei Motive in der Promoterregion von *frühstart* identifiziert die eine verfrühte Expression von *frühstart* verhindern. Mittels EMSA wurde ein weiteres Motiv identifiziert, an das Proteine binden und das für eine starke *frühstart* Expression notwendig ist. Die Analyse des neuen RNA Polymerase II Allels *RPII215X*¹⁶¹ ergab einen Einzelbasenaustausch innerhalb der 3'-untranslatierten Region der RNA Polymerase II, der zu erhöhten Protein- und Transkriptmengen im Embryo führt. Die Hälfte der mutierten Embryonen (unabhängig vom zygotischen Genotyp) durchlaufen nur 12 Kernteilungszyklen und beginnen dann verfrüht mit der Zellularisation. Zusätzlich werden in allen Embryonen die zygotischen Gene *slam* und *frühstart* verfrüht exprimiert sowie die maternalen Transkripte der *string* und *twine* früher abgebaut als im Wildtyp. Die Daten zeigen, dass die Aktivierung zygotischer Gene eine essentielle Rolle bei der zeitlichen Regulation und Koordination der MBT spielt.

Abbreviations

3'UTR	three prime untranslated region
5'UTR	five prime untranslated region
aa	amino acid (s)
ATP	adenosine triphosphate
<i>bcd</i>	<i>bicoid</i> gene
bp	base pairs
cDNA	complementary DNA
<i>cv</i>	<i>crossveinless</i> gene
<i>D.</i>	<i>Drosophila</i>
DAPI	4',6'-Diamidino-2-phenylindole
ddH ₂ O	double distilled water
DNA	deoxyribonucleic acid
DTT	1,4-dithiothreitol
Δ	deletion
<i>E.coli</i>	<i>Escherichia coli</i>
EDTA	ethylenediaminetetraacetic acid
EGTA	ethyleneglycol-bis(β-aminoethyl)-N,N,N',N'-tetraacetic acid
EMSA	Electrophoretic Mobility Shift Assay
<i>frs</i>	<i>frühstart</i> gene
g	gram (s)
GFP	green fluorescent protein
GLC	germline clone
<i>grp</i>	<i>grapes</i> gene
hr	hour (s)
HEPES	N-(2-Hydroxyethyl)piperazine-N'(2-ethanesulfonic acid)
HSP70	heat shock protein 70
Ig	immunoglobulin
<i>in situ</i>	<i>in situ</i> hybridization
IPTG	isopropyl-β-D-thiogalactopyranoside
kb	kilobases
kDa	kilo Dalton
<i>kuk</i>	<i>kugelkern</i> gene
l	liter (s)
MBT	mid-blastula transition
MNK	MAP kinase signal integrating kinase 1
N/A	not available,

<i>nos</i>	<i>nanos</i> gene
Nr.	number
Pol II	RNA polymerase II 215 subunit protein
PMSF	phenylmethanesulfonylfluoride
<i>pn</i>	<i>prune</i> gene
<i>RPII215</i>	<i>RNA polymerase II 215 subunit</i> gene
SDS	Sodium dodecyl sulfate
Slam	<i>slow as molasses</i> protein
<i>slam</i>	<i>slow as molasses</i> gene
<i>sn</i>	<i>singed</i> gene
SNP	Single Nucleotide Polymorphism
<i>stg</i>	<i>string</i> gene
<i>twn</i>	<i>twine</i> gene
<i>v</i>	<i>vermillion</i> gene
<i>w</i>	<i>white</i> gene
WT	Wild type
<i>y</i>	<i>yellow</i> gene
<i>zld</i>	<i>zelda</i> gene
ZGA	zygotic gene activation

1. Introduction

1.1. The Mid-blastula transition

The cleavage stage is the first development process after fertilization in development of animals with big eggs. During the cleavage stage, the large fertilized egg is split into increasingly smaller cells by rapid and synchronized cell divisions. The cleavage cycles are specialized cell cycles, which contain only the S phase and M phase, but lacking the gap phase. The length of cleavage divisions is very short, for example, the average length of the first 8 cycles is 8 min in *Drosophila*. In most animals, these divisions are supported by maternal transcripts and proteins.

The cleavage cycles gradually slow down, eventually stop, and lose synchronicity. This transition is described as “transition blastulenne” first by Jacques Signoret and Jacques Lefresne (KORZH 2009; SIGNORET J. 1971) and Gerhart referred to it as the mid-blastula transition (MBT, Figure 1.) (GERHART 1980).

The further investigation by J. Newport and M. Kirschner revealed that there are other events occurred at mid-blastula transition, includes the onset of zygotic expression, degradation of maternal transcripts and morphological changes (NEWPORT and KIRSCHNER 1982a; NEWPORT and KIRSCHNER 1982b). Mid-blastula transition has been characterized in various model animals (e.g. *Xenopus*, *Danio*, and *Drosophila*) (EDGAR *et al.* 1986; KANE and KIMMEL 1993). Because cleavage cycles is relative simple and the clear cut of proliferation and morphological change, mid-blastula transition can be regarded as a simple model of a switch between cell proliferation and morphogenesis in development.

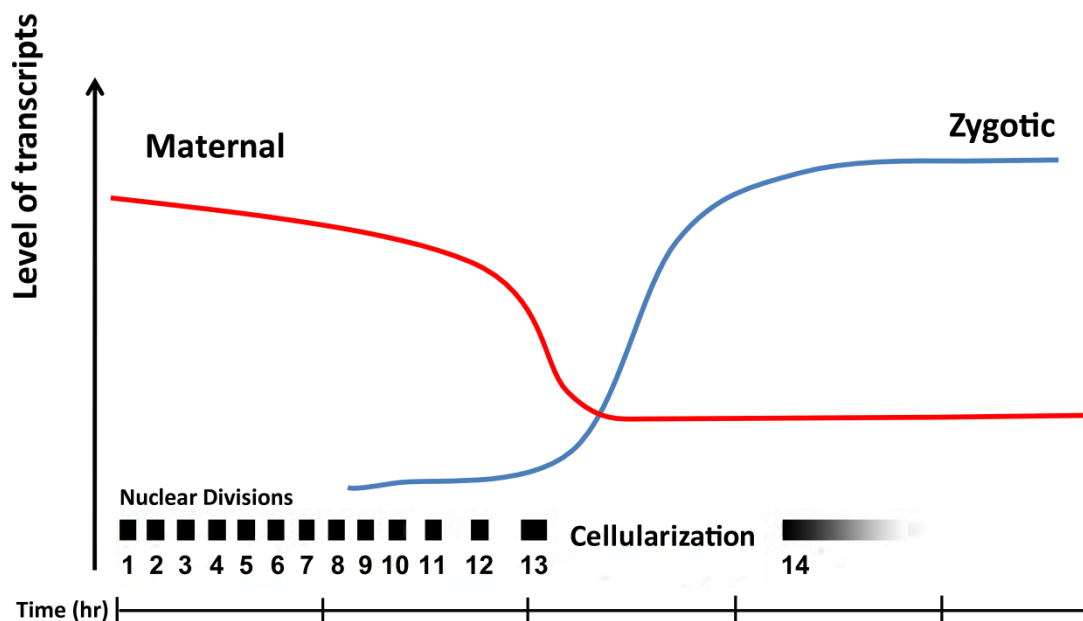


Figure 1: Summary of the events during mid-blastula transition. (a) the rapid nuclear divisions slow down and pause. (b) the maternal transcripts are degraded. (c) Zygotic genes are transcribed (d) cellularization starts

The onset of MBT and the number of cleavage cycles is very precise and robust. The number of cleavage cycles is precisely regulated in the given species, for example, there are 13 cleavage cycles in *Drosophila*, 12 in *Xenopus* and 11 in Zebra fish (KANE and KIMMEL 1993; YASUDA and SCHUBIGER 1992). Even when the embryos develop at various harsh environments; the number of cleavage cycles remains constant and the all the events still occur at the time. For example, the embryogenesis of *Drosophila* take almost two times longer at 18°C than at 25°C, however, the number of cleavage cycles is still 13. Cleavage cycles also have high resistance against UV radiation (YASUDA *et al.* 1991).

1.2. The Cell Cycle during early development of *Drosophila*

In insects, the cleavage stage is slightly different compared to other organisms. The embryo undergoes thirteen rapid and synchronous mitosis without cytokinesis

therefore generate a syncytial blastoderm that contains six thousand nuclei within a bulk cytoplasm (Figure 2B). Some nuclei fall into the yolk and undergo endocycles while other nuclei migrate to the periphery (Figure 2D). Since cycle 8, the degradation of Cyclins could be observed at mitosis (EDGAR *et al.* 1994b). The cell cycles gradually slow down from cycle 8. At cycle 14, the cell cycle pauses and the membrane invaginates from the surface and encloses the nuclei and form individual cells by a specific process called cellularization. After cellularization, the embryo goes into gastrulation and cell cycle is no longer synchronous. The transition is similar to mid-blastula transition in other metazoan.

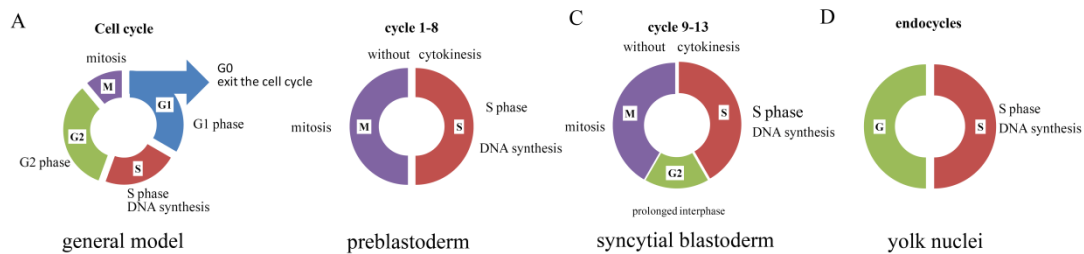


Figure 2: The models of cell cycle during early *Drosophila* development. (A) The general cell cycles contain G1, S, G2 and M phases. (B) the cleavage cycles contain only S and M phases without cytokinesis. (C) After cycle 8, G2 phase presents and interphase is prolonged. (D) the yolk nuclei undergo endocycles, which contain rounds of DNA replication without an intervening mitosis

One factor involved in controlling the timing of MBT is the nucleocytoplasmic ratio (N/C) (NEWPORT and KIRSCHNER 1982a; NEWPORT and KIRSCHNER 1982b). When observing the ligated embryos or the embryos with different ploidy (Figure 3), the cleavage cell cycle pauses when the ratio of DNA to cytoplasm reaches a specific threshold (EDGAR *et al.* 1986; ROTT and SHEVELEVA 1968). In haploid embryo, there is one extra cleavage division compared with diploids; in contrast there is one cleavage less in the tetraploid embryo.

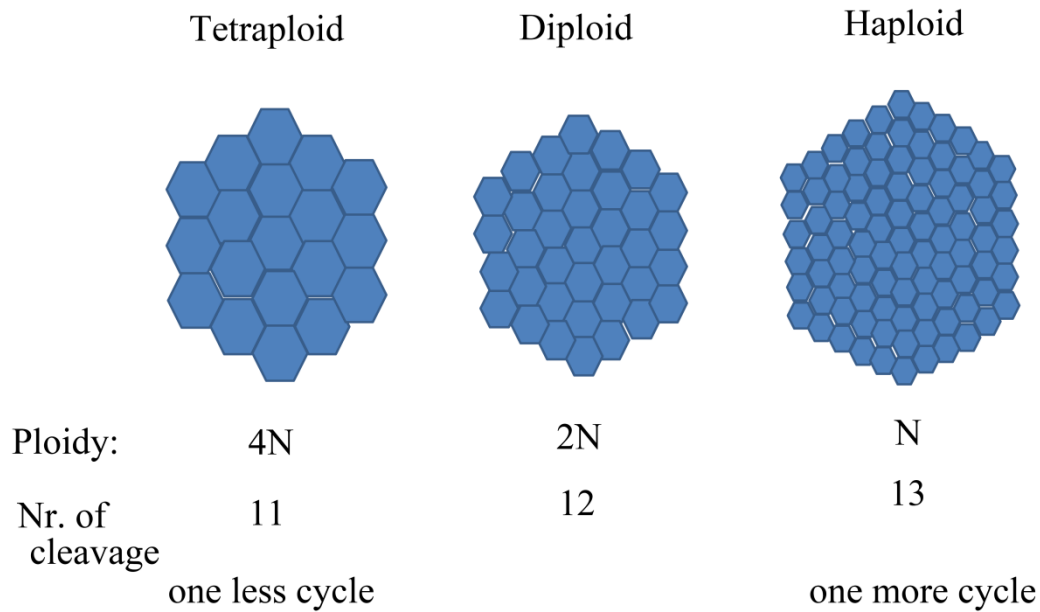


Figure 3: N/C ratio controls number of cleavage cycles in embryos. The wild type (2N) undergoes 12 cleavage cycles. The haploid embryo undergoes one extra cycles while the tetraploid undergoes one cycle less.

In 1984, Newport and Kirschner proposed the titration model. In this model, chromosomes titrate certain unknown cytoplasmic factors repress the transition until its level reaches a critical value. The rate-limiting cytoplasmic factors apparently control DNA replication (NEWPORT and KIRSCHNER 1984; POURQUIE 1998). During the early cleavage cycles, N/C ratio is low and cell cycles proceed. Since there is no cell growth during cleavage stage, N/C ratio became higher and when it reaches a certain threshold, cell cycle stops. It is proposed that there may be a cytosolic factor which would be gradually depleted during DNA duplication, and eventually the amount of this factor is lower than a threshold, the cell cycle stop.

By manipulating chromosomal aberration in *Drosophila*, Lu and colleagues found that the DNA content threshold is required for mitosis stop the cleavage cycle is about 70% of the amount normally present at cycle 14. This threshold between the DNA present at cycle 13 and cycle 14 may ensure the robust decision-making to define the

onset of MBT and tolerate the fluctuations of cytoplasmic volume(LU *et al.* 2009).

The injection of lamda plasmid DNA at level of 2.5ng/embryo is sufficient to severely slow down the cleavage cycle and activates the checkpoint kinase 1 pathway in early *Xenopus* embryo. This level is equivalent to the DNA content of MBT (CONN *et al.* 2004; PENG *et al.* 2007). This result suggests that the sensor for the N/C ratio must sense the amount of DNA directly, but not other chromosome structure or nuclear materials. However, this exact factor remains illusive.

Another specific issue concerning the N/C ratio in *Drosophila* is how individual nucleus responds to N/C ratio. Although all the syncytial nuclei are in the same cytoplasm, there may still be local difference for the composition of cytoplasm. It is possible that the embryo decides to stop the cell cycle as a whole, but it is not true since the patchy embryos containing patches of different nuclear density were observed (Figure 4). This observation also rejects the idea that individual nuclei responds to its surrounding and makes the decision individually. If it were this case, the embryo would show salt and pepper pattern. Therefore the most likely model is that there would be some local communication between neighboring nuclei to decide when to stop the cell cycle collectively (LU *et al.* 2010).

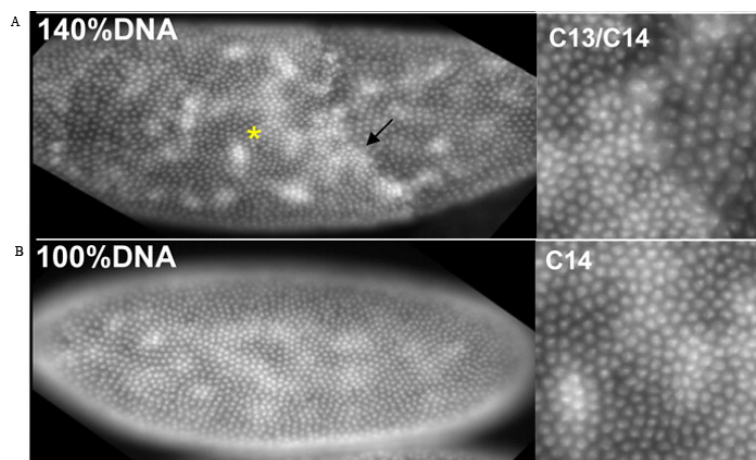


Figure 4: the decision making of cell cycle stop is regional (adapted from Lu 2009). The patchy embryo is the only intermediate phenotype observed when the cell cycle control is altered.

The CDC25 protein phosphatases play an important role in controlling the cell cycle. The Cyclin-dependent kinase is inactive when being phosphorylated on Threonine 14 and Tyrosine 15 by the inhibitory kinases Wee1 and Myt1 (RUSSELL and NURSE 1987a; RUSSELL and NURSE 1987b). CDC25 protein phosphatase dephosphorylate T14 and Y15 of Cdk and promotes cells into mitosis (Figure 5) (EDGAR *et al.* 1994a; EDGAR and O'FARRELL 1990; RUSSELL *et al.* 1989; RUSSELL and NURSE 1986; STRAUSFELD *et al.* 1991).

In *Drosophila*, there are two CDC 25 homologs, *string* and *twine*. Both of them are present maternally in early embryo, and are degraded at cycle 14. 5% of *twine*-overexpressed (6 copies) embryos undergo an extra mitosis, while 10% of the heterozygous *twine* with homozygous *stg* have only 12 mitoses. Therefore, the dose and degradation of CDC25 homologous is required for proper stop of cell cycle at MBT. The degradation of *stg* and *twine* requires the zygotic activation (EDGAR and DATAR 1996; EDGAR *et al.* 1994b).

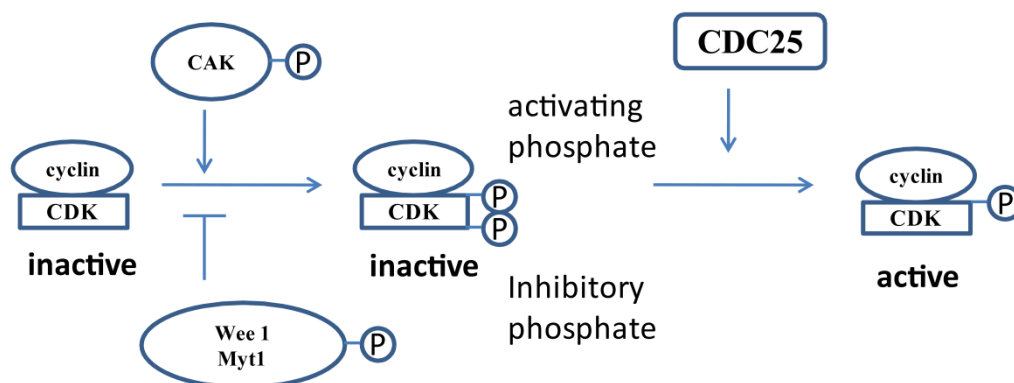


Figure 5: CDC 25 phosphatase activates the cyclin-CDK complex by removing the inhibitory phosphate. The cyclin-CDK is phosphorylated by CAK which activated it, however, cyclin-CDK is also phosphorylated by Wee1/Myt 1 which inhibits cell cycle. The removal of this inhibitory phosphate by CDC25 is essential for cell cycle progression.

Another zygotic contribution to stop the cell cycle is the expression of zygotic inhibitors of cell cycle. The cell cycle inhibitors *frühstarts* and *tribbles* express at early cycle 14 and are sufficient to stop the cell cycle (GROSSHANS *et al.* 2003; GROSSHANS *et al.* 2005).

During the cleavage stage, the DNA damage checkpoint pathway is not activated. The DNA damaging agents UV radiation or injection of DNA double-strand breaks (DSB) fails to activate the checkpoint pathway and prevent the cell cycle progression before MBT. But the experiment show that checkpoint kinase can be activated prior the MBT if the DSBs are co-injected with the sufficient amount of uncut plasmid DNA (roughly equivalent to the DNA content at 10th embryonic division). This result suggests that actually all the components of the DNA checkpoint pathway are supplemented maternally into the embryos but are inactivated by an unknown mechanism and only activated at MBT. Also, the result suggests the activation of DNA checkpoint pathway is controlled by the nuclear-cytoplasmic ratio and the activation of checkpoint pathway is slightly prior MBT. The lack of DNA checkpoint ensures the rapid and synchronous cycles to produce large amount of cells in very short period.

However, the activation of DNA checkpoint pathway is not just the consequence of MBT, but also plays an important role in prolonging the interphase and stop the cleavage cycle. In *Drosophila*, the mutations in checkpoint kinase 1 homologue, *grapes* (*grp*) block the cellularization and repress the gradual increase of interphase in division 11-13.

It is proposed that the function of grapes in increase in cell cycle time is via the phosphorylation on CDC25 phosphatase and leading it to degradation. CDC25 phosphatase dephosphorylates and activates CDKs, therefore, promotes the cell cycle. The removal of CDC25 protein and transcripts is required for the proper stop of cell

cycle at MBT. Therefore, String and Twin, the CDC25 homologous, seems to be good candidate targets for chk 1. However, checkpoint kinase 2, *mnk*, suppresses the cellularization and zygotic activation defects in *grp*, but does not restore cell cycle timing or replication-checkpoint function. This leads to the hypothesis that the lack of *grp* induces the DNA damage, which activates a Chk2-dependent block to developmental progression.

1.3. Degradation of Maternal Transcripts

Prior to the MBT, the early developmental events are driven exclusively by the maternal transcripts and proteins. It is estimated that there are about 6500 to 7700 distinct mRNAs loaded into the eggs (DE RENZIS *et al.* 2007; TADROS *et al.* 2007a; TADROS *et al.* 2007b). Many of these maternal transcripts are degraded at MBT. Among these transcripts, about 1600 distinct mRNAs (20%) would be in unfertilized eggs, indicated a MBT-independent degradation pathway. However, in fertilized and activated embryos, about 33% of maternal transcripts would be degraded depending on MBT (Figure 6). The level of the other maternal transcripts is not obviously changed, which means either they are immediately replaced by zygotic transcripts or they are very stable and not degraded at MBT (DE RENZIS *et al.* 2007; TADROS *et al.* 2007a; TADROS *et al.* 2007b).

Therefore, the degradation of maternal transcripts is mediated by two distinct pathways. The first one is driven by the maternally loaded protein/transcripts, which function even without fertilization or egg activation; the second pathway is dependent on zygotic activation (BASHIRULLAH *et al.* 1999).

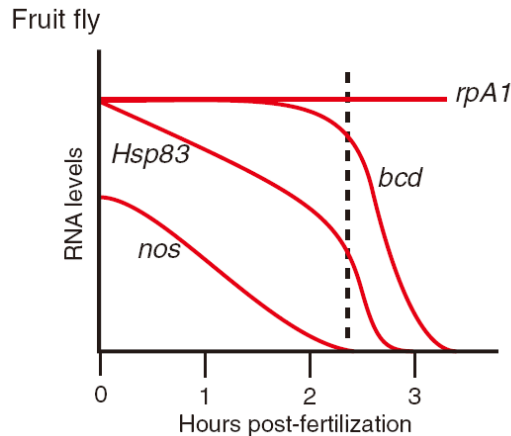


Figure 6: Degradation profiles of maternal transcripts during MZT (adapted from Tadros, 2009). There are different types of maternal transcripts: stable mRNA, like *rpA1*; degraded mainly by maternal pathway, like *nos*, or mainly zygotically, like *bcd*; or by both maternal and zygotic pathways, like *hsp83*.

Bashirullah also identified two loci, *cortex* and *grauzone*, which are required for the maternal degradation pathway. Another RNA binding protein, Smaug (SMG) is identified as a key factor mediating the maternal transcript destabilization and translation repression in early embryos (DAHANUKAR *et al.* 1999; TADROS *et al.* 2007a). SMG can bind to a specific RNA motif, SMG recognition elements (AVIV *et al.* 2003; SMIBERT *et al.* 1996). SMG recruits the CCR4/POP2/NOT-deadenylase complex to the target mRNA, then mediates the deadenylation to remove the poly-A tail of mRNA and leads to degradation (SEMOTOK *et al.* 2008). Piwi-associated RNAs (piRNAs) also involved in CCR4-mediated deadenylation and translation repression (ROUGET *et al.* 2010).

The small non-coding RNA plays an important role in the zygotic degradation pathway. In zebra fish, the zygotic-expressed *miR430* is required and sufficient to promote the degradation of more than 750 maternal transcripts (GIRALDEZ *et al.* 2006). In *Drosophila*, the *miR-309* family of miRNAs also target the maternal transcripts for degradation in a similar manner as the *miR430* in zebrafish (BUSHATI *et al.* 2008).

1.4. Zygotic Gene Activation (ZGA)

Although the major activation of zygotic gene expression is at cycle 14, some zygotic genes, like the sex-determination gene, can be detected as early as in cycle 8 (ERICKSON and CLINE 1993).

Zygotic activation is required for the final pause of the cell cycle, part of the maternal degradation, cellularization and gastrulation (EDGAR and DATAR 1996; EDGAR and SCHUBIGER 1986; NEWPORT and KIRSCHNER 1982b). When α -amanitin, inhibitor of RNA polymerase II, is injected into the early embryo, the cell cycle continues for one additional nuclear division.

Combining the genetics with large chromosome deletion and genome-wide analysis, De Renzis and his colleagues have identified the relative maternal and zygotic contribution for the expression of each individual gene during MBT (DE RENZIS *et al.* 2007). It is estimated that there are 1158 genes which expressed zygotically. Among them, 334 genes can be considered pure zygotic. It means they are not only expressed zygotically but also are absent or at very low level in unfertilized or 0 to 1 hr embryos (DE RENZIS *et al.* 2007). The remaining 824 zygotic genes replace the corresponding maternal transcripts.

Further genome-wide analysis between the haploid and wild-type embryos revealed that there were two subsets of pure zygotic genes. One is N/C dependent, which only contains minority of genes (88 out of 290). The remaining are N/C independent. However, within these two groups, the function of genes is heterogeneous, and the function of genes in these two groups are overlapping (LU *et al.* 2009).

Frühstart (frs) is one of the known zygotic gene responding to N/C ratio. It was reported to involve in the mesoderm invagination (mitotic domain 10) by delaying the

entry into mitosis (GROSSHANS and WIESCHAUS 2000). Further examination showed that *frühstart* was also involved in the pause of the cleavage cell cycle after 13 nuclear divisions, ensuring a proper cell number and timed onset of cellularisation (GROSSHANS *et al.* 2003). *Frs* encode a 90 amino-acids peptide which competes the hydrophobic patch of cyclin E with the subtracts of cyclin/CDK complex(GAWLINSKI *et al.* 2007).

Frs has a narrow expression peak starting only at the early cycle 14, correlates the pause of the cleavage cycles and MBT. The expression of *frs* is delayed to the extra division in haploid embryos (Figure 7), while other zygotic gene, like *nullo*, is still expressed at cycle 14. The expression of *frs* responds to N/C ratio and may serve a curial link between the pause of cell cycle and nucleocytoplasmic ratio. In order to reveal the mechanism how the MBT is initiated and how the number of nuclear division cycles is determined by the N/C ratio, I propose to investigate the transcriptional regulation of *frs*.

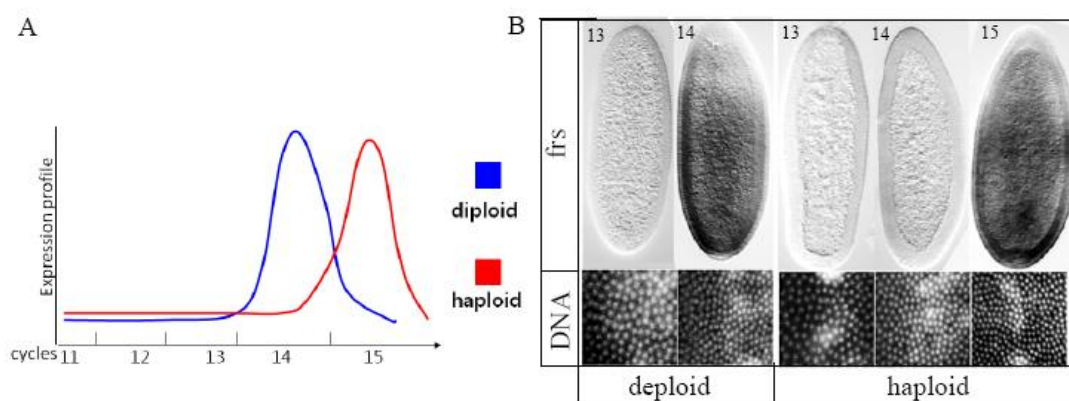


Figure 7: The expression of *frs* as a readout of N/C ratio. (A)the expression profile of *frs*. Blue: diploid, red: haploid. (B)in situ hybridization of *frs* in diploid and haploid embryos (adapted from Grosshans, 2003).

Many zygotic genes share a common motif at their upstream region. This motif is called TAGteam (CAGGTAG) (DE RENZIS *et al.* 2007; ERICKSON and CLINE 1998; TEN BOSCH *et al.* 2006). Through the yeast one -hybrid analysis, Liang and her colleagues identified the zinc-finger transcription factor, Zelda (LIANG *et al.* 2008). Zelda specifically binds to the TAGteam motifs and is required for the expression of early zygotic genes before cellularization. Although Zelda is one of the key activator, *zld* mRNA already presents maternally. Zelda may need to be activated by other factors at MBT, or there may be some other transcription factors involved to give a fine regulation. Since Zelda is required for the expression of N/C dependent and N/C independent zygotic genes, the later idea for the contribution of other factors seems reasonable.

Although the earliest zygotic transcript can be detected at cleavage cycle 8, the majority of the zygotic genes starts at early cycle 14. It is quite reasonable to assume that there is the global inactivation mediated by an epigenetic mechanism. In *Xenopus*, it is showed that the DNA methylation is required for the overall transcriptional silencing before MBT. When the DNA methyltransferase 1 (*xDnmt1*) is depleted, the zygotic transcription activates approximately two cell cycles earlier than normal in *Xenopus* (STANCHEVA and MEEHAN 2000). However, the RNA interference against *Dnmt2*, the only DNA methyltransferase in *Drosophila* genome, causes no obvious effect in early *Drosophila* embryogenesis (KUNERT *et al.* 2003). It remains uncertain whether there is a transcriptional repressor or general silencing mechanism preventing the early zygotic activation before MBT in *Drosophila*. However, SMG is also required for the zygotic gene activation, which can be explained by the degradation of maternal transcript of transcriptional repressor by SMG (Figure 8) (BENOIT *et al.* 2009; TADROS and LIPSHITZ 2009).

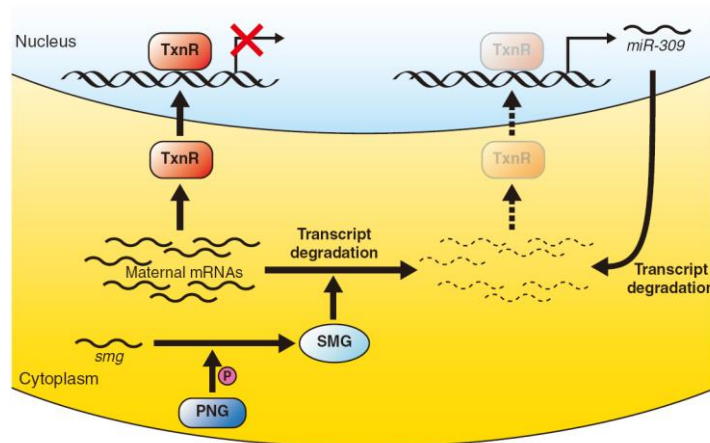


Figure 8: SMG may affect the ZGA by remove transcription repressor (adapted from Tadros, 2009). The maternal expressed transcription repressor like TxnR inhibits the transcription before MBT; when SMG is gradually translated and promotes the degradation of the transcript of transcription repressor therefore reduces the repressor protein and the zygotic gene can be transcribed

1.5. The coordination of events at MBT

Although the features of MBT: the cell cycle pause, the maternal-zygotic transition and cellulization, occur roughly simultaneously. Experiments show that there may not be one single mechanism controlling all events at MBT. Instead, different transitions control different events (YASUDA and SCHUBIGER 1992). Even the single event may be controlled by combination of distinct pathways. For example, the degradation of maternal transcripts is mediated by both maternal and zygotic degradation pathways. Another example is the zygotic genome activation. Two distinct categories of zygotic genes, N/C dependent and N/C independent, are observed. Instead of find a single mechanism controlling the whole MBT, the current challenge is understand how different events coordinate each other at MBT to continue the developmental process smoothly and thoroughly.

Aim of the studies

To further investigating the mechanism how the timing of MBT is controlled, I used two approaches. First, I investigated the regulatory elements controlling *frühstart* (*frs*), whose expression responds to the N/C ratio. Secondly, I investigated the mutant *X161*, which showed premature pause of cell cycle, and caused the embryos underwent only 12 nuclear divisions.

2. Materials and Methods

2.1 Materials

2.1.1 Regents

All standard chemicals were purchased from Sigma-Aldrich (Steinheim, Germany), AppliChem GmbH (Darmstadt, Germany), Serva (Heidelberg, Germany), Merck (Darmstadt, Germany) or Gibco BRL (Eggenstein, Germany) unless otherwise mentioned

2.1.2 Radioactivity

- Adenosine 5'-[γ -³²P]-triphosphate (6000Ci/mmol, 220TBq/mmol), Hartmann Analytic GmbH
- Deoxycytidine 5'-[α -³²P]-triphosphate (6000Ci/mmol, 220TBq/mmol), Hartmann Analytic GmbH

2.1.3 Antibiotics

- Ampicillin, stock (1000X): 100mg/ml, used in a final concentration: 50-200 μ g/ml.
- Chloramphenicol: stock (1000x) 34 mg/ml, used in a final concentration of 34 μ g/ml
- Geneticin (G418): stock (1000X) 75 mg/ml, used in a final concentration of 75 μ g/ml

2.1.4 Enzymes

Restrict enzymes: all enzymes were purchased from Fermentas, New England Biolabs (Ipswich, USA) or Roche Diagnostics GmbH (Penzberg, Germany) and used according to the instructions delivered by the producers unless otherwise mentioned.

The other enzymes used in this study is: Pfu DNA polymerase (prepared in the lab), Protease K (Roche), RNase A (Qiagen), SP6 RNA polymerase (Promega), Taq polymerase (prepared in the lab), T4 DNA ligase (Fermentas), T3 RNA polymerase (Roche), T7 RNA polymerase (prepared in the lab)

2.1.5 RNA probe for in situ hybridization

All the RNA probes were labeled with digoxigenin-UTP (DIG-UTP), the RNA probe used in this study as followed: Dig α EGFP, Dig α slam, Dig α twin, Dig α string, Dig α bottleneck, Dig α nullo, Dig α hairy, Dig α frühstart.

2.1.6 Primary antibodies

Protein Against	Animal	Concentration		Origin
		staining	western	
-CID	rabbit	1:1000		Stefan Heidmann, Bayreuth
-Dig(Alkaline phosphatase)	sheep	1:2000		Roche
-EGFP	rabbit	1:1000		Torrey-Pines Biolabs
-Frühstart	rabbit	1:1000		Princeton
-Frühstart	guinea pig	1:1000		Charles River
- β -galactosidase	mouse	1:1000		Boehringer
-p-Histone H3(S10)	mouse	1:500		Millipore
-kugelkern	rabbit	1:1000		(BRANDT <i>et al.</i> 2006)
-kugelkern	guinea pig	1:1000		Charles River
-Lamin Dmo	mouse	1:1000		By H. Saumweber
-Lamin Dmo	guinea pig	1:1000		By G. Krohne
-Pol II active form, H5	mouse	1:100	1:500	Millipore
-Pol II, Ana 3	mouse		1:1000	Millipore
-Pol II, CTD4H8	mouse		1:250	Millipore
-Pol II, 8WG16	mouse		1:1000	Millipore
-Slam	rabbit	1:5000		Charles River
-Slam	guinea pig	1:5000		Charles River
- α -Tublin	mouse		1:5 \times 10 ⁶	Sigma
- γ -Tublin	mouse	1:1000		Sigma

2.1.7 Secondary Antibodies

All the secondary antibodies used in this study were obtained from Invitrogen.

2.1.8 Other reagents used in immunostainings

- DAPI (4',6'-Diamino-2-phenylindole): DNA staining, in a final concentration of 0.4 µg/ml (Sigma-Aldrich)
- oligreen (Molecular Probes, desiccate at -20°C): dilute 1:500 (stock, store at 4°C), stain at further 1:100 (strong) with 50 µg/ml RNaseA for at least 30 min.
- Phalloidin-Alex 488: used for actin staining, in a final concentration of 6 nM (Molecular Probes)
- Mounting medium: Aquapolymount (Polysciences, Eppelheim)

2.1.9 Buffer

- Genomic DNA extraction buffer:

30 mM	Tris/HCl (pH 8)
100 mM	NaCl
19 mM	EDTA
- DEPC water:

2ml	diethyl pyrocarbonate
1 l	water
- PBS:

130 mM	NaCl
7 mM	Na ₂ HPO ₄
3 mM	NaH ₂ PO ₄
	adjust to pH 7.4
- PBST:

0,2 %	Tween 20
	PBS
- Fixation solution:

5ml	PBS
0,5 ml	Formaldehyde (37%)
5ml	Heptane

-TAE:	40mM Tris-Ac 1mM EDTA
- TE:	10mM Tris/HCl (pH8,0) 1 mM EDTA
- 6xLadderbuffer:	10 mM Tris/HCl (pH 7,6) 0,03 % Bromophenol blue 0,03 % Xylenocyanol FF 60% Glycerine 60 mM EDTA
For <i>in situ</i> Hybridisation	
- NTP+Dig labeling mix (10x):	10 mM ATP 10 mM GTP 10 mM CTP 6,5 mM UTP 3,5 mM Dig-11-UTP (Roche)
- Transcription buffer (10x):	400mM Tris/HCl, pH 8,0 60mM MgCl ₂ 100 mM DTT 20 mM Spermidine 100 mM NaCl
- NBT/BCIP:	75 mg/ml Nitrobluetetrazolium 50 mg/ml BCIP (X-phosphate, Sigma)
- Hybridisation solution:	50 % formamide 5x SSC 50 µg/ml heparin 100 µg/ml tRNA
- AP buffer:	100mM NaCl 50 mM MgCl ₂ 100 mM Tris pH 9,5 0,2 % Tween 20

Fur medi plasmid DNA purification	50 mM	Tris/HCl
- Resuspension Buffer S1	10 mM	EDTA
	100 µg/ml	RNase A
		adjusted to pH 8,0
- Lysis Buffer S2:	200 mM	NaOH
	1 %	SDS
- Neutralization Buffer S3:	2.8 M	potassium acetate
		adjusted to pH 5,1
- Equilibration Buffer N2:	100 mM	Tris
	15 %	ethanol
	900 mM	KCl
	0.15 %	Triton X-100
		adjusted to pH 6,3 with H ₂ PO ₄
- Wash Buffer N3:	100mM	Tris
	15 %	ethanol
	1.15 M	KCl
		adjusted to pH 6.3 with H ₂ PO ₄
- Elution Buffer N5:	100 mM	Tris
	15 %	ethanol
	1 M	KCl
		adjusted to pH 8.5 with H ₂ PO ₄
For min prep of plasmid-DNA		
- Solution I:	50 mM	Tris/HCl, pH 8
	10 mM	EDTA
- Solution II:	1 %	SDS
	0.2 M	NaOH
- Solution III:	3 M	potassium acetate
		adjusted to pH 5.4

	250mM	Tris
For isolation and fractionation of nuclei		
-Buffer A	350mM	sucrose
	15mM	Hepes/KOH pH7.5
	10mM	KCl
	5mM	MgCl ₂
	500mM	EGTA
	1mM	DTT
-Buffer B	800mM	sucrose
	15mM	Hepes/KOH pH7.5
	10mM	KCl
	5mM	MgCl ₂
	500mM	EGTA
	1mM	DTT
-Buffer C	15mM	Hepes/KOH pH7.5
	10mM	KCl
	3mM	MgCl ₂
	1mM	DTT
-High salt buffer	15mM	Hepes/KOH pH7.5
	1M	NaCl
	1mM	DTT
For EMSA		
-5X Tris-glycine buffer:	12.5mM	EDTA
	2M	glycine
-2X binding buffer:	20mM	HEPES pH7.9
	20%	glycerol
	0.2mM	EDTA
	1mM	tetrasodium pyrophosphate
	0.5mM	PMSF
-6X loading buffer:	0.25%	bromophenol blue

0.25% xylene cyanol

40% sucrose

For western blot

-Wet transfer buffer

25mM Tris

175mM Glycine

20% Methanol

2.1.10 Media for bacterial culture

- LB: 10 g bactotryptone, 5 g yeast extract, 10 g NaCl in 1l water, autoclaved.

-LB plate: 10 g bactotryptone, 5 g yeast extract, 10 g NaCl, 15g agar in 1l water, autoclaved, then add required antibiotic at 55°C

2.1.11 Fly food

10 l water together with 128 g thread agar was cooked for 2 h, till the agar is completely dissolved. 400 g fresh baker yeast, 160 g soja bean meal and 1,28 kg maize meal was suspended in 4 l water, mixed and was added to the agar and cooked another 2 h. 1,28 kg malt extract and 350 g sugar beet molasses was suspended in 2 l water and was added to the mixture. The food was cooked for 30 min and afterwards it will be cool down below 60°C. 24 g Nipagin (solved in ethanol) and 150 ml propionic acid was added, mixed and the fly food was filled up in vials. The vials were closed with plags and stored at 18°C.

2.1.12 Apple juice plates

70 g agar was dissolved in 3 l of water. In 1 l apple juice was dissolved 100 g of sugar in a 60 °C water bath. 40 ml Nipagin-solution (15 % Nipagin in ethanol) was added to the apple juice. The sweetened apple juice was added to the agar, mixed and cool down to 60°C. The apple juice agar was poured in Petri dishes and stored at 4°C.

2.1.13 Oligonucleotides

Molecular Cloning

Nr.	Sequence
SV1	ggc tcg agt aca tgg tgg tgg gga gat g
SV5	gga tcg ata ata act gct agg ctg gc
SV6	ggc tcg agc gaa ttc ctt tct aat tta ttg c
SV7	ggc tcg agg cga gaa ttt tct gcg gaa at
HS1	gtc gac ctg cgg aaa ttt taa tta tga gc
HS2	gtc gac agt aat ggg ttt tag tct acc gc
HS3	gtc gac agt gga tat aaa gaa ggc cgt g
HS4	gtc gac aat atc tgc gcg gaa aat aca g
HS5	gtc gac agt gac aga tgt gga aaa cgg ata ag
HS6	gtc gac cta atc cct ttt taa tgc gtt cag
HS7	gtc gac agt gac aga tgt gga aaa cgg
HS8	gtc gac taa tgg gtt tta gtc tac cgc
HS9	gtc gac gca cca taa aag tga cag atg tg
HS10	gtc gac ctc ata att aaa att tcc gca g
HS11	gaa ttc atg gtg agc aag ggc
HS12	gaa ttc cta ctt gta cag ctc gtc c
HS13	cgc ctc gag ggc agt gat tcc gat tta gca
HS14	cgc ctc gag aga gac acc cgc aaa gag
HS15	cgc ctc gag agt ggg ttc ttt cac ctg
HS16	cgc gaa ttc atg gtg agc aag ggc
HS17	cgc gaa ttc ctt gta cag ctc gtc c
HS18	cta taa gtc gac agt gga tat aaa gaa ggc cgt g
HS19	tcc act gtc gac aat atc tgc gcg gaa aat aca g
HS20	tat gac gtc gac gca cca taa aag tga cag atg tg
HS21	tgg tgc gtc gac ctc ata att aaa att tcc gca g
HS22	gga aat ttt aat tat gag gtc gac gca cca taa aag tg
HS23	gta gac taa aac cca tta gga gtc gac gtc gta att ctg aac gca
HS24	tgc gtt cag aat tac gac gtc gac tcc taa tgg gtt tta gtc tac
HS25	ctc gcg taa ttc tga acg gga gtc gac gtc att ag cga gaa ttt tct gcg
HS26	c gca gaa aat tct cgc t aat gac gtc gac tcc cgt tca gaa tta cgc gag
HS27	agg gat tag cga gaa tt gga gtc gac gtc ttt aat tat gag cag gta g
HS28	c tac ctg ctc ata att aaa gac gtc gac tcc aa ttc tcg cta atc cct
HS29	cag gta gca cca taa aag gtc gac aca tg gga aaa cgg ata agc tg
HS30	ca gct tat ccg ttt tcc ca tgt gtc gac ctt tta tgg tgc tac ctg
HS31	ctg tat ttt ccg cgc a gga gtc gac gtc agt cct gaa att gca cac
HS32	gtg tgc aat ttc agg act gac gtc gac tcc t gcg cgg aaa ata cag
HS33	g atg tgg aaa acg gat a gga gtc gac gtc att gca gat att tat ggc ag
HS34	ct gcc ata aat atc tgc aat gac gtc gac tcc t atc cgt ttt cca cat c
HS35	ctg cgg aaa ttt taa tta tga g gtc gac gca cca taa aag tga cag atg

HS36	cat ctg tca ctt tta tgg tgc gtc gac ctc ata att aaa att tcc gca g
HS37	gcg aagett tggag aacgt tgta gcggtg
HS40	cgc atc gat tgg aga acg ttg tta gcg gtg
HS41	cgc ctc gag tgt gga aaa cgg ata agc
HS42	cgc ctc gag gat tgg att att gaa agc
HS43	cgc ctc gag ctt taa gga att att atc
HS44	cgcatcgatggagaacgttgtagcggtg
HS45	cgcggtacccaacccgctcatctcg
HS46	ccggtcgaccatgcagccgccgactg
HS47	cg ctc gaggatgttgagacatatcctg
HS48	cc gatc gat cga gcg gcg ggc ata tat ac
HS49	ccg ggtacccatgcagccgccgactg
HS50	gca gga att cga tat caa gc
HS51	ccg atc gat tgt gca att tca gga ctg c
HS129	cgc ctc gag gac ttt atg gcg gta gac
HS130	cgc ctc gag ccc att act acc tgc teg
HS351	cgctctagaccactgcatccgcgctggg
HS352	gccgcccgcgagtgcccgcactggctctc
HS357	ctccccagcacgtcccgaactccgggcccgtcaag
HS358	cttgaccgccccggagttcgggacgtgctgggggag
HS363	agcctgagaaacggctacca
HS364	agctgggagtggttaatttacg
HS365	ctagctcagtcggtagagcatga
HS366	ccaacgtgggctcgaac

Oligos for the EMSA

Nr.	Sequence
HS52	agc ttg cat ctt cag tta tcg gtt atg cgg cgt tta ag
HS53	tcg act taa acg ccg cat aac cga taa ctg aag atg ca
HS54	cgg agt act gtc ctc cgc gga gta ctg tcc tcc gcg gag tac tgt cct cc
HS55	gga gga cag tac tcc gcg gag gac agt act ccg cgg agg aca gta ctc cg
HS56	att ctg aac gca tta aaa agg gat tag cga gaa tt
HS57	aat tct cgc taa tcc ctt ttt aat gcg ttc aga at
HS58	ttt ccg cgc aga tat tta tgg cag tcc tga aa
HS59	ttt cag gac tgc cat aaa tat ctg cgc gga aa
HS52	agc ttg cat ctt cag tta tcg gtt atg cgg cgt tta ag

HS53	tcg act taa acg ccg cat aac cga taa ctg aag atg ca
HS54	cgg agt act gtc ctc cgc gga gta ctg tcc tcc gcg gag tac tgt cct cc
HS55	gga gga cag tac tcc gcg gag gac agt act ccg cgg agg aca gta ctc cg
HS56	att ctg aac gca tta aaa agg gat tag cga gaa tt
HS57	aat tct cgc taa tcc ctt ttt aat gcg ttc aga at
HS58	ttt ccg cgc aga tat tta tgg cag tcc tga aa
HS59	ttt cag gac tgc cat aaa tat ctg cgc gga aa
HS63	cag tcc tga aat tgc ac
HS64	gtg caa ttt cag gac tg
HS65	gga aaa cgg ata agc tgt att ttc cgc gca
HS66	tgc gcg gaa aat aca gct tat ccg ttt tcc
HS67	acc ata aaa gtg aca gat gtg gaa aac gga
HS68	tcc gtt ttc cac atc tgt cac ttt tat ggt
HS69	ttt aat tat gag cag gta gca cca taa aag
HS70	ctt tta tgg tgc tac ctg ctc ata att aaa
HS71	gcg aga att ttc tgc gga aat ttt aat tat g
HS72	cat aat taa aat ttc cgc aga aaa ttc tcg c
HS73	Cattactacctgctcgcgtaattctgaacg
HS74	Cgttcagaattacgcgagcaggtagtaatg
HS75	gac taa aac cca tta cta cct gct cgc gta
HS76	tac gcg agc agg tag taa tgg gtt tta gtc
HS77	agg cgg act tta tgg cgg tag act aaa acc
HS78	ggt ttt agt cta ccg cca taa agt ccg cct
HS79	aat tta ttg cga ttt gta aaa ggc gga ctt
HS80	aag tcc gcc ttt tac aaa tcg caa taa att
HS81	ctc gag cga att cct ttc taa ttt att gcg
HS82	cgc aat aaa tta gaa agg aat tcg ctc gag
HS83	tta tgg tgc tac ctg ctc
HS84	att atg agc agg tag cac cat a
HS85	tat ggt gct acc tgc tca taa t
HS86	aat tta ttg c
HS87	gca ata aat t
HS88	gat ttg taa a
HS89	ttt aca aat c
HS90	agg cgg act t
HS91	aag tcc gcc t
HS92	tat ggc ggt a

HS93	tac cgc cat a
HS94	gac taa aac c
HS95	ggt ttt agt c
HS96	Atttgtaaaggcggactttatggcggtag
HS97	Ctaccgccataaagtccgccttttacaat
HS98	Ttgcgattgtaaaaggcggactttatggcggtagactaa
HS99	Ttagtctaccgccataaagtccgccttttacaatcgcaa
HS100	Cgaattcctttctaatttattgcgattgtaaa
HS101	Tttacaatcgcaataaattagaagggaattcg
HS102	Tttctaatttattgcgattgtaaaaggcg
HS103	Cgccttttacaatcgcaataaattagaaa
HS104	Attgcgattgtaaaaggcggactttatgg
HS105	Ccataaagtccgccttttacaatcgcaat
HS106	Gatttgtaaaggcggactttatggcggtta
HS107	Taccgccataaagtccgccttttacaatc
HS108	Gtaaaaggcggactttatggcggtagacta
HS109	Tagtctaccgccataaagtccgccttttac
HS110	Gactttatggcggtagactaaaaccatta
HS111	Taatgggttttagtctaccgccataaagtc
HS112	Tatggcggtagactaaaaccattactacc
HS113	Ggtagtaatgggttttagtctaccgccata
HS114	Cggtagactaaaaccattactacctgctc
HS115	Gagcaggtagtaatgggttttagtctaccg
HS116	aatttattgcgattgtaaaaggcggactttatggcggtagactaaaacc
HS117	gaaattgttacgaattcc ga gtc gac gtc att a gattgtaaaaggcggac
HS118	gtccgccttttacaatctaatagacgtcgactcggaattcgtacaatttc
HS119	cctttctaatttattgc ga gtc gac gtc att a gactttatggcggtagac
HS120	gtctaccgccataaagtctaatagacgtcgactcgcaataaattagaagg
HS121	ctaatttattgcgattgtaaa ga gtc gac gtc att a cggtagactaaaacc
HS122	gggttttagtctaccgtaatagacgtcgactctttacaatcgcaataaattag
HS123	gtaaaaggcggactttatgg ga gtc gac gtc att a cattactacctgctcgcg
HS124	cgcgagcaggtagtaataatgacgtcgactccataaagtccgccttttac
HS127-bio	bio-ccc tgg aca gca aga agt att c
SV5-biotin	bio-cct cga gcg aat tcc ttt cta att tat tgc

SNP mapping

Nr.	Sequence
HS131	tcc tcg cat tca ttt ctc gca ca
HS132	acg gct ctc gct ttc tcc ttc ca
HS133	ctt gtg tgc gtg cgt gtg tgt gt
HS134	cct gct gcg gtt tca gtt gtc att tt
HS135	tcg gtg tgc gtt ttg ttc tgg ttt t
HS136	tgg aca cag cag gag cag agt agg tg
HS137	cac agt ccg cgt caa gag caa ca
HS138	agc cac atc ttc atc gtc ttc agc atc
HS139	ttt ttg cca ttt ctg ctg ta
HS140	gaa cat ttg tag cgt gca gat
HS155	Gacaaaggcttcggcgatct
HS156	tga aga ttc ttg gcg agc cg
HS157	ttt tct tga ggg gcc tgg ga
HS158	ggg aca ctg aag cgc taa gg
HS159	cca ttc agc aag ccc ctg tt
HS160	tgg gta tcg ggt agt cga gc
HS161	cct cgt gtg gca agc gaa ta
HS162	tct tgg cac gtt gtt gtc gt
HS164	acg agt gtt ggc ctg tcg gg
HS165	ggc cca gga gca agg caa ga
HS166	ggc aca tgc cac acg cac aa
HS167	gcc act gcc ttt tgc acc cc
HS176	tcttggggtgatcacgcagc
HS177	cat ggg tcc gca gaa cac g
HS178	tcc tcg cat tca ttt ctc gc
HS179	ggc tct cgc ttt ctc ctt c
HS180	cat cca tcc aac cat cca tcc
HS181	cga atg cca aga gcc aaa cac
HS182	tgc ttc ctt gca ccc tta att tg
HS183	cga ttt tcc gtc ccg tct gat
HS184	cag cca gga tta cat ggg tgt c
HS185	gtt ttt cgg cat ttc ggg ttt c
HS186	gtc gac cgc cca aat gtc gc
HS187	gcc ctc ccc cac ctt tcc ac
HS188	agt ggt ggg gcg gaa atg gg
HS189	cgg aaa cgg aag cgg aag cg

HS190	cga aca aat ggg cgg ggt gc
HS191	ggg acg gca gaa acg ggg aa
HS192	ctc tgg gct ccc cta tcc cc
HS193	ctg cag aag gac gac ccc ac
HS194	cac gat caa gcc cgc gtt tc
HS195	agc atc ccc aac gaa cga cc
HS196	cgg gga aga cca cgc atc tc
HS197	cgg ctc tcg cca tct ctg tc
HS198	agt caa gag cgg tga gtg cg
HS199	tgg cag gag gtg cgg ttt tt
HS200	aaa aac gcc gac tgc aca gc
HS201	gat gga gaa ggg ttg ggc cg
HS202	gtc gca ggc ccc ttt tcg ta
HS203	agc ggg atg gca tca agg tg
HS204	gtt tgc ggg tgc ggc ttt gg
HS205	att ggc ctt ggg tca gcc gc
HS206	cag cgc tcc tgg gaa cca gc
HS207	act ccg cag gct ttt ccg cc
HS215	gcc agc aaa ctg acc aca ga
HS216	aat gca act gca gcg aaa gc
HS217	ggt gga ggg agg aac gta ca
HS218	aca ggc gtt gtt gct gtc at
HS219	cca aaa gaa acg cac gcg aa
HS230	aat tcg gag agc gga agt gc
HS231	ata ttt cgc cct gca tgc gt
HS232	tcg cgg gaa cgt ttc ttc tc
HS233	tgc agc agc ggt act gaa tc
HS234	agc gtt ttg ggt ctg gga ac
HS235	gaa ggg cag taa ctc gct gg
HS236	ggc ggc ttc ttc ttc gct ta
HS237	cgg tgt atc atg tgg cag ca
HS238	cgg aat gcc tca ctc act gg
HS239	gtg gcc caa aaa gcg cca gc
HS240	ctg tct gcc agc aac ccc cg
HS241	gcg gga aac act gct ccg ct
HS242	ctg gtc ctt ggc cgc cct tg
HS243	cct cca tag ccc cca ccc cc

HS244	agt ttc agc ttc gcc ccg cc
HS245	gtc cgt gtc ctt gcc cct gc
HS246	gac tgc cgc aca gcc gga at
HS247	atc gcc tgg cgt ggc caa aa
HS248	cgt tgc gat gcg tta gcg gc
HS249	gcc cca aag ctg ctc cgg tt
HS250	ttc tgc tcg ctt ggg tgg cg
HS251	ggg aag ggc acg cac aga cc
HS252	ttg cca att gcc cac ccg ca
HS253	ttc agc atg ccg ccg ttg at
HS254	cgc ctc ccc tct ctc gct ca
HS255	tca ccg gcg tat cgg agg ga
HS256	tcg ata gga acc tgc gcg gc
HS257	gcg atc ggt ggg tgc tgc ta
HS258	tcc ctc cga tac gcc ggt ga
HS259	cat ccg gca gct ggc cac aa
HS260	aat gcg acg tga gcg gag gc
HS261	ggc agc acg cga ttc cga gt
HS262	ttg tgg cca gct gcc gga tg
HS263	ctg ttc gtt ttc cct ttg gtg
HS264	cgt cat cgt cat cct cgt cct
HS265	cgt tcc cca tct acc ttc att tc
HS266	act gtt cct ctc act tgg aca cct

Oligos for sequencing

Nr.	Sequence
HS279	gtcaaagttcagagctttc
HS280	cagaggacgaatcctaac
HS281	ctaaccttaccgcaataaag
HS282	ggatttgacttttctacc
HS283	agaagaagaaccggagccgg
HS284	agccccaatgtaagctcg
HS285	agactggtaggcgaatgtac
HS286	caaggagttcaagctgccgc
HS287	gatttcggcagcaacagctc
HS288	aaagtccaatccactcacc

HS290	gtgttgatgttggtacag
HS291	gcaacatctagctgcttag
HS292	acgtcttaaactgaatttgc
HS293	aagagcctctgcacccagtg
HS294	cacccaaaactcaggctgtc
HS295	acatgcacaacgatccgaat
HS296	tagaagagcgaattgatgaa
HS297	cagtggaaagtgcgagcagtg
HS298	aaaggtgacctgctgctgcacgtc
HS299	tcagcatcgtccaggcacag
HS307	gcacttctgatgatggctgcc
HS308	cgaccgaaaagtgtgactgc
HS309	tgagaaggatgagcgaggcc
HS310	gcggcaaggcatgatcctga
HS311	aaatcggcctggaaggcttc
HS312	acagccaagtaccgagaattcc
HS313	caccagcaaatttgttggc
HS314	cacaattaaagcatgccgac
HS315	ggctatctgaagactttccc
HS316	gacgatctatgtgagtataatc
HS317	gcggcatttaagcactaaag
HS320	gaacagagcggacacccccg
HS321	atccatgtcctcgcgcccc
HS322	gcgtaagcgcctggcctacg
HS323	tccacgaaaccgcgcgactc
HS324	tgacaagactggtggttcggcc
HS325	cgtcctctcgagcagccac
HS326	ggacgaagacgaggccgtc
HS327	gggacgtgctgggggagc
HS328	ctttcggtcggcgttgtcc
HS329	tccagtaacgcgagcaggac
HS330	agcttcgcaagaacgaggcc
HS331	tgaacctgtcgtgtacatgcc
HS332	tcgtcttataaaggctatggagtcg
HS333	gcgtttgagtggttggtcgg
HS334	cggctgctttgaccttctgc
HS335	tgcaagtccacgttacgcatc

HS336	tgctggccatagaagtatctgtgg
HS337	gtcggcatgcgagccttc
HS338	caggcaccaccatacac
HS339	tatggccattgggctgtgctc
HS340	acatgccaacatctccgatag
HS341	ttttccgctgactgcacacag
HS342	ttttgttagccgatgcaagc
HS343	cgtaacacctcatactcgccg
HS344	cggtgccacacctatggatac
HS345	gagcgaagactgaggaaggag
HS346	gccaacgtcagacactattttagc
HS347	tggcagtagatcggtgacg
HS348	cgcgagcaggacaacaataac
HS349	cgggcatatcgtgtccactag
HS350	cgtccagttgaggagacaatg

Oligos for QPCR

Nr.	Sequence
HS353	tatcccaggtattgcttgtgtggg
HS354	gcagtatcgataagacctcaccgacc
HS355	atcgagcacggcatcatcac
HS356	cacgcgcagctcgttga
HS363	agcctgagaaacggctacca
HS364	agctgggagtggttaattacg
HS365	ctagctcagtcggttagagcatga
HS366	ccaacgtgggctcgaac

2.1.14 vectors

The following vectors were used in this study:

- pBS-KS(+) (Stratagene, Waldbronn)
- pCasper 4 (Lab J. Grosshans)
- pATTB (Lab Basler)

2.1.15 EST clones & BAC clones

RE30267

136G02

161G23

2.1.16. Column

PD-10 desalting column GE Healthcare Life Science, Uppsala, Sweden

G-25 Sephadex column GE Healthcare Life Science, Uppsala, Sweden

2.1.17. Kits

- MiniElute Gel extraction Kit Quiagen, Hilden

- Plasmid Midi Kit Nucleobond AX Macherey-Nagel, Düren

-Expand High Fidelity PCR System Roche, Mannheim

2.1.18. Bacterial cell lines- E.coli DH5- α F⁻, ϕ 80dlacZ Δ M15, Δ (lacZYA-argF)U169, *deoR*, *recA1*, *endA1*,
hsdR17(rK⁻, mK⁺), *phoA*, *supE44*, λ ⁻, *thi-1*, *gyrA96*, *relA1***2.1.19. Fly stocks**

Most fly stocks were obtained from the Bloomington Drosophila Stock Center at Indiana University (<http://flystocks.bio.indiana.edu/>) unless otherwise mentioned

-*x9* from Vogt EMS collection (VOGT *et al.* 2006)-*X161* from Vogt EMS collection (VOGT *et al.* 2006)-*y*, *pn*, *cv*, *v*, *FRT*^{18E} prepared by Grosshans-*OvoD*, *FRT*^{18E}

-histone::GFP (3rd) prepared by Grosshans

-*nullo*/FM7; *Cad::GFP, histone::RFP* prepared by Grosshans

-*nullo*/FM7; *sqh-meo::GFP* prepared by Grosshans

-*C(1)A, y1/Y/FM0*

- *P{w[+mC]=ovoD1-18}P4.1, P{ry[+t7.2]=hsp70-flp}1, y[1] w[1118] sn(SHIBUTANI et al.) P{ry[+t7.2]=neoFRT}19A/C(1)DX, y[1] w[1] f[1]*

-*w[1118] sn(SHIBUTANI et al.) P{neoFRT}19A*

-*y1 arm1/FM7c*

-*Df(1)BSC351, w[1118]/FM7h*

-*Df(1)svr, N ras fw / Dp(1;Y)y 67g19.1 / C(1)DX, y f*

-*Dp(1;f)R, y[+]/y dor[8]*

-*Df(1)w258-45, y /Y/C(1)DX, y w f; Dp(1;3)w[vco]*

-*Df(1)64c18, g sd /Dp(1;2;Y)w[+] /C(1)DX, y w f*

-*Dp(1;2)w-ec, ec cm ct sn/C(1)DX, y w f*

-*Df(1)dhd81, w/C(1)DX, y f; Dp(1;2)4FRDup /+*

-*Df(1)JC70/Dp(1;Y)dx[+]5, y[+]/C(1)M5*

-*Df(1)ct-J4, In(1)dl-49, f/C(1)DX, y w f; Dp(1;3)sn[13a1]/+*

-*Df(1)GE202/Y & C(1)A, y/Y; Dp(1;2)sn[+]72d/Dp(1;2)bw[D]*

-*Dp(1;Y)619, y[+] B[S]/w oc/C(1)DX, y fy nej v f/Dp(1;Y)FF1, y[+]/C(1)DX, y w f*

-*Df(1)v-L15, y/C(1)DX, y w f; Dp(1;2)v[+]7*

-*Dp(1;Y)BSC1, y[+]/w P{w[+mC]=lacW}l(1)G0060/C(1)RA, y*

-*Df(1)v-N48, f[*]/Dp(1;Y)y[+]v[+]#3/C(1)DX, y f*

-*C(1;Y)6, y w P{w[+*]=white-un4} BE1305 mew[023] / C(1)RM, y pn v;Dp(1;f)y[+]*

-*C(1;Y)1, Df(1)g, y f B/C(1)A, y/Dp(1;f)LJ9, y[+] g[+] na[+] Ste[+]*

-*Df(1)19, f/C(1)DX, y w f; Dp(1;4)r[+]*

-*Dp(1;Y)W73, y B, f[+], B[S]/C(1)DX, y f/y baz[EH171]*

-*Df(1)os[UE69]/C(1)DX, y f/Dp(1;Y)W39, y[+]*

-Df(1)R20, y/C(1)DX, y w f/Dp(1;Y)y[+]mal[+]

-Df(1)A113/C(1)DX, y w f; Dp(1;2)w[+]64b/+

-Df(1)dx81, w[*]/Dp(1;Y)dx[+]1/C(1)M5

-Df(1)w258-45, y/Y/C(1)DX, y w f; Dp(1;3)w[vco], Pr

Dp(1;Y)BSC47

Dp(1;Y)BSC49

Dp(1;Y)BSC50

Dp(1;Y)BSC52

Dp(1;Y)BSC54

Dp(1;Y)BSC56

Dp(1;3)DC233

Dp(1;3)DC234

Dp(1;3)DC235

Dp(1;3)DC237

Dp(1;3)DC238

Dp(1;3)DC239

Dp(1;3)DC240

Dp(1;3)DC241

Dp(1;3)DC243

Dp(1;3)DC246

RPII2151

RPII215G0040

Df(1)BSC287

Df(1)BSC288

Df(1)BSC541

Df(1)BSC544

Df(1)BSC658

Df(1)BSC722

Generated in this work

-w, *X161*, *f*, *FRT^{18E}/FM7h*

-y, *pn*, *cv*, *v*, *X161^{m10+m12}*, *f*, *FRT^{18E}/FM7h*

-y, *pn*, *cv*, *v*, *X161^{m12}*, *f*, *FRT^{18E}/FM7h*

-y, *pn*, *cv*, *v*, *RPII215^{X161}*, *FRT^{18E}/FM7h*

-*X161*; *Tft/CyO*

-*X161*; $\Delta 7/TM3$

-*X161*; *Cad&his*

-*X161*; *sqh-meoGFP*

-*OVO*; $\Delta 19/TM3$

-*OVO*; *Cad&his*

-*OVO*; *sqh-meoGFP*

-*OVO*; *histoneGFP*

2.1.20. Agarose gel electrophoresis

- | | |
|-------------------------------|------------------------------|
| - Gel electrophoresis chamber | ZMBH fine mechanics workshop |
| - Voltage source | ThermoEC 135-90 |

2.1.21. Microscopy

- | | |
|--|------------|
| - Injection-microscope | Carl Zeiss |
| - Leica MZ125 | Leica |
| - Zeiss Axioplan 2 Fluorescence microscope | Carl Zeiss |

- Zeiss Axiovert 200 M Ultra-View Spinning
Dsc confocal microscope Carl Zeiss

- Zeiss Stemi 2000 Carl Zeiss

2.1.22. Other materials

- Coverslips	Menzel
-Electrophoresis cuvet	peqLab
- Fly vials	Greiner
- Glass pipetts (20 ml, 10 ml, 5 ml, 2 ml)	Silber Brandt
- Pasteur pipetts	Brandt
- Petri dishes	Greiner
- Pipetboy	IBS Integra Biosciences
- Pipettes (1000 μ l, 200 μ l, 20 μ l, 2 μ l)	Gilson
- Pipett tips (1000 μ l, 200 μ l, 2 μ l)	Eppendorf, Hamburg
- Reaction tubes (50 ml, 30 ml, 15 ml, 1,5 ml)	Sarstedt, Nürnber
- Teaction tubes (2 ml, 1,5 ml)	Eppendorf
- Transfer pipetts	Sarstedt, Nürnberg
- SperFrost Plus Slides	Menzel
- 10S VoltaLef Halocarbon Oil	Lehmann & Voss & Co.
- 3S VoltaLef Halocarbon Oil	Lehmann & Voss & Co.

2.1.23. OtherEquipments

- Agarose gel rigistrator	Paytest IDA
- Cetrifuge 5415D	Eppendorf, Hamburg
- Centrifuge 5417R	Eppendorf, Hamburg
- Electroporator	Gene Pulser™, BIO-RAD
- Glass needle maker	Narishige PN-30
- Heating block	Techne Dri-Block
- IDA Gel Documentation System	Raytest
- Microinjection	FemtoJet, Eppendorf
Multi Cyclor PTC-200	MJ Research
- NanoDrop-2000 spectrophotometer	peqLab, Erlangen
- Rotator Wheel	neoLab Rotomix
- Speed Vac Concentrator 5301	Eppendorf, Hamburg
- Thermomixer confort	Eppendorf, Hamburg
- Vortexer	Scientific Industries
- Waterbath	Julabo

21.24. Software

- Adobe Design Premium CS2	Adobe
- Axio Vision Rel. 4.8	Carl Zeiss
- ImageJ 1.38x	NIH
-LSM Image	Carl Zeiss
- Lasergene	GATC biotech
-Vector NTI 9.0	Invitrogen
-EndNote X4	Thomson Reuters

2.2 Methods

2.2.1 DNA sequencing

DNA sequencing was done either in cooperation with the sequencing service of the department of developmental biochemistry, GZMB, University of Göttingen or the sequencing service from SeqLab, Göttingen.

2.2.2 Extraction of Genomic DNA from a single fly

The single fly was grinded in 30µl of buffer B with 200µg/ml proteinase K, then adding 2µl 10% SDS. The homogenized fly was incubated 1 to 4 hours at 37°C. After incubation, 3µl 3M NaCl was added, then the phenol/chloroform extraction was performed with 1:1 volume. The aqua phase was transferred to new tube, and 50µl EtOH was added, and incubated on ice for 20min. The DNA was precipitated by centrifuging for 10 min at 14,000 rpm. The DNA was dissolved into 30µl TE buffer after washing with 70% EtOH.

2.2.3 PCR

PCR reactions were performed using Taq or Pfu DNA polymerase. For standard PCR reactions the following reagents were mixed: 50-200 ng DNA template, 0,4 µM forward and reverse primers, 50 µM dNTP (each), 10x PCR buffer (polymerase dependent), 1-2 units (per 50 µl of reaction) Taq or Pfu polymerase. The reactions were performed under the following conditions:

Step 1 (initial denaturation): 95°C for 1 min

Step 2 (denaturation): 95°C for 30 sec

Step 3 (annealing): 50-60°C (depending on the annealing temperature of the respective oligos) for 1min

Step 4 (elongation): 72°C for 1min per kb to be amplified

Step 5: repetition of steps 2-4 for 30 times

Step 6 (final elongation): 72°C for 7 min

2.2.4. Quantitative real time polymerase chain reaction (QPCR)

The quantitative real time polymerase chain reaction (QPCR) was performed with oligreen fluorescence. The primers against actin were used as internal control.

2.2.5. Molecular Cloning

The general method for molecular cloning was followed Sambrook, 2001 (SAMBROOK and RUSSELL 2001) and the website of Grosshans' lab (<http://wwwuser.gwdg.de/~jgrossh/method.html>)

2.2.6. Motif predication by MEME program

The motif predication was performed on the MEME website (BUSKE *et al.* 2010) (http://meme.sdsc.edu/meme4_6_1/intro.html). The maximum number of motifs to find was set to 10, the length of motifs was from 6bp to 25bp. Other setting was as default.

2.2.7. Antibody Staining

Dechorionate embryos with 50-100% Clorox for 90 sec, then fix the embryos with the mix of 5ml 4% formaldehyde in PBS and 5ml heptanes for 30 min on the shaker (100-200 rpm). After fixation, remove the fix-reactant and add 5ml methanol. Devitellinize the embryos by shocking vigorously for 30 sec. The embryos without vitelline membranes would fall down. Suck the embryos and store in methanol at -20 °C. When doing the staining, rinse once with fresh methanol and wash with 50% methanol/PBST for 5 min. Rinse 3X PBST then wash 2X 5 min with PBST. Block

with 5% BSA, then add 1st antibody and incubate overnight at 4°C. Rinse 4 times and wash 4 times of 15 min. Then Add 2nd antibody and incubate for 1 hour at room temperature. After incubation, rinse 4 times and wash 4 times with PBST for 15 min. The embryos may be stained with DAPI (8mg/ml) for 2min. Wash 2 times with PBST for 5 min. Then lineup and mount on the cover slips with aqua-polymount.

2.2.8 Preparation of antisense Dig-labeling RNA probe

The plasmid containing the proper cDNA was linearized at the 5' end of the cDNA by a proper restriction enzyme. Setup the transcription reaction as following:

- 1µl DNA (linearised 1µg)
- 2µl 10x NTP+Dig labeling mix
- 2µl 10x transcription buffer
- 2µl RNA polymerase (40U of SP6)
- 1µl RNase inhibitor (20U)
- 12µl DEPC-treated water

Incubated at 37°C for two hours, then, the DNA was removed by 15min DNase I treatment. The RNA is precipitated by adding 0.8 µl 0,5M EDTA, 2 µl 5M LiCl, 75 µl ethanol (-20°C) and incubated at 4°C for longer than 30min, then the RNA is spun for 10min at 14,000 RPM and washed with 70% ethanol for 5min. The RNA is dissolved in 20µl DEPC-treated water and adjusted to 1mg/ml.

2.2.9. In situ hybridization with alkaline phosphatase

Dechorionate embryos with 50-100% Clorox for 90 sec, then fix the embryos with the mix of 5ml 4% formaldehyde in PBS and 5ml heptanes for 30 min on the shaker (100-200 rpm). After fixation, remove the fix-reactant and add 5ml methanol.

Devitellinize the embryos by shocking vigorously for 30 sec. The embryos without vitelline membranes would fall down. Suck the embryos and store in methanol at -20 °C. When doing the staining, rinse once with fresh methanol and wash with 50% methanol/PBST for 5 min. Rinse 3X PBST then wash 2X 5 min with PBST. Wash with 50% hybridization solution (hyb sol) in PBST for 10 min at room temperature. Then wash with 100% hyb sol for 10 min at RT. Prehybridization with 100% hyb sol for 1hr at 55°C or higher temperature. Meanwhile, prepare the probe. Add 2ul dig-labeled probe and 1ul tRNA into 20ul water boil for 5min then chill on ice, then add 200ul ice-cold hyb sol. Incubate the embryos in the hyb sol with probe at selected temperature overnight. Rinse 3 times with pre-warmed hyb sol and wash 3 times for 30min. Then rehydrate with series of pre-warmed hyb sol and PBST mixture: 80%, 60%, 40% and 20%. Afterward, block for 30min with 5% BSA in PBST. Then incubate with Dig antibody at 1 to 1000 dilutions for 1hr. Rinse 3 times and wash 4times for 15min with PBST. Wash 3 times for 5min with AP buffer. Incubate the embryos in 1ml AP buffer with 4.5 ul NBT and 3.5 ul BCIP until the signal becomes visible. Terminate the reaction with PBST and dehydrate with ethanol and incubate in 100% ethanol for 20min to remove the non-specific staining. Then rehydrate with series of ethanol/PBST mixture with gradually increased concentration of PBST. The embryos are visualized together with DAPI for marking the nuclei.

2.2.10. Isolation and fractionation of nuclei for EMSA

1g embryos were collected, dechorionated and frozen in liquid nitrogen. Homogenize the embryos with buffer A. Spin the lysate for 10 min at 4,000 rpm, discard the supernatant and suspend the pellet gently in 1ml buffer A. Then put the nuclear fraction carefully on 2ml of buffer B in a 15ml tube. Spin for 10 min at 4,600 rpm with swing-out rotor. Suspend the pellet in 200 µl, transfer to a new tube. Spin

and wash with buffer C twice. Spin and suspend the pellet in 500 μ l high salt buffer, incubate for 1 min. Spin for 10min at 13,000 rpm at 4°C. Save the supernatant (high salt extract), and suspend the pellet in 500 μ l high salt buffer, and spin again 10min at 13,000 rpm and collect the supernatant (high salt extract II). The nuclear protein extract was transferred to 2X binding buffer with buffer exchange column (PG-10)

2.2.11. Prepare the radio-labelled DNA probe

The probes were prepared with either T4 polynucleotide kinase or PCR (LANIEL *et al.* 2001). For end-labeling with T4 polynucleotide kinase, the complementary strands of oligos were mixed, heated 5°C above the melting temperature for 5 min, and let cool to room temperature. Place the double-stranded oligos at 4°C for 2 hr.

Setup the phosphorylation reaction as below:

ds-oligos	5 μ l (250ng)
10X kinase buffer	5 μ l
[γ ³²]ATP	3 μ l (30 μ Ci)
T4 polynucleotide kinase	2 μ l
Add ddH ₂ O	50 μ l

Incubate at 37°C for 2 hr

The DNA probe was purified by the G-25 Sephadex column (GE Healthcare, Uppsala, Sweden) and adjust the concentration to 30,000 cpm/ μ l.

For the PCR method, it was followed the common PCR protocol with 5 μ l 6000 Ci/mmol [α ³²]dCTP. The DNA probe was purified by the G-25 Sephadex column (GE Healthcare, Uppsala, Sweden) and adjust the concentration to 30,000 cpm/ μ l.

2.2.12. Electrophoretic Mobility Shift Assay (EMSA)

The basic protocol is performed according to the common protocol with few modification (LANIEL *et al.* 2001). The nuclear protein extract was transfer to 2X binding buffer

Nuclear extract	10.0 ul (in 2X binding buffer)
DTT (20mM)	1.2ul
ZnOAC (50um)	1.2ul
Poly(dI:dC) (1mg/ml)	1.0ul
KCl (1M)	2.4ul final:200mM
MgCl ₂ (100mM)	0.6ul final: 2mM
Probe	2.0ul
Cold Oligos	3.6ul

The DNA-protein interacting reaction was set up at 25°C for 15min. The electrophoresis was performed with 6% polyacrylamide gel and 0.5X tris-glycine buffer at 10mA for 2.5hr. The gel is dried and illuminated with Imaging plate BAS-MS 2040 (Fujifilm) and FUJIFILM FLA-3000 Image Reader.

2.2.13. Western Blotting

The staged embryos were collected on the apple juice plate, and dechorionated with bleach, then weighted and frozen in liquid nitrogen. The embryo were homogenized in 2X Lämmli buffer with the volume to make the final concentration 20embryos/ μ l (100embryos=1mg). Boil for 5 min

The protein extracts were loaded on the SDS page. Run the page at 15 to 25mA for 1hr. The protein was transferred to the membrane with wet transfer method for 3 hr at 110V. Use 5% milk for blocking for 30min. Then incubate the membrane with first antibody at 4°C overnight. Wash the membrane 6 times with PBT for 7min each, then incubate it with 2nd antibody at RT for 2hr. Then wash 6 times with PBT for 7min each.

Soak the membrane with the reagent for peroxidase for 1min. then illuminate the film in the dark room.

2.2.14. Isolation of total RNA and cDNA synthesis

Total RNA was isolated from 10mg staged *Drosophila* embryos using 500 μ l TRIzol reagent. Homogenize the sample, then incubate at RT for 5 minutes. Add 100 μ l chloroform and shake for 15 sec, incubate for 2-3 min at RT. Centrifuge at 12000g for 15 min at 4°C. Transfer the aqueous phase to a new tube. Add 250 μ l 100% isopropanol and incubate at RT for 10min. Centrifuge at 12000g for 10 min at 4°C. Wash with 75% ethanol and dry the RNA pellet. Dissolve the RNA in DEPC-treated water and adjust the concentration to 1 μ g/ μ l.

cDNA synthesis was performed with Reverse Transcriptase, Oligo-d(T) and 1 μ g of RNA as template in a final volume of 20 μ l. The cDNA was subsequently used as template for PCR.

2.2.15. Generation of Germline Clones

The germline clone was performed following the instruction by Chou and Perrimon (CHOU and PERRIMON 1992) with minor modifications. The heat shock for inducing flippase was performed at 37°C for 90min per day for two days after hatching.

2.2.16. Injection of α -amanitin into embryos

The injection of α -amanitin, RNA polymerase II inhibitor, was performed following the instruction by Schubiger and Edgar (SCHUBIGER and EDGAR 1994). The concentration used was 500 μ g/ml. The injection was performed in embryos of 0 to 30

minutes. The embryos were placed in S10 hydrocarbon oil for one hour, then recorded under spinning disc microscope.

2.2.17. Generating Transgenic flies

The transgenic flies were generated with either P-element transposon system and a ϕ C31-based integration system (ASHBURNER 1989; BISCHOF *et al.* 2007).

For the P-element transposon system, mix 3 μ g DNA of target genes on pCasper4 vector with 1 μ g of pDelta2-3 turbo vector and perform the ethanol precipitation and dissolve in ddH₂O to the concentration of 0.8 μ g/ μ l.

The embryos of *w* or *yw* were collected from the apple-juice plates, lined up on agar plate and transferred to a glass slide, dried for 10 min, then covered by hydrocarbon oil (Votalef H3S, ARKEMA, France). The DNA was injected with a glass needle at the posterior end of the embryos. Then leave the injected embryos at 18°C for 48 hr. Transfer the larvae to a new food vial with the needle. After eclosion, collect the adult flies and cross them with the double balancers. Select the F1 flies with eye color and cross them with double balancers. Decide which chromosome the transgene is by linkage with the dominate markers of F2 and setup stocks.

For ϕ C31-based integration system, the transgenes were inserted into the attB vectors. The embryos of *attP-zh86Fb/nos- ϕ -zh102D* (integrated at 3rd chromosome) were used for injection. The transgenic flies were selected by eye color and setup stocks as the P-element inserted transgenic flies.

2.2.18. Mapping with duplication and deficiency

All the genomic and sequence data of *Drosophila melanogaster* is from the Fly Base (<http://flybase.org/>) (TWEEDIE *et al.* 2009).

For the complement test with duplications, the mutant females were collected and crossed with the males containing the molecular defined duplication either attached on 3rd chromosome (POPODI *et al.* 2010) or attached on Y chromosome (COOK *et al.* 2010). The male progeny was collected. If the mutant male progeny with duplication is viable, it means the duplication line can complement the mutation, and the mutation is located within the region of duplication.

For the complement test with deficiencies, the mutant females were first crossed with the males with complemented-duplication on Y chromosome. Then the viable mutant male progeny was collected and crossed with the females from deficiency lines. If the mutant/deficiency females are lethal and can not be found, the deficiency can not complement the mutation. It means the mutation is located within the region of the deficiency.

2.2.19. Mapping with Single-Nucleotide Polymorphism (SNP)

The general procedure and strategy followed the instruction from Berger, *et al* (2001) and Chen, *et al*(2007) and is illustrated in figure (BERGER *et al.* 2001; CHEN *et al.* 2008). The SNP were obtained by the direct sequencing of specific region on X chromosome between stocks *w X161 f FRT^{18E}/FM7, FM7c/FM7c, FM7h/FM7h, y pn cv v FRT^{18E}(B437)* and *w sn neoFRT^{19A}*(Table). The genomic DNA of single recombinant fly was extracted and used as the template for PCR and sequencing

Table 1 : The Summary of SNP used in this study. The primers in bold are using as primers for sequencing

Number	Cyto resion	position	X161	B437	FRT19	FM0	FM7h	Left flank	Right flank	PCR primers
1	9F	10816046	A	G	G	G	G	CAATCATCCCATACCACCCA	TCATCTCACCTAGTCGATAG	HS196/HS197
2	9F	10816060-1	CT	TC	TC	TC	TC	CACCCAGTCATCTCACCTAG	GATAGAGTTACCATTTAAAT	HS196/HS197
3	11A	12373767-8	--	CT	CT	CT	CT	GATTACCATCTTATACTACT	ACACATACCGTTTTTAGTCA	HS194/HS195
4	12A	13444753	A	T	A	A	A	TATTAACGCCCCATTAAAG	CCATTTCCTTCAGTGCTCCC	HS179/HS178
5	12A	13444671	A	C	A	A	A	ACATACCTACCCACATCTCA	ATATACCTTCTATGCTAAG	HS179/HS178
6	12A	13444662	C	C	C	C	C	AGCTGTTACATACCTACCCA	ATCTCAGATATACCCTTCTA	HS179/HS178
7	12A	13444641	T	G	T	T	T	TTTTTTATAAATGCCACACC	AGCTGTTACATACCTACCCA	HS179/HS178
8	12D	13801573	A	G	G	G	G	TGCCACCTACAATATGTATG	CTTAGGTGTCGCCTTTGTGG	HS161/HS162
9	12D	13801916	C	T	C	C	C	TTAAATTAGATGCCCATACA	ACAAAACAAAACGAGATCAG	HS161/HS162
10	12D	13801921	G	A	G	G	G	TTAGATGCCCATACACACAA	ACAAAACGAGATCAGCCGCC	HS161/HS162
11	13A	14862598	T	G	G	G	G	ATCACCATCTCCGCATCTCC	CATCTCCTCATCTGCGGACG	HS165/HS164
12	13A	14862463	A	T	T	T	T	TTAATTATATGCATTAAAGG	ACTGGGCAGAGAGGCAGCAG	HS165/HS164
13	13A	14862200	G	A	A	A	G	TCGGGTAATACGACTTTAAA	CGTTACAATAAGCTCGTTTA	HS165/HS164
14	13F	15755025	G	A	A	A	A	TTCCTCTTTTTTTTAGTAT	CCATCCCATCCGCGAGATAA	HS183/HS182
15	14B	16048476	A	C	A	A	A	GCCGCTTAATTACAAAACG	AAGAAGTCAAATTACTAGCC	HS202/HS203

3. Results

3.1 The genomic regulatory elements of *frs*

3.1.1 The conservation of the promoter region of *frs*

The N/C ratio is the key measurement for the size of cells and play an important role controlling the number of cleavage cycles (UMEN 2005). N/C ratio is also a factor controlling the expression of some zygotic genes. However, how cell senses the N/C ratio and how N/C ratio mediates the transcription remains unknown. To fulfill this gap, we investigated the genomic regulatory elements of *frs*, one of the known genes whose expression was respond to N/C ratio (GROSSHANS *et al.* 2003).

We first used the bioinformatic approach to predict the possible genomic regulatory elements. Based on the blast of *frs* protein sequence against the translated nucleotide database, *frs* orthologs can be found only in *Drosophila* genus, but not in the genome of two mosquitoes, *Anopheles gambiae* and *Aedes aegypti*. The sequence comparison of *frs* genomic region revealed that -500 to 0 bp upstream of the *frs* transcription start site showed a high similarity (75%, figure 9A), even higher than the coding region of *frs*. This high conservation suggested that the regulatory elements of *frs* may locate in this region.

3.1.2 The *frs* promoter-driven GFP reporter construct

In order to investigate the genomic regulatory elements, we generated the EGFP reporter construct driven by the 1.3kb genomic sequence between *frs* and the upstream gene, cg7841 (*frs*1.3::GFP). The transgene containing the genomic fragment including this 1.3 kb region and *frs* gene can fully rescue the *frs* mutant, therefore it is considered to contain full genomic regulatory modules for *frs* expression (GROSSHANS *et al.* 2003). In our reporter construct, we replaced the *frs* coding region to EGFP, and

add the 3'UTR region from heat shock protein 70, which enhances the translation. The other region, including transcription start site, 5'UTR, promoter region and upstream region were from *frs* genomic DNA and was identical as endogenous *frs* locus.

The GFP expression of *frs1.3::GFP* can fully represented the endogenous *frs* expression (Figure 10 B and C). The expression started in early cycle 14 of wild type embryos. In maternal haploid mutant embryos, the peak of expression was in cycle 15. This result indicated this reporter system could reflect the expression of *frs* and can be used for the further analysis. This result also suggested that the genomic regulatory element located within this region.

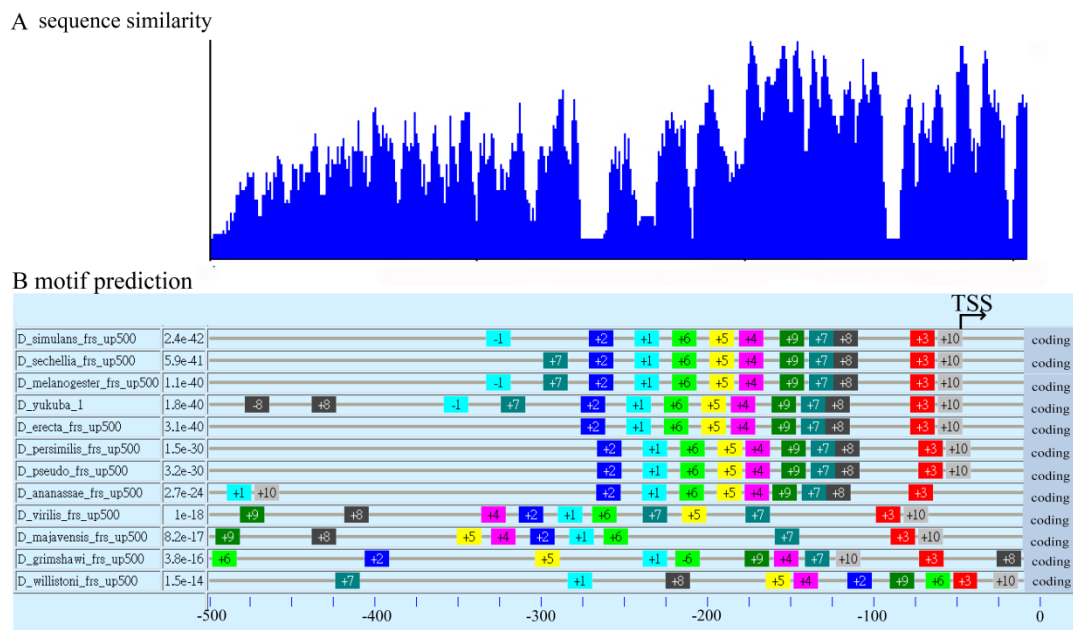


Figure 9: The summary of the motifs in 500bp upstream region of *frs* gene. (A) the graph of the sequence similarity for the sequence alignment of 500bp upstream region of 12 *frs* orthologs. The sequence conservation is 75% by Align X (Vector NTI). (B) the conserved motifs predicted by MEME program. The predicted motifs are mainly located with 300bp upstream of *frs* coding sequence. The arrangement of the motifs is identical in melanogaster and obscura group. The motif 3 and 10 represent the transcription start site (TSS).

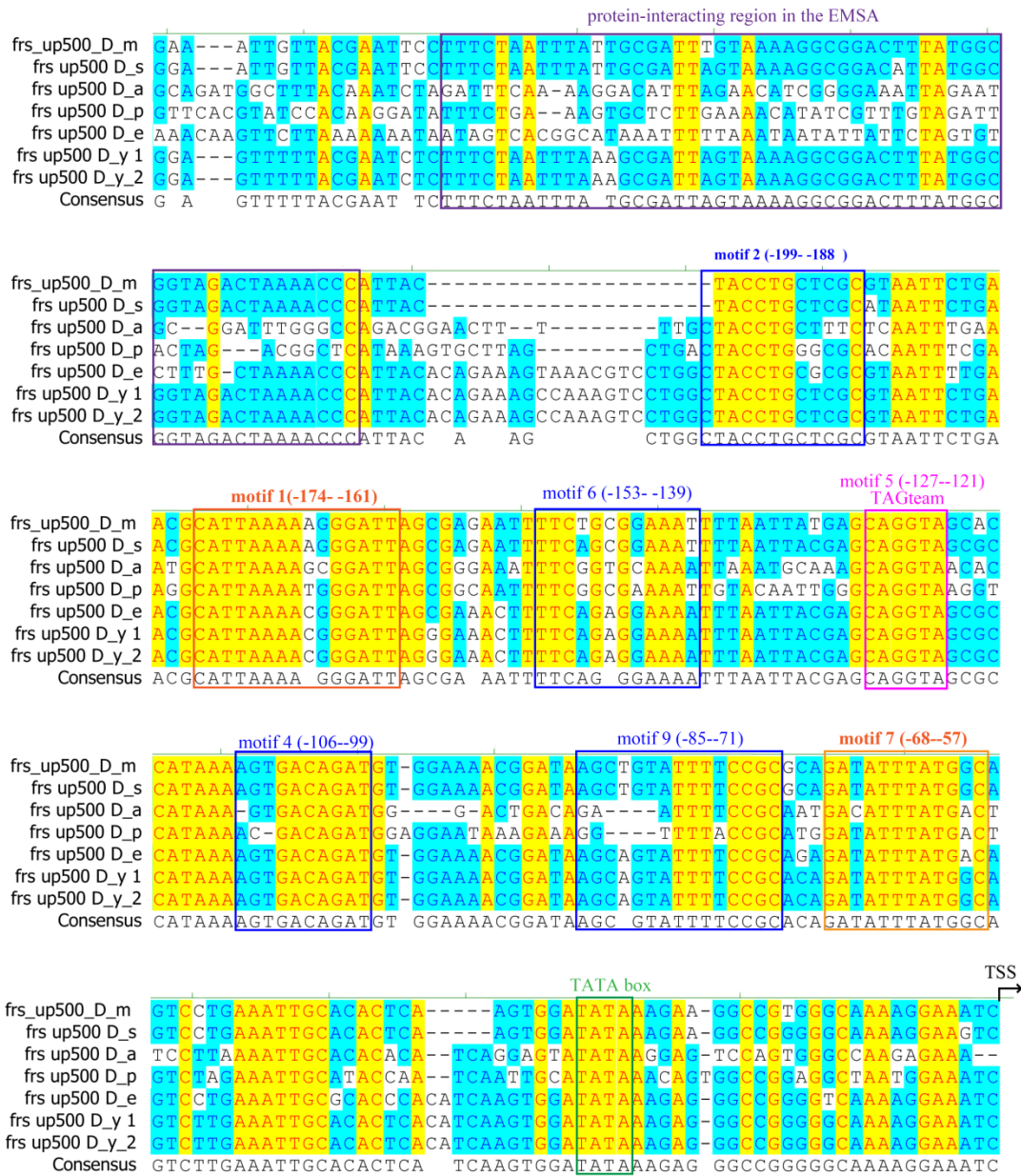
C. sequencing alignment of frs promoter region in 6 *Drosophila* species

Figure 9(continued): The sequence alignment of upstream region of 7 *frs* orthologs in 6 species in melanogaster group(C). The violet box marks the protein-binding region found in EMSA. The orange boxes mark the two motifs which prevent premature expression in reporter assay. The blue boxes mark the predicted motifs which were substituted in the reporter assay and gave no change of expression. The pick and green box mark TAGteam motif and TATA box respectively. The transcription start site (TSS) is at the end of the sequence. D_m: *D. melanogaster*; D_s: *D. simulans*; D_a: *D. ananassae*; D_p: *D. persimilis*; D_e: *D. erecta*; D_y: *D. yakuba*. There are two *frs* orthologs in *D. yakuba* due to the genome duplication during evolution.

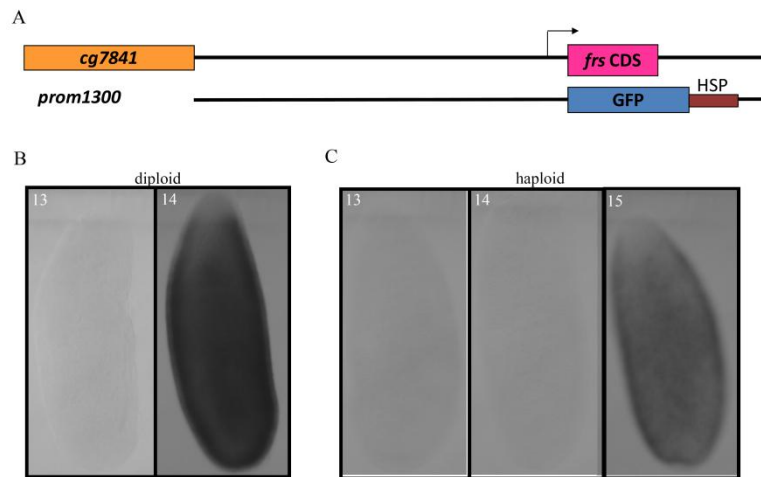


Figure 10: The GFP reporter construct can represent the endogenous *frs* expression. (A) the diagram of the reporter construct. The full length of intergenetic region is placed upstream of GFP coding sequence, flanking by the 3'UTR of HSP 70. The *in situ* hybridization of GFP starts at cycle 14 in diploid embryos (B) and at cycle 15 in haploid embryos (C).

To narrow down the minimal regulatory region, we generated more reporter constructs with shorter genomic upstream sequences. The *frs260::GFP* with 260bp upstream region could fully drive the *frühstart* expression (Figure 11C). However, the expression of the *frs180::GFP* was greatly reduced and there was no signal in *frs100::GFP* (Figure 11B). This 260bp region is sufficient to drive *frs* expression and the region between -260bp to -180bp may be required for the expression of *frs*. To further narrow down this region, three deletion constructs, $\Delta(-265 \text{ to } -215)::\text{GFP}$, $\Delta(-216 \text{ to } -q76)::\text{GFP}$ and $\Delta(-265 \text{ to } -176)::\text{GFP}$ at this region were generated. However, no expression was detected in these three reporters.

One possibility is that the enhancer which directs the *frs* expression is deleted in all of these constructs. However, it is also possible that the proper spacing between the promoter and the enhancer was disturbed. The deletions are at 150bp upstream of transcription start site, and since the average sequence to form a smoothly graded bend is about 200bp. The result of deletion construct may due to the shortening of the space but not the deletion of the enhancers.

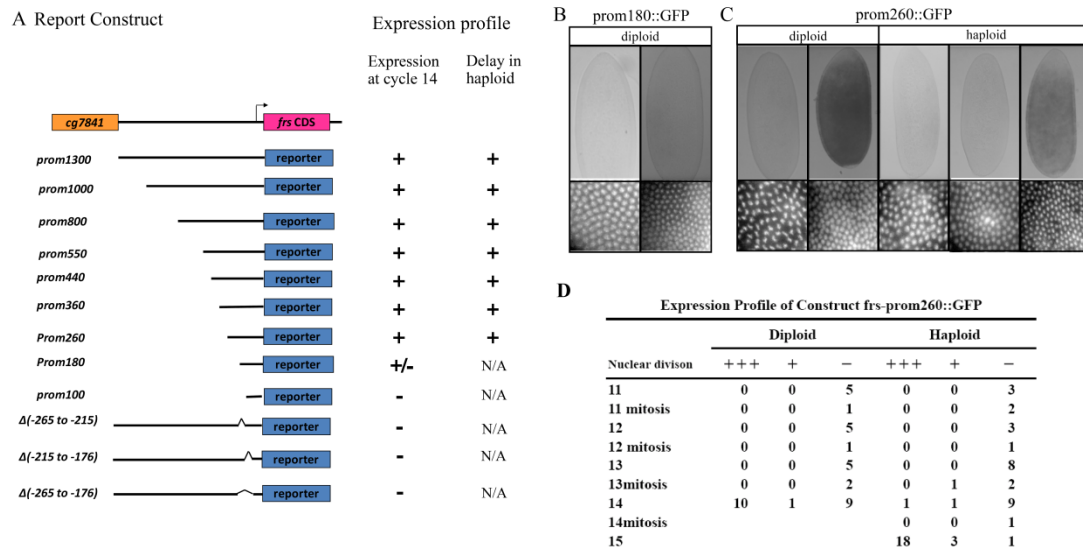


Figure 11: The *prom 260* is the minimal genomic regulatory region for *frs* expression. (A) the summary of the reporter with different length and deletion. The reporter with promoter region shorter than 180bp gives no expression (B). The expression of *prom 260::GFP* show similar expression profile as endogenous *frs* in both diploid and haploid embryos (C and D).

3.1.3 The substitution constructs

To avoid disturbing the spacing between the promoter and transcription factor binding site, we changed our strategy. Instead of making deletion constructs, we generated a new set of reporter constructs with short substitutions within *frühstart* genomic regulatory region. We used the MEME program (BAILEY and ELKAN 1995) to predict conserved motifs in these 330 bp region (Figure 9B and C). Based on this prediction, we made short substitutions (from 6 to 15bp) within this region, including TAGteam motif (CAGGTA) which was showed to be the enhancer for early zygotic activation (LIANG *et al.* 2008).

Among our 7 substitution constructs (Figure 9C and 12), two constructs *prom(-68--57)::GFP* (motif: GATATTTATGGC) and *prom(-174--161)::GFP* (motif: CATTAAAAAGGGATT) show the premature expression at cycle 13 in wild type embryos (Figure 12). In haploid background, the expression could be detected as early in cycle 13; however, the majority signal was at cycle 14 (Figure 13). Although the expression of these two constructs starts prematurely, it still delays in haploid embryos.

		Expression profile	
		Expression starts at	Delay in haploid
Frs prom ss -199- -188		14	+
Frs prom ss -174- -161		13	+
Frs prom ss -153- -139		14	+
Frs prom ss -127--121		14	+
Frs prom ss -106--99		14	+
Frs prom ss -85--71		14	+
Frs prom ss -68--57		13	+

Figure 12: Summary of the motif-substitution reporters. The substitution of two motifs *prom(-68--57)* and *prom (-174- -161)* (grey box) leads the premature expression at cycle 13 in diploid background, however, in haploid embryos, the expression starts at cycle 14 in haploid, which is one cycle later than in diploid.

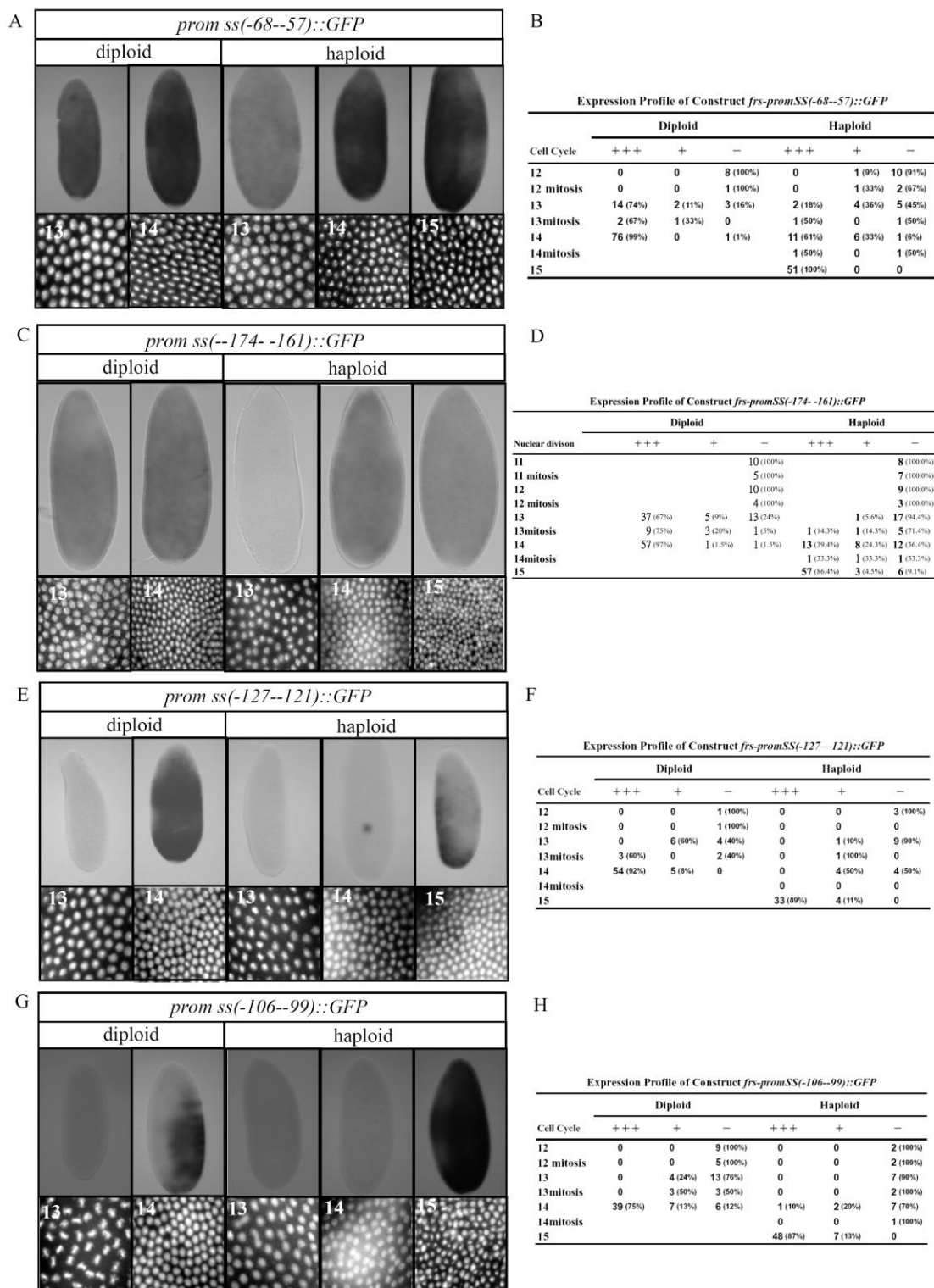


Figure 13: two motifs (-68--57) and (-174- -161) prevent the frs expression at cycle 13.

A and B, in situ of GFP in *ss(-68--57)::GFP*.

C and D, in situ of GFP in *ss(-174- -161)::GFP*

E and F, in situ of GFP in *ss(-127--121)::GFP*.

G and H, in situ of GFP in *ss(-106--99)::GFP*

3.1.4. The -260 to -211bp upstream region is a preotin binding motif

In order to investigate the DNA-protein interaction in *frs* promoter region, the electrophoretic mobility shift assay was performed. Two different p³²-labeled PCR products covering -279--110bp upstream region were used as probes. The nuclear extract from 0.5-1.5 hr embryos were used to identify the specific DNA-protein interaction prior or in the early cellularization. There was a strong shift of the -279--110bp DNA fragment with the 0.5-1.5 hr extract and the shift pattern was changed to two lower shifts (Figure 14).

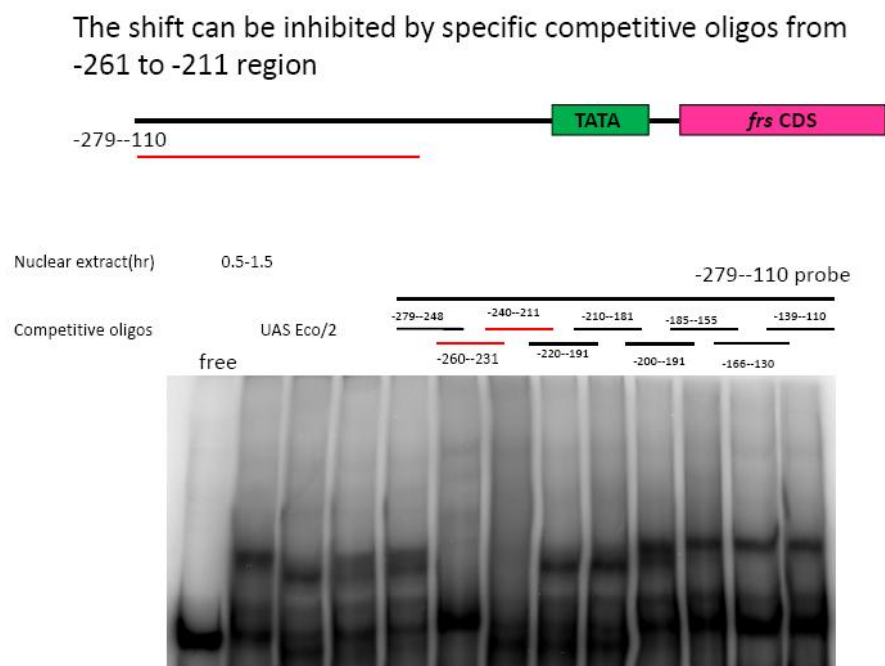


Figure 14: One DNA-protein interacting motif locates at -279bp to 211bp upstream of *frs*. The probe (-279 to -110 bp upstream of *frs* gene) was generated by PCR. One specific shift was obtained with nuclear extract of 0.5 to 1 hr embryo.

To further narrow down the protein interacting motifs and confirm the specific interaction, the non-labeled double-stranded oligos were added to compete the interaction with probes. Two oligos -260--231 and -240--211 could compete the DNA-protein interaction with dose-dependent manner (Figure 15). Thus, a protein interacting region was mapped to -260 to -211 upstream of *frs* gene (Figure 9C).

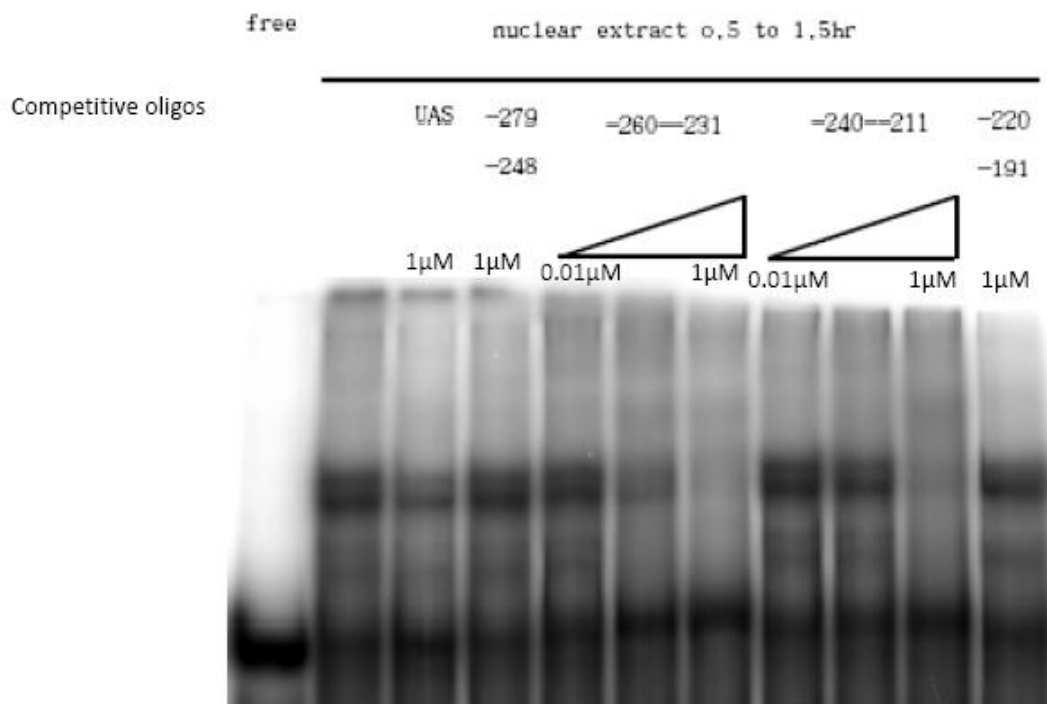


Figure 15: The cold oligos competed to the shift in dose-dependent manner. Two oligos -260 to -231bp and -240 to -211bp can compete to the radio-labeled probe in dose-dependent manner. However, the oligos of flanking sequence did not compete to the shift.

In summary, I narrowed down the functional *frs* regulatory region to 260bp upstream region. The -260bp to -180bp is required for the expression of *frs* and also showed a specific DNA-protein interacting. Secondly, I identified two motifs, GATATTTATGGC and CATTAAAAAGGGATT, which prevented the premature *frs* expression at cycle 13. However, I didn't find the elements, which responds to N/C ratio.

3.2. The Genetic Analysis of *RPII215*^{X161}

3.2.1 X161 germline clone undergoes only 12 nuclear divisions

To gain further insight for *Drosophila* development, one EMS-induced mutagenesis was performed in Tübingen (VOGT 2006; VOGT *et al.* 2006). Previous in our lab, a genetic screen with this EMS-mutant collection was performed in order to identify the candidate maternal genes required for the early *Drosophila* screen. The mutants were selected for the defects observed by the DIC time-lapse imaging. One mutant, X161, on X chromosome, showed the premature entry of the cellularization with lower nuclear density (Figure 16A).

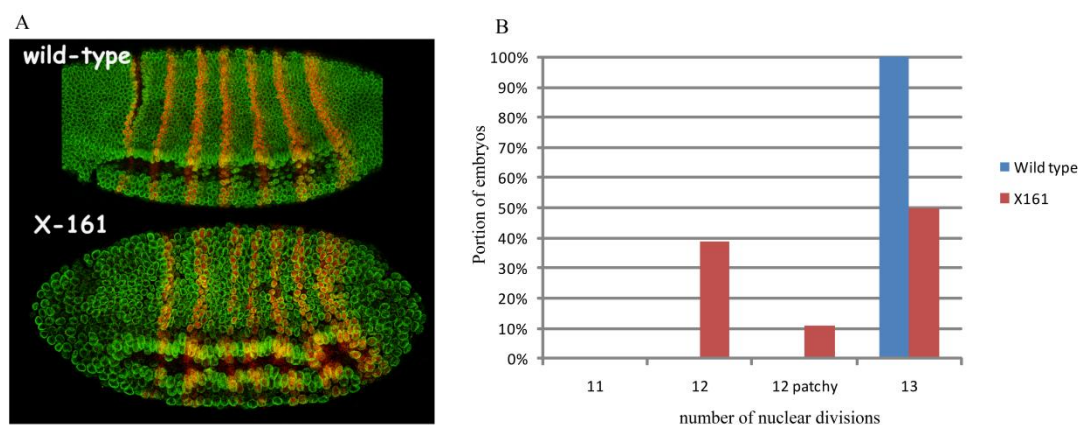


Figure 16: *X161* GLC embryos undergo one division less. (A) Half number of cells in stage 6 *X161* GLC embryo compared to wild type. Green: Kuk, Orange: Eve. (B) Bar graph showing the penetrance of cell cycle phenotype in *X161* GLC. 40% of *X161* GLC

Live imaging with differential interference contrast microscopy (DIC) and fluorescence imaging with histoneRFP confirmed the reduced number of nuclear divisions. The result showed that 40% of embryos had one division less than the wild type (Figure 16B and Table 2). 10% of the embryos are patched embryos with mixed

territories of nuclei in cycle 13 and cycle 14. The remaining 50% of embryos underwent the normal number of divisions. Despite the normal number of nuclear division in these embryos, the interphase of cycle 13 in the X161 GLC with 13 nuclear divisions was extended to about 20 min at 21°C, compared to 12 min in wild type (Figure 17 and Table 3). In patchy embryos, the interphase 13 is further prolonged to more than 30 min. The length of the interphase and mitosis of cycle 11 and 12 was not different to wild type.

Table 2: Summary of the number of cleavage cycles in different background.

Genotype/cross	number of nuclear divisions				
	12	12patchy	13	13patchy	14
Wild type	0	0	128	0	0
<i>X161 FRT^{18E} /FM7</i>	0	0	46	0	0
<i>X161 FRT^{18E} GLC</i>	24	5	27	0	0
haploid <i>X161 GLC</i>	16	3	11	1	5
<i>RPII215^{X161} FRT^{19A} GLC</i>	4	5	15	0	0
<i>2X Dp(1;3)DC241</i>	0	0	16	0	0
<i>X161/X161; frs/frs</i>	36	11	48	0	0
WT +water	0	0	34	0	0
WT + α -amanitin	0	0	2	0	21
<i>RPII215^{X161} +water</i>	11	7	12	0	0
<i>RPII215^{X161} +α-amanitin</i>	0	0	21	0	0

The *X161 FRT^{18E}* refers to the original X161 line which contain two mutations on X chromosome. The *RPII215^{X161} FRT^{19A}* refers the “cleaned” X161 line which only was recombined with viable marker chromosomes distal and proximal to *RPII215^{X161}*.

The mutant embryos went into the normal cellularization and gastrulation, even with fewer cells. The seven eve stripes in the X161 GLC suggests anterior-posterior patterning is not affected. The proper morphology of the ventral furrow suggests that the dorsal-ventral patterning is correct during gastrulation (Figure 16A). Since there were few larvae hatched (>1%), further defects may occur during later embryonic stages in addition to the reduced cell number in half of the embryos. We did not

investigate these potential phenotypes.

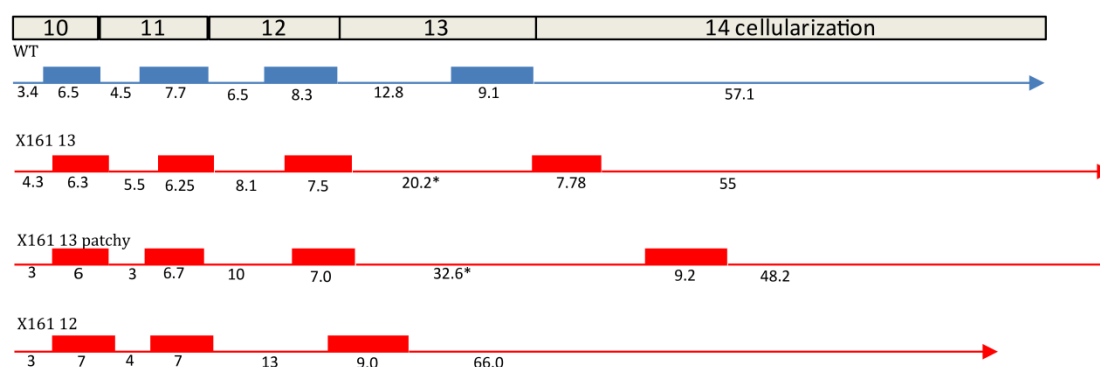


Figure 17: length of interphase and mitosis in wild type and *X161* GLC. The interphase 13 of *X161* is significantly longer than in WT ($P < 0.05$). The lines represents the length of interphase, the column represents mitosis. The number below the line indicates the time (min). WT is in blue and *X161* is in red.

Table 3: The time length of nuclear division after cycle 10

		Divisions								
embryos		10I	10M	11I	11M	12I	12M	13I	13M	14I cellularization
WT	(n:18)	3.4±0.9	6.5±1.1	4.5±1.0	7.7±0.9	6.5±1.1	8.3±1.0	12.8±2.3	9.1±2.5	57.1±4.4
<i>X161</i> 13	(n:8)	4.3±0.9	6.3±0.9	5.5±1.0	6.25±0.4	8.1±1.9	7.5±0.9	20.2*±2.3	7.78±2.25	55.4±8.7
<i>X161</i> patchy	(n:3)	3	6	3	6.7±0.5	10±2.0	7.0±0.8	32.6*±4.4	9.2±1.5	48.2±9.5
<i>X161</i> 12	(n:3)	3	7	4±1	7.0±0.8	13±4.5	9.0±1.4	66.0±12.0		

The unit of time is minutes, the number after “±” indicates the standard deviation.

3.2.2. *X161* does not affect the cell cycle

The premature stop of the mitosis in *X161* may be due to the complete arrest of cell cycle machinery. Alternatively, the mutation of *X161* may only affect the timing and the number of the cleavage divisions. To test these two possibilities, following experiments were performed.

In previous studies, it is showed that the premature arrest of nuclear divisions often

leads to the uncoupling of the DNA duplication and the centrosome duplication (McClelland and O'Farrell 2008). If this phenomenon happened in *X161* mutant, there would be more than 2 centrosomes per nuclei. However, antibody staining for γ -tubulin revealed that there were two centrosomes per nuclei during interphase 14 in *X161* (Figure 18 C). Despite the correct pairing of the centrosome cycles, we observed that the distance between the pairs of centrosomes was longer in *X161* GLC embryos. The result clearly shows that there is no extra centrosome duplication in *X161* GLC embryos.

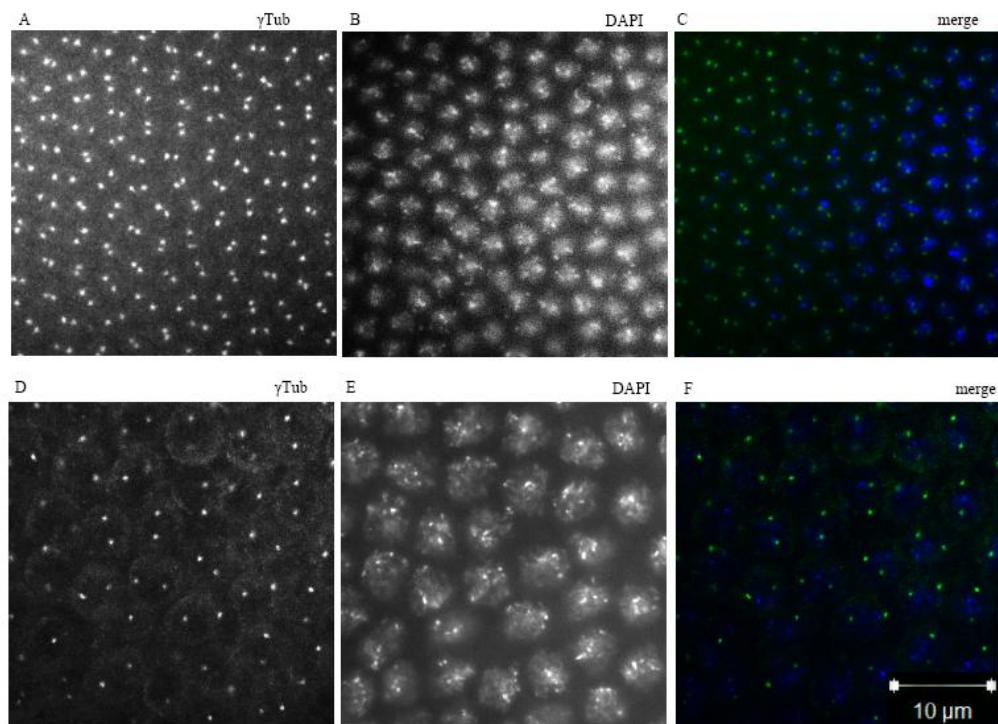


Figure 18: Centrosome cycle is not affected in *X161*. There is no extra centrosome duplication in *X161* GLC after cell cycle stop (D to F) as in wild type (A to C). The embryos were in late cellularization, but *X161* GLC was at cycle 13 while wild type was at cycle 14. γ -tubulin marks the centrosomes in green, DAPI marks DNA in blue, the scale bar: 10 μ m

Following cellularization, the mitosis 14 occurs in an asynchronous manner in 25 different domains. With few exceptions, cells enter mitosis according to the

expression of *string* (EDGAR *et al.* 1994a; FOE 1989). To test whether the timing and patterning of mitosis 14 is affected by *X161*, we performed the *in situ* hybridization of *string* and the staining with the mitotic marker, phospho-Histone H3 (S10) antibody (HAU *et al.* 2006). The expression of *string* was generally similar to wild type. The mitosis always occurred in the region where *string* is expressed (Figure 19 B and C). In embryos with patches, we observed higher expression level of *string* in the patches with lower nuclear densities. This may be due to the longer period of time after exit from mitosis 13. We also noticed that the mitotic pattern was slightly advanced as compared to the gastrulation movement (compare Figure 19 A and C) as it is also seen in *trbl* and *frs* mutants (GROSSHANS and WIESCHAUS 2000). To summary, *X161* specifically affected the counting mechanism of the nuclear divisions, but it did not disturb the general cell cycle mechanism.

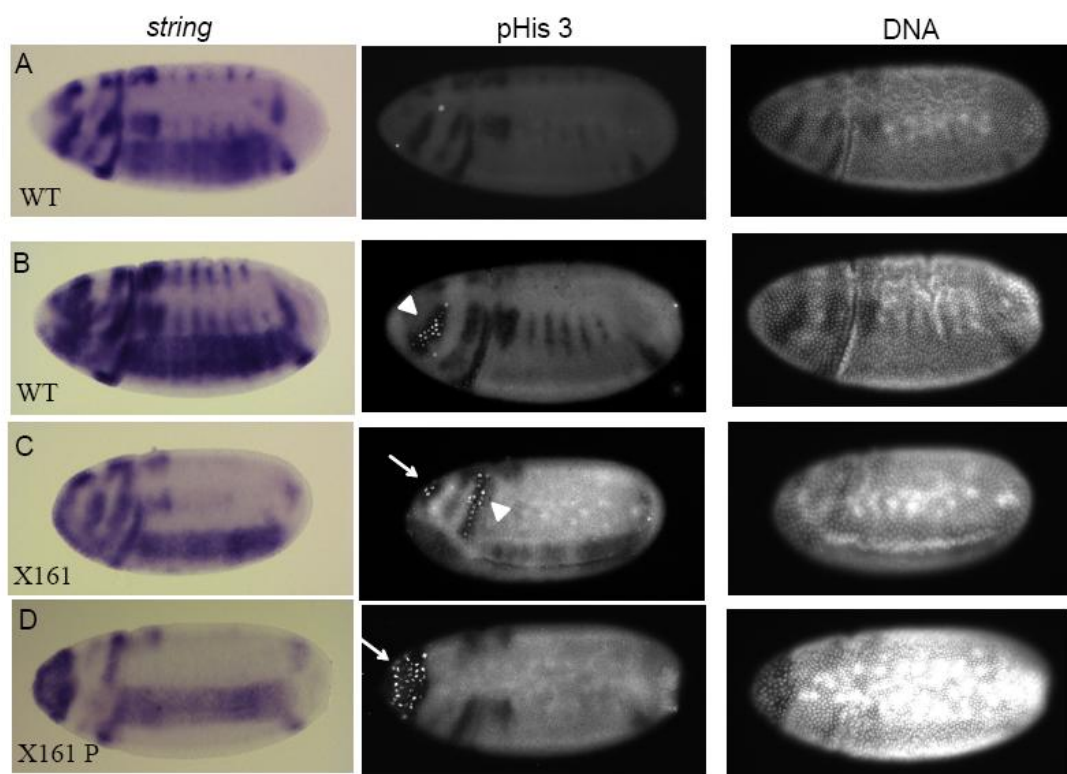


Figure 19: The mitosis 14 occurred according to the mitotic domains in wild type (A, B.) and *X161* embryo (C, patchy, D, the same stage as A). Arrowhead indicates the mitotic cells at cephalic furrow. Arrow indicates the ectopic mitosis at head region in *X161*. pH3 (S10) staining marks the cells at mitosis, *in situ* of *stg* marks the mitotic domain.

3.2.3. The X161 mutant does not affect the ploidy of the nuclei.

Since the number of cleavage cycles is controlled by the N/C ratio. It is possible that the premature stop of cell cycle in X161 mutant is due to tetraploidy of the embryos. To test this hypothesis, we stained for CID protein. CID is the *Drosophila* homologue of the CENP-A centromere-specific H3-like protein which localizes at centromeres (BLOWER and KARPEN 2001), allowing to count the number of chromosomes in one nucleus. There are 8 dots of CID staining in each X161 nucleus during interphase similar to wild type (Figure 20). It indicated that the chromosome number and ploidy is not affected in X161 embryos.

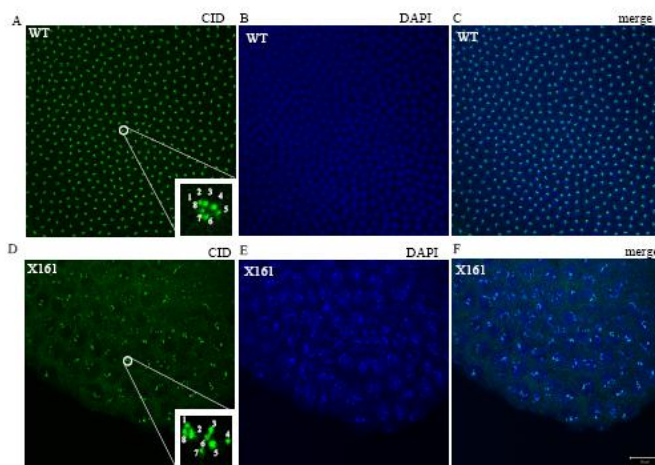


Figure 20: X161 GLC embryos contain normal set of chromosomes in wild type (A, B, C), or in X161 (C, D, E). Notice that the cell density of X161 is less than in WT. Centromeres are marked by CID, DNA/nuclei are marked by DAPI. Green: CID, blue: DAPI, scale bar: 20 μ m.

3.2.4. The X161 phenotype in haploid embryos

Haploid embryos undergo an extra mitosis before cellularization (EDGAR *et al.* 1986), which is opposite to the phenotype of X161, allowing to establish genetic epistasis. Such embryos were produced by crossing females bearing X161 germline clones with male homozygotes for *ms(3)K81*. *Ms(3)K81* prevents the union of maternal and paternal pronuclei but still allows development to continue with haploid

maternal genome (YASUDA *et al.* 1995). The haploid X161 embryos undergo viable number of nuclear divisions. The embryos at cycle 13, cycle 14 and cycle 15 could be observed (Figure 21B and Table 2).. One patchy embryo even contained three compartments of different nuclear density (Figure 21A). This result indicated that X161 and haploid are not epistatic to each other, and suggests that they act in distinct processes to control the cell cycles.

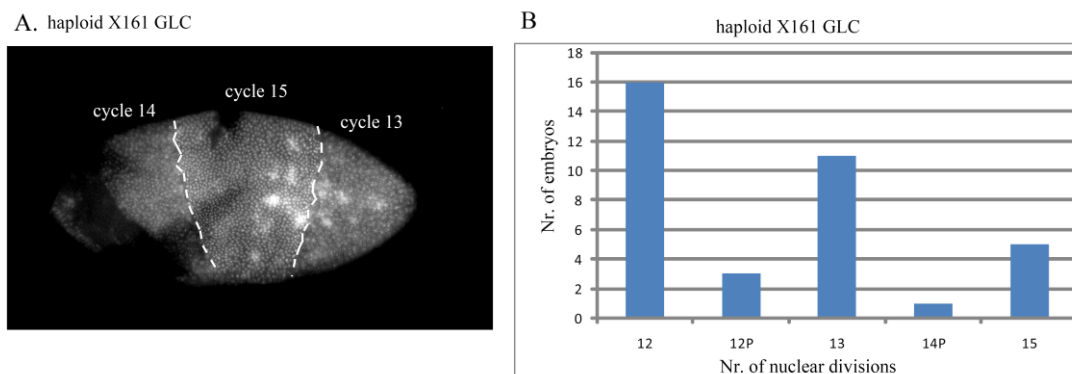


Figure 21: Epistasis of *X161* and haploid mutants. *X161* and N/C ratio work in parallel to control the number of nuclear divisions. The haploid X161 GLC show complicated patched embryos (A). The number of nuclear divisions in haploid *X161* embryos is summarized in (B). About 50% of haploid embryos undergo 12 nuclear divisions, 34% undergo 13 divisions and 15% undergo 14 divisions.

3.2.5. Partial rescue of the phenotype by zygotic activation

Since only half of the embryos had a reduced number of nuclear divisions, X161 may show a zygotic rescue. To test this hypothesis, *X161* females were crossed to males with a marked X-chromosome (FM7c, P{ry[+t7.2]=ftz/lacZ}YH1) (KLÄMBT *et al.* 1991). Zygotically heterozygous (female) embryos therefore could be separated with hemizygous males by the staining of β -galactosidase to mark the female. The embryos at stage 5 and 6 were collected and checked for nuclear density from both male and females. 87% of the male embryos showed the premature stop of nuclear division, compared with the female (52%) (Table 2). Although there was still 50% of

females show the phenotype, the male has higher portion of defect. It suggests there is a partial rescue for the premature stop, but not fully. This result also confirms that the extension of length of interphase 13 in all the *X161* embryos is a strictly maternal phenotype.

3.2.6. Cellularization occurs immediately after cell cycle stop

In wild type, cellularization immediately starts after exit mitosis 13. To test whether such a link is also observed in *X161* embryos with premature stop of cell cycle, we used time-lapse imaging with Moesin::GFP to visualize the progression of cellularization. Unlike the result of cyclin RNAi treatment (MCCLELAND and O'FARRELL 2008), cellularization in *X161* mutant started after last mitosis (Figure 22). The progression of cellularization in interphase 13 is 10min slower than in interphase 14. Since the average time of cycle 13 is 36 min, it is unlikely that cellularization starts at an absolute time after fertilization. However, inhibition of the cell cycle was not sufficient to forestall cellularization, which is based on the experiment of RNAi against mitotic cyclins (MCCLELAND and O'FARRELL 2008). We proposed that the difference result of these two experiments is due to the premature activation of zygotic genome in *X161*.

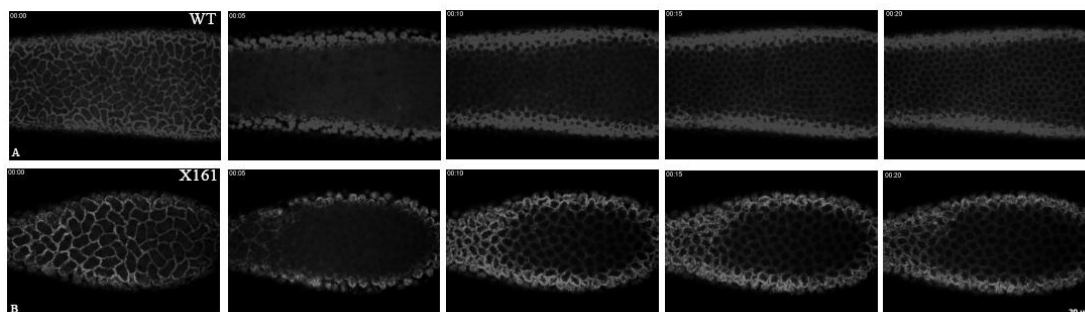


Figure 22: The cellularization occurred immediately after last mitosis. (A) is wild type at cycle 14 and (B) is *X161* embryos at cycle 13. The movie was obtained with meosin::GFP to mark the furrow canal. Scale bar is 20 μ m.

3.2.7. X161 causes premature degradation of *cdc25* homologs

The degradation of the maternal transcripts *cdc25* homologs, *string* (*stg*) and *twine* (*twn*), plays an important role in proper stop of cell cycle (EDGAR and DATAR 1996). It is possible that the degradation of *stg* and *twn* is changed in X161 mutant. In wild type embryos, the maternal transcripts of *stg* and *twn* are abundant until the mid-cellularization in interphase 14. In the embryos with premature stop, the expression of *stg* and *twn* disappeared in mid-cellularization of cycle 13 (Figure 23). Since degradation of *stg* and *twn* followed the premature onset of cellularization in interphase 13, the degradation may be the consequence but not the cause of the premature stop of nuclear division. Although we did not perform a genome-wide analysis, it is quite likely that some other maternal transcripts, if not all, may be also degraded prematurely in X161 mutants.

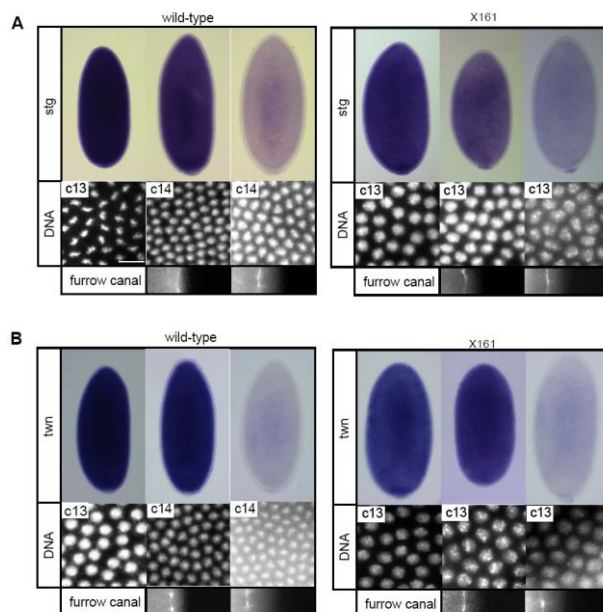


Figure 23: Expression of *stg* and *twn*. The *in situ* hybridization of *stg* (A) and *twn*(B) in WT and X161 embryos. The cycle is decided by the nuclear density. The furrow canal is marked by the immunostaining against Slam. Scale bar: 10 μ m as all the following nuclear density pictures.

3.2.8. X161 causes premature expression of zygotic genes

The stop of nuclear divisions and onset of cellularization require the zygotic gene expression (EDGAR and DATAR 1996). The embryos injected with the RNA polymerase II inhibitor, α -amanitin, do not cellularize and undergo one extra nuclear division. This data suggested that zygotically expressed mitotic inhibitors are involved in pausing the nuclear division at cycle 14. At least two mitotic inhibitor *tribbles* and *frühstart* have been identified (GROSSHANS *et al.* 2003). Expression of mitotic inhibitors is sufficient to pause the cell cycle.

To test whether the premature stop of cell cycle in X161 is due to the premature expression of zygotic cell cycle inhibitors, the expression profile of *frs* was analysed by in situ hybridization. In wild type, the major peak of *frs* expression showed up at early interphase 14 (Figure 24A). In X161, the peak of *frs* expression is at interphase 13 (Figure 24B). We concluded that the expression starts one cycle earlier, immediately following the exit of mitosis 12.

Since cellularization starts immediately after mitosis 12 in half of X161 embryos, the zygotic genes, which are required for cellularization, may be expressed prematurely as well. Therefore, we analysed expression of *slow as molasses* (*slam*). *Slam* is required for the slow phase of cellularization (LECUIT *et al.* 2002). In wild type, the expression of *slam* starts at late interphase 13 and has the major peak at early cycle 14. The expression of *slam* was detected as early as interphase 12 in X161 embryos (Figure 24C and D). It may be the reason why the cellularization can occur prematurely in the X161 embryo but not in other mutant embryos.

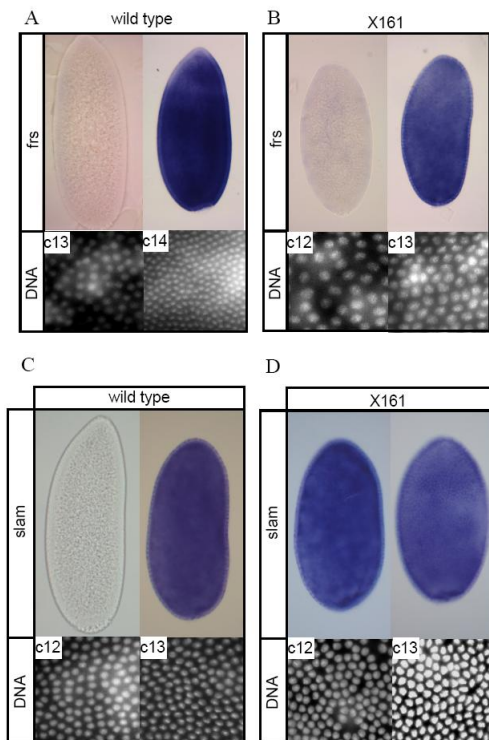


Figure 24: Expression of *frs* and *slam*. The *in situ* hybridization of *frs* (A, B) and *slam* (C, D) in WT and X161 embryos. The cycle is decided by the nuclear density .

The microarray comparison between diploid and haploid embryos revealed that there are two clusters of zygotic genes, N/C dependent and N/C independent (LU *et al.* 2009). *Frs* belongs to the N/C dependent cluster and *slam* belongs to the N/C independent cluster. Both *frs* and *slam* are expressed prematurely in *X161* mutant. This suggests that onset of zygotic gene activation is affected in *X161* embryos.

3.2.9. The *X161 frs* double mutant could not rescue premature cell cycle pause

It is showed that the premature stop of cell cycle in *X161* mutants requires the zygotic activation. *frühstart* is a good candidate of the zygotic gene that mediates the inhibition of cell cycle. *Frs* is the cell cycle inhibitor which blocks the substrate binding site (hydrophobic patch) of cyclin (GAWLINSKI *et al.* 2007) , and its expression is precisely at early interphase 14 in wild type embryos (GROSSHANS *et al.* 2003). However, the expression of *frs* could be detected as early as in interphase 12 in

X161 mutant. It is possible that *X161* pauses the cell cycle via regulating the expression of *frs*. To test this possibility, *X161, frs* double mutant was generated. The penetrance of the double mutant was as the same as *X161* alone. It suggested that *frs* was not required for pause of cell cycle in *X161*. This is consistent with the previous result that *frs* is only one of several zygotic mitotic inhibitors (GROSSHANS *et al.* 2003). In summary, *frs* may be involved in the premature stop of cell cycle, but there are redundant cell cycle inhibitors. Therefore, *frs* alone is not required for the premature entry of MBT.

3.2.10. The premature cell cycle pause requires the expression of zygotic genes

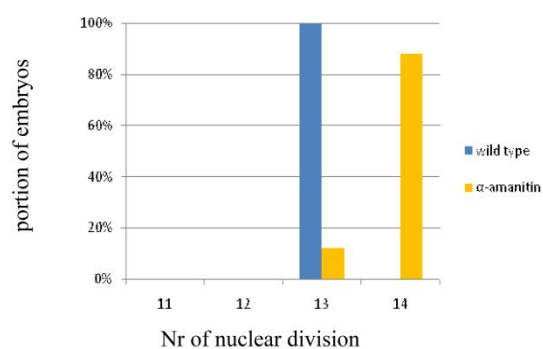
Since we observed the premature expression of zygotic genes, the question was raised whether zygotic expression is required for the cell cycle phenotype. One possibility is that *X161* affected the cell cycle directly, or by maternal cell cycle regulators, such as *CycB* and *grapes* (EDGAR 1995; SIBON *et al.* 1997). The other possibility is that *X161* cause the premature stop of cell cycle via the expression of zygotic genes (Figure 25A). To distinguish these two hypotheses, the expression of zygotic genes was blocked by the injection of α -amanitin, inhibitor of RNA polymerase II, is performed. If the expression of zygotic genes is required, the injection of α -amanitin would revert the cell cycle phenotype to 13 or 14 nuclear divisions. The result showed that all the injected *X161* germline clone embryos underwent at least 13 nuclear divisions, while 50% of the embryo injected with water still underwent 12 divisions. The result suggested the zygotic activation is required for the premature stop of cell cycle in *X161* GLC embryos (Figure 25C). In wild type embryos, the injection of α -amanitin cause an extra mitosis. However in *X161* embryo (Figure 25B), the injection of α -amanitin also caused severe nuclear fallout and nuclear fusion (Figure 25 E and F). Therefore, the further imaging could not be

recorded.

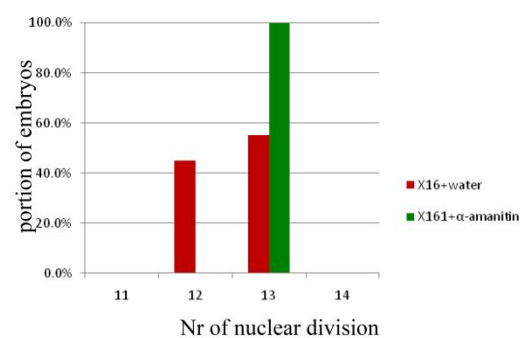
A



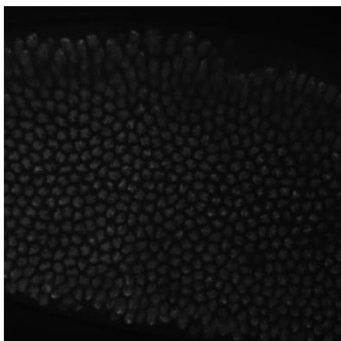
Hypothesis	Predicted results
X161 directly affect the cell cycle	Nr. of cleavage cycles 12/13
Zygotic gene expression is required	13



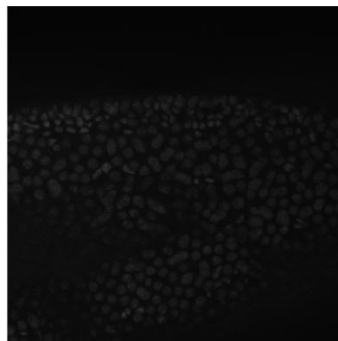
C



D. WT + water



E. WT+ α -amanitin



F. X161+ α -amanitin

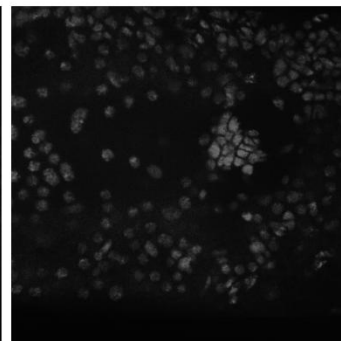


Figure 25: *X161* requires zygotic gene expression. (A) summary of the predicted results of α -amanitin injection. (B) α -amanitin caused extra cell cycle in wild type (93%). (C) α -amanitin rescued the premature cell cycle stop phenotype of X161 GLC. The α -amanitin caused the moderate nuclear fallout and fusion (E) and severe fallout and fusion in X161 (F), which was not occurred whe injected with water (D)

3.2.11. Isolation of X161 genes

The initial approach to map *x161* was the complement test with the X-chromosome duplication kit. However, no duplication could complement the lethality of X161 (table 4). There are gaps in the duplication kit, although it covers more than 90% of X

chromosome, It is possible that X161 is within one of these gaps. Another possible explanation is that there may be more than one lethal mutations on X161 X chromosome.

To narrow down the position of X161, the linkage map of meiotic recombination was performed with a marker chromosome carrying visible markers (Figure 26). The lethal mutation locates between *vermillion* (cytomap: 33.0) and *forked* (cytomap: 56.7). With the calculation using the recombination between *white* and *crossveinless* as reference, the genetic distance between *crossveinless* and the mutant is 30.3 cM and between *forked* and the mutant is 9.5. The calculation from the proximal and distal markers estimated the position of the mutation at at 44 to 47 at the recombination map, which is roughly at 12 to 13 in the cytological map.

Table 4: the complement test of original X161 line with duplication kit

Number	Duplication	Bar male	WT male
901	1Lt--2B18	66	0
761	1A3--3A2	173	0
1527	2C1--3C5	121	0
936	2D2--3D3	146	0
1319	3C1-2;3E7-8	111	0
5594	3C2;3F + 3F;4E3 + 4E3;5A1-2	146	0
5279	4C11;6D8 + 1A1;1B4 (Dp)	91	0
948	6C;7C9-D1	116	0
1879	7A8--8A5	64	0
5678	7D;8B3-D7 + 16A1;16A1 + 20B;20Fh	53	0
5292	8C-D;9B + 1A1;1B2	122	0
929	9A2;10C2	143	0
5596	1A1;1B1-2 + 10C1-2;11D3-8	187	0
3560	9F4;10E3-4 + 1A1;1B2 + 20B;20Fh	114	0
5459	11D--12B7	170	0
3219	12A6-10;13A2-5 + 1A1;1B3-4	134	0
5273	13F1-4;16A1 + probably X tip segment 1A1;1A	98	0
1537	15B1--16F	148	0
1538	16F1-4;18A5-7 + 1A1;1B2 + 19E5-7;20Fh	110	0
3033	18F1;20Fh + 1A1;1B2	160	0
940	3D6-E1;4F5, 4E3;5A1-2	178	34
5281	5A8-9;6D8	145	0
1527Pr	2C1;3C5	117	1

3.2.12. Mapping with Single nucleotide polymorphisms and chromosome cleaning

To further narrow down the X161 mutation, the mapping with SNP was performed. X161 flies crossed with the marker line, $y, pn, cv, v, f, FRT18E$, and the recombinants were collected and checked for SNPs.

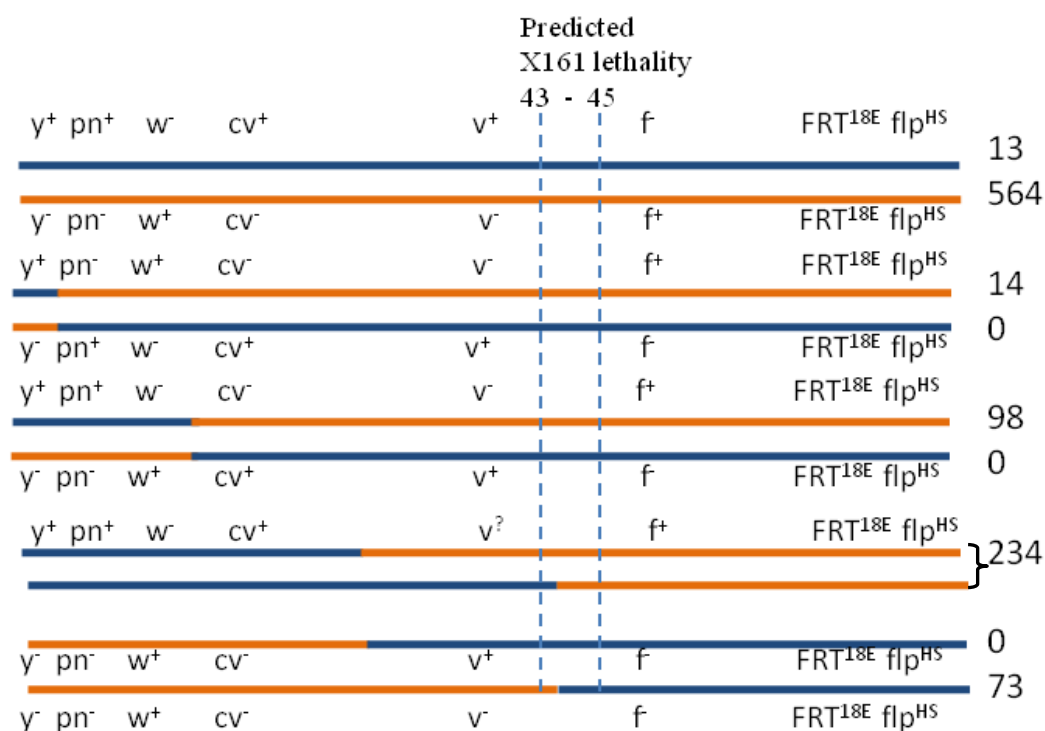


Figure 26: Mapping of *X161* by meiotic recombination. The summary of the meiotic recombination between $w^-, X161, f, FRT18E$ (blue) and the marker chromosome $y, pn, cv, v, f, FRT18E$ (orange). The number indicated the F1 progenies of specific genotype. The blue dash line illustrates the approximate region *X161* mutation locates. The blue line indicates the region from mutant chromosome, the orange, from the marker chromosome.

5 of 48 $v^- f$ viable males show the SNP from X161 at 11A and SNP from B437 at 9F. This result narrowed the location of the mutant down to 9F to 11A (Figure28A). However, the 7 of 13 lethal female recombinants (distal: marker and proximal: mutant) contained the marker SNP at 11. This result suggested that there was another mutation was proximal to 11 which was inconsistent with the result from the male

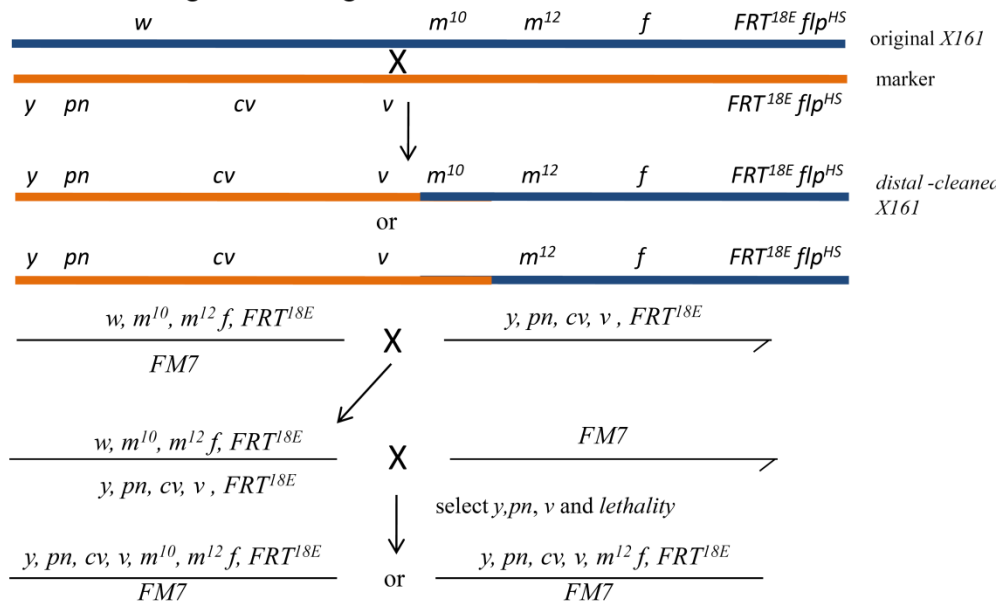
recombinants.

To explain this conflict result, I assumed that there may be two mutations on the X161 chromosome. First mutation m^{10} is between 9 and 11 and is a true lethal mutation. The other mutation m^{12} located proximal to 11 and is actually a semi-lethal mutation because there were few escapers of male recombinants carrying this mutation. Since at this stage, the m^{12} mutation was isolated (Figure 27A). The germline clone analysis showed that m^{12} mutation didn't have maternal effect and could not generate the phenotype observed in original X161. Therefore, the m^{10} may be the mutation that caused the phenotype.

Based on this assumption, another round of recombination was performed to separate these two mutations and isolate the m^{10} mutation (Figure 27B). The $y, pn, cv, v, x161^{m^{10}+m^{12}}, f, FRT^{18E}$ flies were crossed with the fly, $w^{118} sn^3 P\{neoFRT\}^{19A}$. The flies were treated with G418 to select the flies which contained $P\{neoFRT\}^{19A}$ then progenies were crossed *FMO* balancer and the recombinants with v^- and *forked*⁺ were picked up and setup stocks. Further SNP analysis with the SNP at 11 was performed to select the stocks whose proximal mutations were removed.

All the recombinants were tested by germline clones to check for the maternal effect. All the GLC embryos from the viable recombinants hatched, the GLC from all the recombinants containing m^{10} mutation did not hatched and showed premature cellularization phenotype similar to *X161* (Table 2). This result indicated the phenotype was linked to the lethality. And the m^{10} mutation was indeed the mutation we were looking for.

A. Chromosome Cleaning for distal region



B. Chromosome Cleaning for proximal region

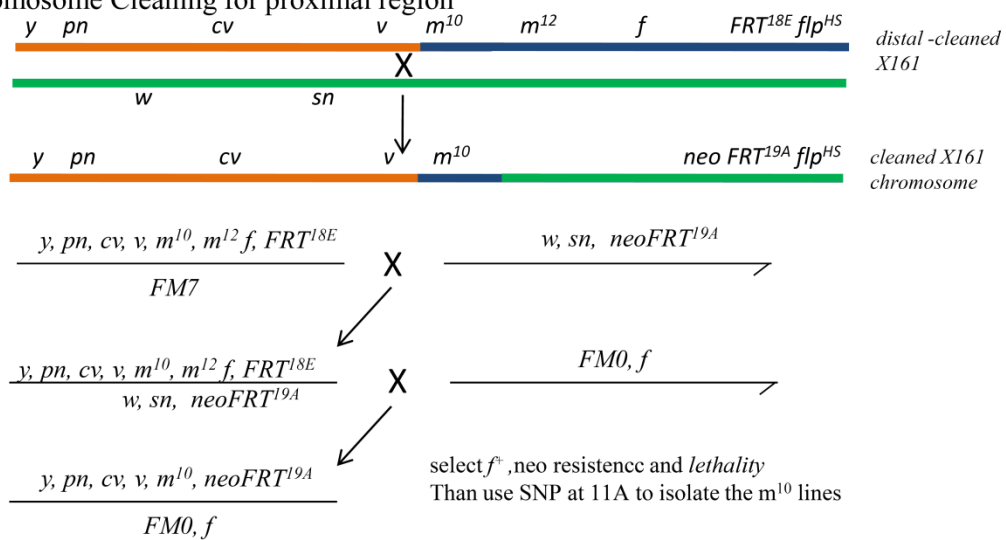


Figure 27: The crossing-scheme of chromosome cleaning for X161. There two mutation, one at cyto 10 and one between 12 and 14 on the X chromosome of X161. The first chromosome cleaning (A) cleaned the X chromosome distal to v , and isolate the lines containing only m^{12} mutation. The second chromosome cleaning (B) cleaned the proximal region and isolate the lines containing only m^{10} , which is $RPII215^{X161}$.

Table 5: the complement of the <i>X161^{ml}</i> , <i>FRT^{9AE}</i> with duplication and deficiency lines.				
Duplication				
Stock Nr.	Genotype	Duplicated region	FM0	WT
929	Df(1)v-L15, y/C(1)DX, y w f; Dp(1;2)v[+]7	9A2;10C2	66	0
5596	Dp(1;Y)BSC1, y[+]/w	10C1-2;11D3-8	177	30
3560	Df(1)v-N48, f[*]/Dp(1;Y)y[+]v[+]#3/C(1)DX, y f	9F4;10E3-4 + 1A1;1B2	245	45
29771	Dp(1;Y)BSC47	10B3;11A1	113	1
29773	Dp(1;Y)BSC49	10B3;11A1	84	1
29774	Dp(1;Y)BSC50	10B13-10C5;11A1	61	4
29776	Dp(1;Y)BSC52	10C5-10C7;11A1	182	0
29778	Dp(1;Y)BSC54	10C7-10D5;11A1	72	0
29780	Dp(1;Y)BSC56	10D5-10E2;11A1	63	0
30352	Dp(1;3)DC233	9F13;10A3;65B2	36	0
30353	Dp(1;3)DC234	10A3;10A8;65B2	86	0
30354	Dp(1;3)DC235	10A6;10B1;65B2	31	0
30356	Dp(1;3)DC237	10B2;10B5;65B2	52	0
30357	Dp(1;3)DC238	10B3;10B12;65B2	50	0
30358	Dp(1;3)DC239	10B8;10B15;65B2	53	0
30359	Dp(1;3)DC240	10B14;10C5;65B2	143	0
30360	Dp(1;3)DC241	10C2;10D1;65B2	127	69
30361	Dp(1;3)DC243	10D4;10E2;65B2	135	0
30364	Dp(1;3)DC246	10F1;10F7;65B2	105	0
Deficiency				
Stock Nr.	Genotype	Duplicated region	Df/FM0	X161/Df
23672	Df(1)BSC287	10A10;10B11	45	59
23673	Df(1)BSC288	10B2;10B11	9	6
25069	Df(1)BSC541	10E1;10F1	13	15
25072	Df(1)BSC544	10E4;11B9	21	30
26510	Df(1)BSC658	10B3;10C10	65	0
26574	Df(1)BSC722	10B3;10E1	38	0
1512	RPII215 ¹		193	0
11547	RPII215 ^{G0040}		34	0

3.2.13. *X161* is a novel allele of RNA polymerase II 215 subunit

These new x161 recombinants are used for the complement test with duplication kit. Indeed, the chromosome-cleaned x161 could be complemented by two duplication lines 3560 and 5596, which narrowed the region of X161 as 9F to 10E. The further complement test with molecular-defined duplications and deficiencies was performed and narrowed to a 20KB region, from X: 11,446,970 to 11,466,244 (table 4, and figure 28A). There are 4 genes within this region, cg 1572, PGRP-SA, RNA polymerase II, and cg11699. The sequencing was performed for the genomic region of all four genes, which including the coding region, 5' UTR, 3'UTR and the 1kb upstream. The sequencing revealed that there was a single nucleotide exchange from A to T at 40bp of the 3'UTR of RNA polymerase II 215 subunit (Figure 28 C and D).

To confirm that the *X161* would be an allele of RNA polymerase II 215, the *X161* was crossed with two lethal alleles, *RPII215^{G0040}* and *RPII215^l* (GREENLEAF et al. 1980). *X161* failed to complement both (Table 4). Although the genomic rescue experiment is missing, combining the sequencing and complement test data still provides the convincing evidence that *X161* is an allele of *RPII215* (*RPII215^{X161}* distinguishes from *X161* in following section).

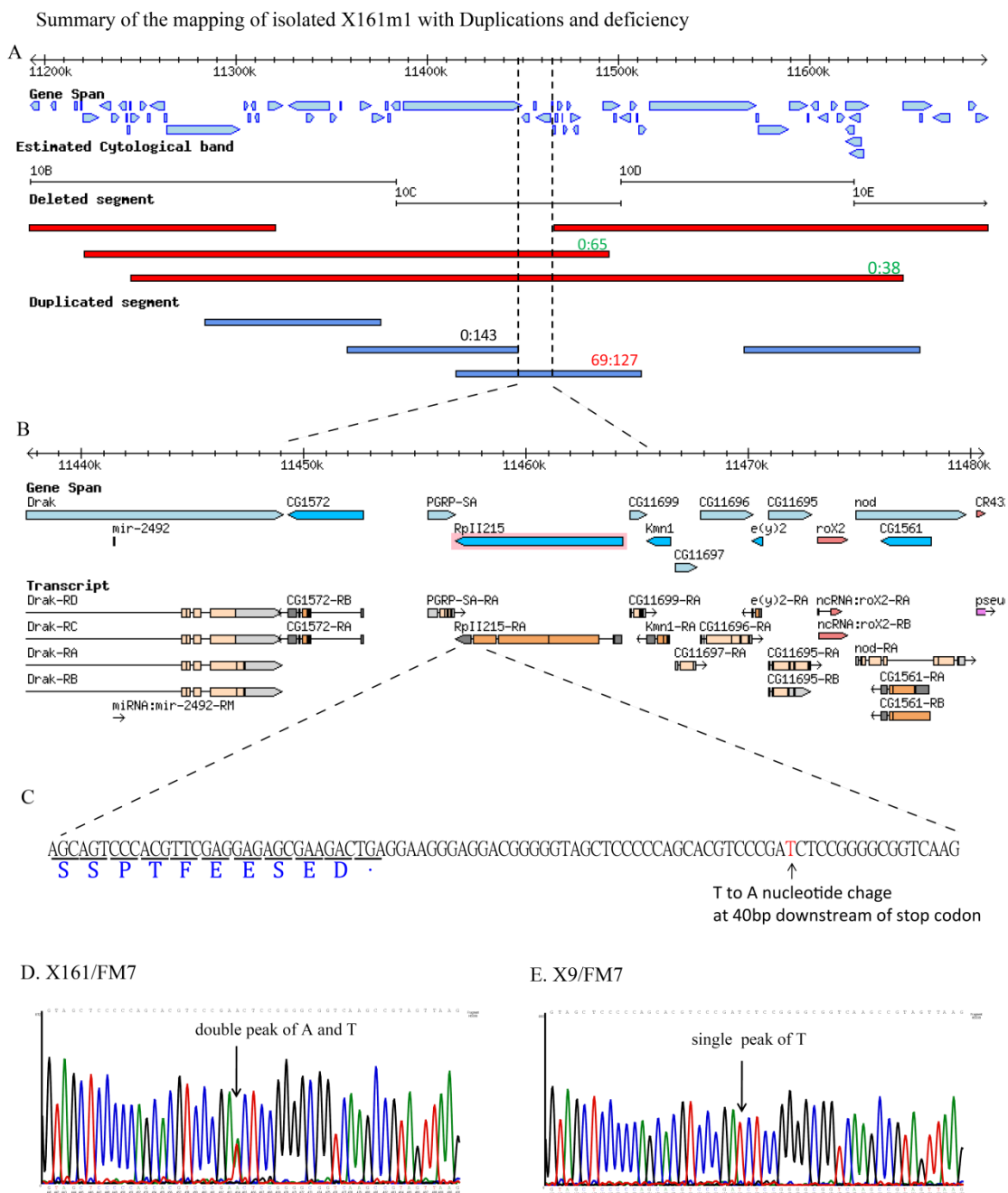


Figure 28: *RPII215^{X161}* is a novel allele of *RNA polymerase II 215*. The complement test with duplications and deficiencies narrowed down to four candidate genes (A & B). The enlarged illustration of the first 50bp region of 3'UTR of *RPII215* (C) The sequencing graph of the X161/FM7 show the double peak (T to A) at the point mutation of X161 (D), but show only single peak of T in the control line X9/FM7 (E). The position of X161 mutation is indicated by the arrow.

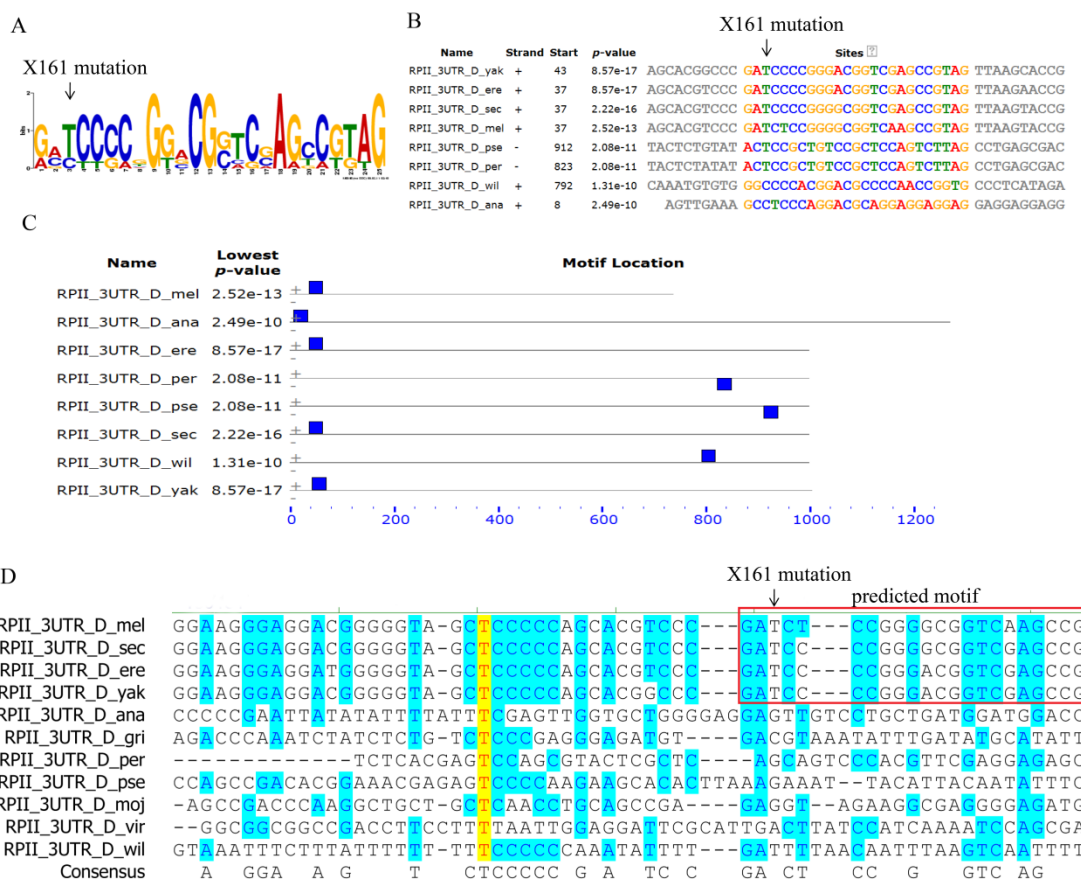


Figure 29: Motif prediction of X161 mutation site. (A) The weight matrix of the predicted motif locates the X161 mutation site at 3’UTR of *RPII 215*. (B) the sequence of this motif from 8 *Drosophila* species. (C) the location of this motif at 3’UTR of the RPII in different species. (D) the sequence alignment of the first 50bp of 3’UTR of RPII 215. The red box indicates the predicted motif by MEME program.

3.2.14. The prediction of X161 mutation site

Next, I tried to use bioinformatic apporcah to predict the molecular nature of X161 mutation. The sequence alignment show that the first 50bp of RPII 215 3’UTR is conserved within 4 species in the melanogaster subgroup (Figure 29 D, red box). The motif prediction by MEME program also predicted one 25bp motif located at X161 mutation site (Figure 29A, B and C).

Since the microRNAs paly an important role controlling the translation and RNA stability at early development (BUSHATI *et al.* 2008), we first checked whether there is

potential miRNA binding site at 3'UTR of RPII 215 based on the data from miRNA-Target predictions for *Drosophila* miRNAs at EMBL (STARK *et al.* 2005; STARK *et al.* 2003). No miRNA binding site is reported at 3'UTR of RPII 215. No piRNA binding site could be found at X161 mutation region with the blast of known piRNA database (SAI LAKSHMI and AGRAWAL 2008). We have not tested any the interaction of RNA-binding protein. However, Smaug, for example, may be a good candidate may bind to this position.

3.2.15. Dynamics of RNA pol mRNA and protein

Since *RPII215^{X161}* mutation occurred at 3'UTR, it should not affect amino acid sequence. We hypothesized that the mutation may affect the translation rate or mRNA level. The western blotting against RNA polymerase II was performed. In wild type, there was low level of RNA pol II protein in 0 to 1 hr embryos (Figure 30A). Benoit and colleagues also obtained similar result (BENOIT *et al.* 2009). Both the active form and the total lever of Pol II protein gradually increase during the development. In *RPII215^{X161}* embryos, there is already high level of active Pol II protein at 0 to 1 hr embryos; however, the amount of Pol II remains constant.

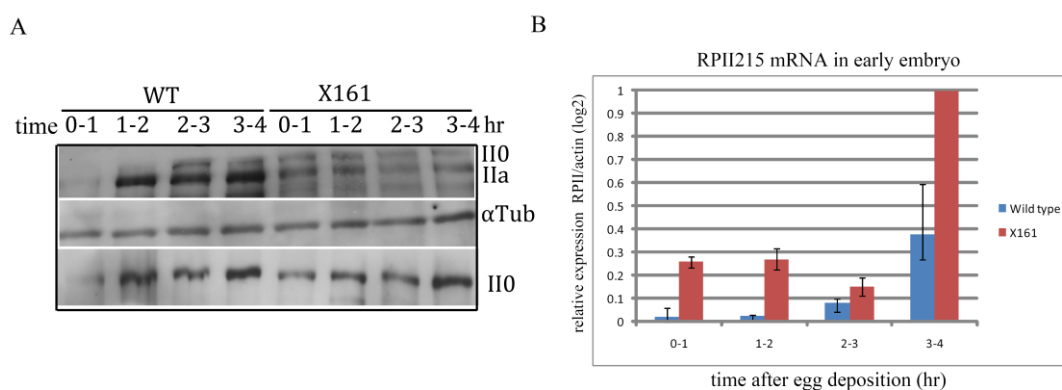


Figure 30: The dynamics of RPII215 protein and transcripts. (A) The western blot of RNA polymerase II 215 in early embryo. II0 is active form of Pol II IIa, inactive form. Pol II by ARNA3-a antibody, and II0 was by H5. The number above each lane indicates the collecting time (unit: hr) after egg deposition. II0 is the phosphorylated and active form of Pol II (B) the QPCR of RPII215 relative to actin. The overall level is significantly higher in *X161* embryos.

Next, we investigated the dynamics of RNA polymerase II transcripts with quantitative PCR. The dynamic of Pol II mRNA show similar pattern as the protein. The level of transcripts is low for 0-2 hr, but the level rises from 2hr and boost during 3 to 4 hr (Figure 30B). This result was contrary to the current genome-wide RNA sequencing result on flybase, that the level of RPII 215 transcripts was stable during whole life cycle (Figure 31) (DAINES *et al.* 2011). This may due to the different scale and experimental procedure. In X161 embryos, the initial level of Pol II mRNA is much higher than in wild type (Figure 30B). The high level of RNA polymerase II protein and transcripts is quite unexpected. It is unclear whether the rate of translation is higher in X161 at 0 to 2 hr. However, the high level of active form of pol II protein at the 0 to 1 hr may suggest that the accumulation of pol II protein and transcripts already start during oogenesis.

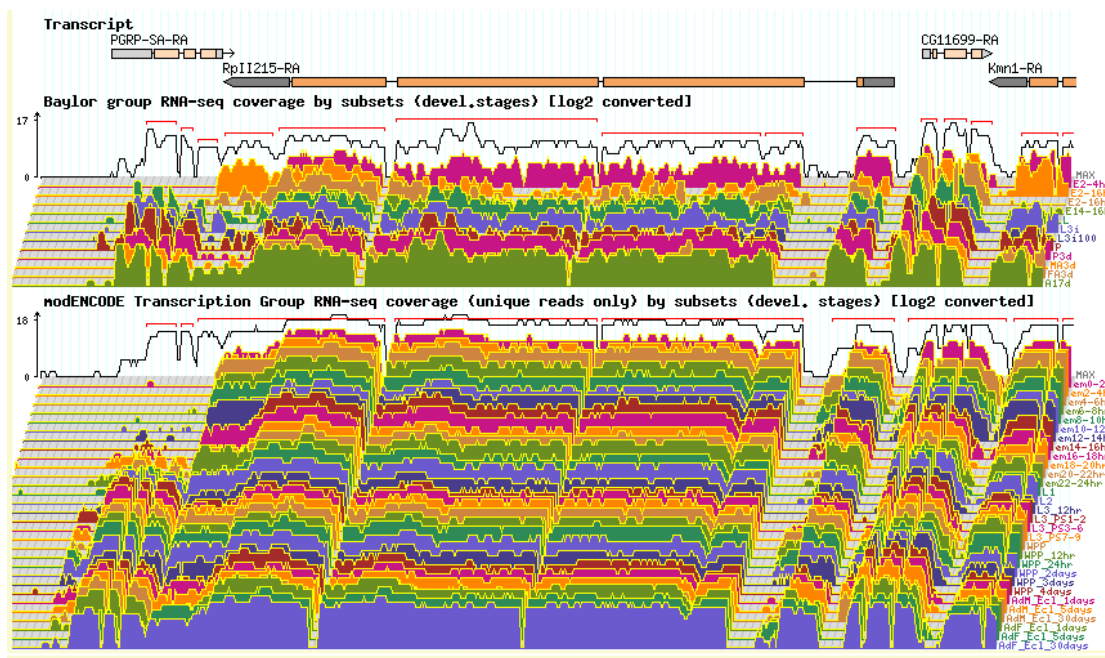


Figure 31: the RNA-seq of *RPII 215* in *Drosophila* (adapted from Daines 2011). The level of *RPII 215* of 0-2 hr and 2-4 hr is similar, which is contrary to the QPCR result in Figure 29B.

4. Discussion

4.1. Dissection of *frs* genomic regulatory module

4.1.1. The genomic regulatory modules of *frs* expression

In this study, we investigated the genomic regulatory elements of *frs* in order to provide the link between the N/C ratio and the zygotic gene expression. Although we did not achieve this initial goal, our reporter assay narrowed the core genomic regulatory region of *frs* to the 260bp upstream region upstream of its transcription start site. The -260bp to -180bp region is required for the transcription of *frs*. The deletion of the region dramatically reduced the expression. We also identified two transcription silencers at the genomic regulatory region of *frühstart*. *prom(-68--57)::GFP* and *prom(-174- -161)::GFP* drives the leaky expression at cycle 13, although the expression still delayed in haploid embryos (Figure 32). However, it supports the idea that there would be transcription repressor to prevent the premature activation of *frs*. Since *Frs* is a cell cycle inhibitor which is sufficient to arrest the cell cycle, the expression of *frs* needs to be restrictively controlled at temporal aspect. The transcription repressor combined with activator can set a sharp expression broader than the activator alone (DAVIDSON 2001).

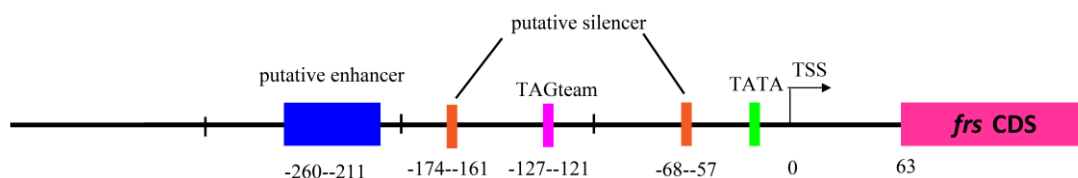


Figure 31: the genomic regulatory region of *frs*. The putative enhancer and the protein-binding region is in blue. Two putative silencers (in orange) prevent the premature expression at cycle 13. The TAGteam motif is in pink, TATA box in green. The number below indicate the distance (bp) from the transcription start site.

In our EMSA assay, we identified one protein-binding motif at -260bp to -211bp at the region is required for the strong expression of *frs* (Figure 32). This motif may be an enhancer for the transcription activation. This region is conserved within *D. melanogaster*, *D. simulans*, and *D. yakuba* (all in melanogaster subgroup), but quite variable in other species. This may be the reason why this motif is not over-presented in MEME predication. We did not attempt to purify the protein binding to this motif. But it is worth to investigate it with DNA affinity chromatography or yeast-one hybrid screen.

We could not detect any DNA-protein interaction at the region of *prom(-68--57)* and *prom(-174- -161)* in our EMSA assay using nuclear extract from the early embryo. EMSA is proved to be a very powerful tool for investigating the interaction between nuclear acid and proteins and is widely used in DNA and RNA researches. However, the binding interaction of EMSA is performed *in vitro* at reaction tube supplied by the artificial buffer. The DNA probe using in EMSA are usually short (less than 500bp) and is without histone or DNA modification. Therefore, the EMSA could not fully provide the microenvironment identical to the transcription factors encounter in nuclei, especially the weak DNA-protein binding or the binding required other factors. Another reason is the abundance of transcription factors. The amount of transcription factor is relative low compared to other nuclear protein. In early cleavage stage, the number of nuclei is fewer than in syncytial blastoderm or later stage. Therefore, the nuclear extract we used in this study may not contain sufficient transcription factor to mediated the shift in EMSA. The third possibly is that this motif may not be directly involved in protein binding. Although this two motifs are required for the repression at cycle 13, it may mediate the repression by change the local DNA topology, for example, the motif makes it more difficult to bend DNA and form the loop which is

required for the interaction between transcription activator and RNA polymerase II complex (TADROS *et al.* 2007a).

4.1.2. The TAGteam motif is not required for frs expression

The transcription of *frs* is largely decreased in the microarray analysis of *zelda* mutant, and about 5 to 10% of *zelda* mutant embryos undergo extra mitosis as in *frs* mutant (LIANG *et al.* 2008). These two results suggest that the expression of *frs* requires the transcription factor Zelda. The Zelda binds specifically to the TAGteam DNA motif (CAGGTAG). There is one CAGGTA motif located at 127 to 121 bp upstream of the *frs* transcription start site. However, in our study, substitution of this motif did not alter the expression of the reporter. It suggests that TAGteam motif is not required for the expression of *frs*. It is possible that there is alternative Zelda binding site which is not a typical cAGGTA motif or that Zelda indirectly affect *frs* expression by controlling other transcription factor.

4.1.3. In situ hybridization as a tool studying temparol expression

In our study, we use in situ hybridization as read out of reporter constructs for several reasons: first, the early cell cycles in drosophila are short. the interphase 13 takes about 20min. The normal translation and activation of GFP takes at least 30min, as other reporter protein, like luciferase. Second, the RNA level is what we were really interested in, although the preotin level correlate with mRNA level, but it is still indirect. Second, we use the nuclear density as an indicator which cycles the embryo is. Therefore, the embryo needs to be fixed and stained by DAPI. The in situ hybridization is very powerful for investigation of spatial expression, since it provides more expression. However, it could only provide qualitative data but not quantitative

data. This caused some problem in this study. The staining was sometimes faint and difficult to decide whether it is expressed.

Lu has showed that it is possible to hand-select the staged embryos for each cycle with the histone-RFP labeling the nuclei under fluorescence stereo microscope (LU *et al.* 2009). It would be a better detection method for our study to use QPCR for hand-select staged embryos.

4.1.4. The N/C ratio and number of cleavage cycles

The relation between N/C ratio and number of cleavage cycles is known for almost one hundred years (KORZH 2009). However, the molecular link between N/C ratio and cell cycle mechanism remain unclear. Lu and Wieschaus has identified 88 zygotic genes whose expression delay in haploid embryos (LU *et al.* 2009). Based on this finding and the previous work about *frs* in our lab, we hypothesized that the *frs* can provide the missing link between N/C ratio and cell cycle control. Because the expression of *frs* is respond to N/C ratio and Frs is a cell cycle inhibitor. Although we identified two cis-motifs which prevent premature expression at cycle 13, we could not identify the element responsive to the N/C ratio. One possibility is that this element may be an activator which is required for *frs* expression, therefore, we could not identify it via deletion or substitution constructs. To test this, we would need to add the minimal *frs* regulatory module to the promoter of the zygotic gene which is not regulated by N/C ratio and see whether the fusion promoter can response to the N/C ratio.

4.1.5. Outlook for the investigation of *frs* genomic regulatory elements

So far we could not identify the elements responsive to the N/C ratio. We would like to improve this study by following: first, using quantitative method to measure

the level of transcripts. Second, use yeast-one hybrid screen to identify candidate DNA-protein interaction (SIEWEKE 2000). The advantage of yeast-one hybrid system is the interaction is in vivo, and it can identify the candidate proteins which bind to the DNA. We hope that we could eventually identify the cis and trans factors which respond to N/C ratio and provide the missing link between N/C ratio and cell cycle stop.

4.2. The Role of RPII215 in controlling the onset of MBT

4.2.1. *RPII 215^{X161}* is a novel allele of RNA polymerase 215 subunit

In this study, we reported a special allele of RNA polymerase II 215, *RPII 215^{X161}*, which contains one single T to A mutation at 40bp downstream of the stop codon. Several lines of evidences supported this conclusion. First, the sequencing result showed there was only one point mutation within the genomic region of four candidate genes. Second, two *RPII215* allele, *RPII215^{G0040}* and *RPII215^l* can not complement the lethality. Third, the duplication line *Dp(1;3)DC241* rescued both the lethality and maternal effect. *RPII 215^{X161}* caused the premature onset of MBT, which includes the cell cycle pause, maternal-zygotic transition and cellularization. Since the mutation occurs at 3'UTR, we assume it may affect the translation efficiency and RNA level as it changes the level of both transcripts and protein.

We could not find putative factor binding to X161 mutation site, therefore could not provide the molecular evidence how the X161 point mutation caused the phenotype. But the data of western and QPCR show that even the initial amount of Pol II protein and transcripts is high in 0 to 1hr embryos. It suggests the accumulation of Pol II may already start during oogenesis. This raises another question: whether the level of other maternal transcripts also increase in the egg. The genome-wide analysis of

unfertilized eggs would help to clarify it.

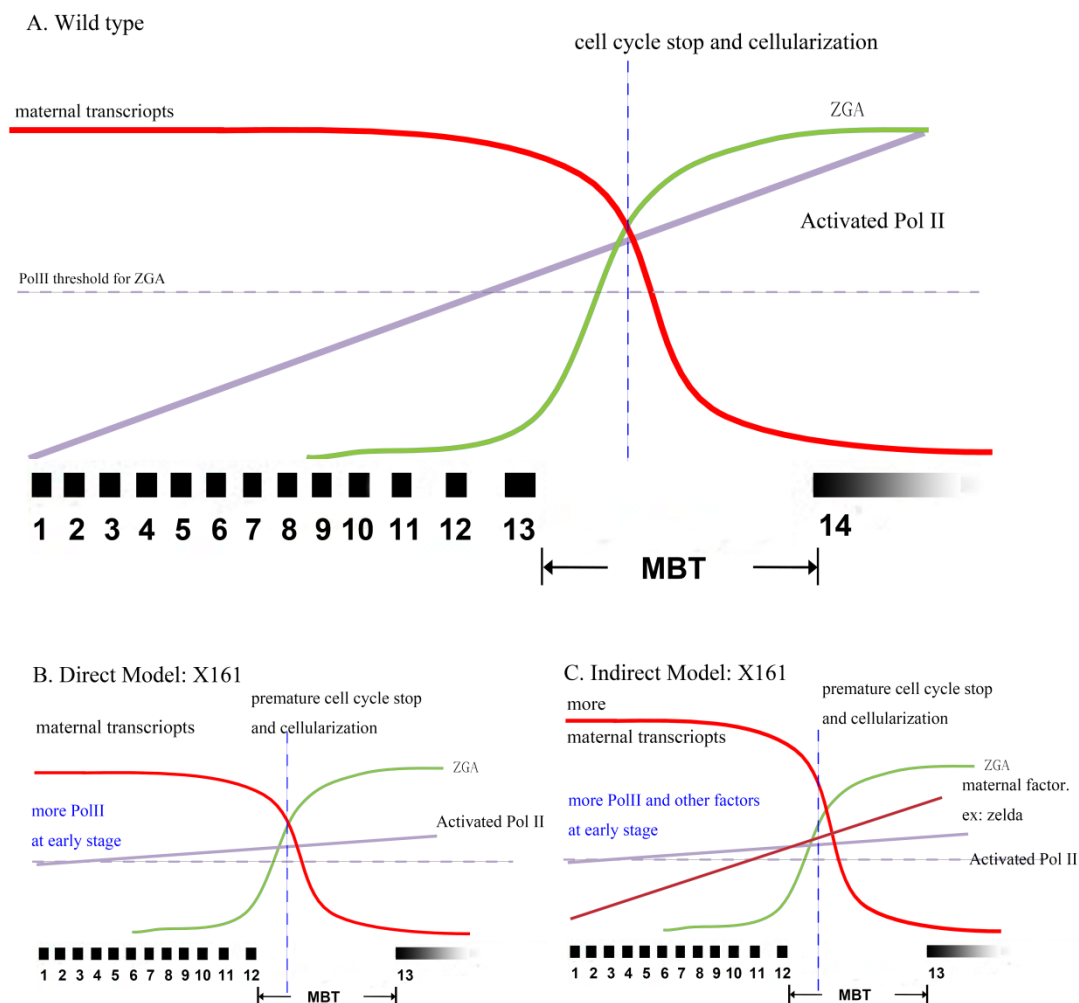


Figure 33: The models for phenotype of X161 mutant. In wild type (A), the active Pol II protein gradually increases and enables the zygotic gene expression with the help of transcription factor. In direct model (B), the higher amount of Pol II protein in preblastoderm is the main force driving the

4.2.2. Two models for *RPII 215^{X161}* phenotype

Based on the western blot and QPCR, we proposed two models to explain how *RPII 215^{X161}* causes the premature onset of MBT. In wild type, the level of RNA polymerase II protein is low after egg deposition, but is gradually increased by translation. When the amount of Pol II protein reaches a threshold, it starts the transcription of zygotic genes with the help of transcription factors (Figure 33A). Zygotic-expressed factors inhibit the cell cycle progression and promote

cellularization.

In our first model, the direct model (figure 33B), *RPII 215^{X161}* affect the translation of Pol II protein, and generat high amount of active Pol II protein in preblastoderm. Pol II protein therefore forces the premature zygotic gene activation and eventually initiates mid-blastula transition.

The indirect model (Figure 33C) emphasizes the change during oogenesis. The amount of Pol II protein is already higher in oogenesis. This may affect the transcription of many maternal genes. The amount of many maternal transcripts are higher in the egg as *RPII215*, probably the protein as well. These premature translated maternal proteins, like Zelda and Smaug, together with Pol II protein promote the premature expression of zygotic genes, and lead to premature MBT.

No matter how *RPII 215^{X161}* promotes the premature zygotic gene expression. The expression of zygotic genes is required for the premature onset of MBT, as the α -amanitin injection showed.

4.2.3. The Regulation of onset of Zygotic Gene Activation

Even that the amount of active Pol II protein was much higher in preblastoderm of *RPII 215^{X16}*; zygotic genes we tested were expressed only one cycle earlier than in wild type. This suggests that other factors are also required for zygotic gene expression (Figure 34). During the early nuclear divisions there are only S phase and M phase, which the DNA is either during DNA synthesis or packed into compact chromosome structure. This inhibits transcription. This may explain why there is no or very less transcription until cycle 10 when the interphase is prolonged. However, the length of interphase 12 did not prolonged in *X161* embryos, but is able to transcript the sufficint amount of zygotic genes required for MBT. It suggested that prolonged

gap phase may be required passively, but it is not the switch for onset of zygotic gene activation. Another possible negative factor for transcription in early divisions is the epigenetic modification on DNA or histones. The DNAs are highly methylated and the transcription of zygotic genome is repressed in vertebrates (FENG *et al.* 2010). There would be also transcription repressors contributed to the inhibition of transcription in early embryo and define a sharp cut of expression as our *frs* project showed. Removal of these repressors is also required for the zygotic gene expression. This may mediate partly by the RNA degradation of the repressor transcripts by RNA-binding protein Smaug (BENOIT *et al.* 2009; TADROS and LIPSHITZ 2009). Another requirement is the availability of transcription activator. The main transcription activator for zygotic genes is Zelda. Zelda protein can be detected only after cycle 10 (LIANG *et al.* 2011; NIEN *et al.* 2011). Zygotic gene activation is regulated by multiple factors to setup at proper timing. In this study, we found out that the accumulation of RNA polymerase II is not only required but also sufficient to promote zygotic gene activation and MBT.

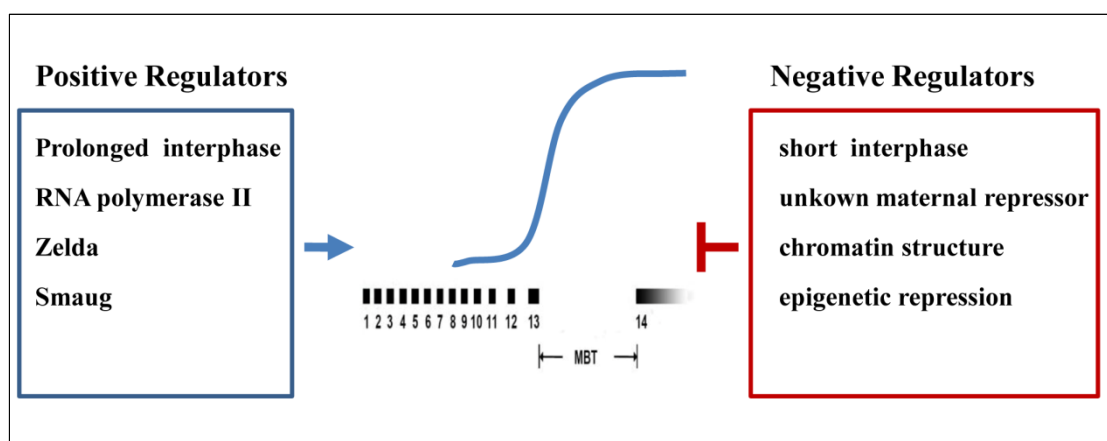


Figure 34: Summary of the known and predicted factors controlling the onset of ZGA. Blue box lists the known factors may promote ZGA, including the prolonged interphase, the accumulation of active Pol II, translation of transcription factor Zelda, and translation of RNA binding protein Smaug. The red box lists the negative factors for ZGA, including the rapid cell cycle, maternal transcription repressor, compact chromosome structure, and epigenetic repression, like DNA methylation

4.2.4. The Coupling of Cell Cycle Pause and Cellularization

McClelland and O'Farrell have performed the experiment with RNAi against mitotic cyclin in early embryos (MCCLELLAND and O'FARRELL 2008). The embryo with RNAi against Cyclin A and Cyclin B would stop cell cycle prematurely, and the cellularization still began at the absolute time of the development. It leads to the conclusion that the uncoupling of the cell cycle and cellularization, and suggests cell cycle and cellularization are controlled by different mechanism (MCCLELLAND and O'FARRELL 2008). However, in X161 germline clone, the cellularization do occurred immediately after the last mitosis. We propose that the result causes the different outcome is the premature expression of cellularization-related zygotic genes, such as *nullo* and *slam*. We hypothesis that as long as these proteins required for cellularization are presented in embryo, the furrow channel invagination would start during interphase.

4.2.5. Role of zygotic transcription in timing and coordination of MBT

MBT describes the assembling of changes occur at roughly the same time. However, these events may not be controlled by the same mechanism (YASUDA and SCHUBIGER 1992). However, our data put the zygotic activation at the center of MBT, and therefore coordinate all the other events (Figure 35). The cell cycle control at MBT required the zygotic cell cycle inhibitor, like Frs, and also the zygotic mediated removal of *stg* and *twi* transcripts. The degradation of maternal transcripts may contribute to the zygotic gene expression, but the majority of maternal transcripts is depredated by zygotic-expressed miRNAs. Finally the cellularization also required the zygotic genes, like *slam* and *nullo*.

The regulation of zygotic genes is not homogenous. There are two categories, N/C

dependent and N/C independent. These two different regulations can sense the internal cue (via the N/C ratio) to generate sufficient number of reasonable-size cells, but also can sense the environment cue (probably by N/C independent mechanism) to ensure the smooth and successful development at different conditions. Therefore, the coordination of two distinct regulatory pathways for zygotic gene activation makes the development more flexible and robust.

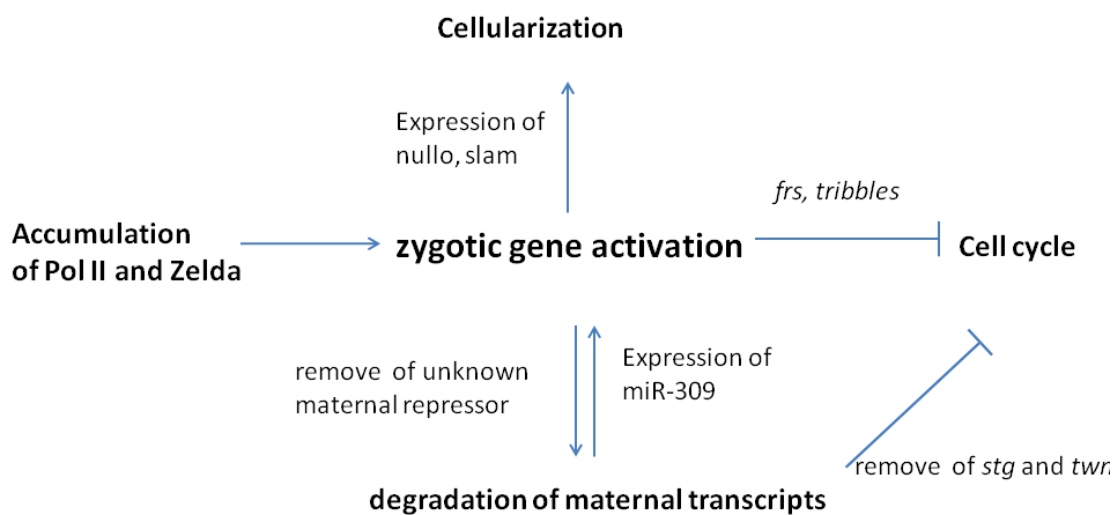


Figure 35: The role of zygotic gene activation during mid-blastula transition. The zygotic genes are required and sufficient to trigger the other events on MBT

5. References

- ASHBURNER, M., 1989 *Drosophila, A laboratory manual*. Cold Spring Harbor Press, Cold Spring Harbor, New York.
- AVIV, T., Z. LIN, S. LAU, L. M. RENDL, F. SICHERI *et al.*, 2003 The RNA-binding SAM domain of Smaug defines a new family of post-transcriptional regulators. *Nat Struct Biol* **10**: 614-621.
- BAILEY, T. L., and C. ELKAN, 1995 The value of prior knowledge in discovering motifs with MEME. *Proc Int Conf Intell Syst Mol Biol* **3**: 21-29.
- BASHIRULLAH, A., S. R. HALSELL, R. L. COOPERSTOCK, M. KLOC, A. KARAIKAKIS *et al.*, 1999 Joint action of two RNA degradation pathways controls the timing of maternal transcript elimination at the midblastula transition in *Drosophila melanogaster*. *Embo J* **18**: 2610-2620.
- BENOIT, B., C. H. HE, F. ZHANG, S. M. VOTRUBA, W. TADROS *et al.*, 2009 An essential role for the RNA-binding protein Smaug during the *Drosophila* maternal-to-zygotic transition. *Development* **136**: 923-932.
- BERGER, J., T. SUZUKI, K. A. SENTI, J. STUBBS, G. SCHAFFNER *et al.*, 2001 Genetic mapping with SNP markers in *Drosophila*. *Nat Genet* **29**: 475-481.
- BISCHOF, J., R. K. MAEDA, M. HEDIGER, F. KARCH and K. BASLER, 2007 An optimized transgenesis system for *Drosophila* using germ-line-specific ϕ C31 integrases. *Proceedings of the National Academy of Sciences* **104**: 3312-3317.
- BLOWER, M. D., and G. H. KARPEN, 2001 The role of *Drosophila* CID in kinetochore formation, cell-cycle progression and heterochromatin interactions. *Nat Cell Biol* **3**: 730-739.
- BRANDT, A., F. PAPAGIANNOULI, N. WAGNER, M. WILSCH-BRAUNINGER, M. BRAUN *et al.*, 2006 Developmental control of nuclear size and shape by Kugelkern and Kurzkern. *Curr Biol* **16**: 543-552.
- BUSHATI, N., A. STARK, J. BRENNECKE and S. M. COHEN, 2008 Temporal reciprocity of miRNAs and their targets during the maternal-to-zygotic transition in *Drosophila*. *Curr Biol* **18**: 501-506.
- BUSKE, F. A., M. BODEN, D. C. BAUER and T. L. BAILEY, 2010 Assigning roles to DNA regulatory motifs using comparative genomics. *Bioinformatics* **26**: 860-866.
- CHEN, D., A. AHLFORD, F. SCHNORRER, I. KALCHHAUSER, M. FELLNER *et al.*, 2008 High-resolution, high-throughput SNP mapping in *Drosophila melanogaster*. *Nat Methods* **5**: 323-329.
- CHOU, T. B., and N. PERRIMON, 1992 Use of a yeast site-specific recombinase to produce female germline chimeras in *Drosophila*. *Genetics* **131**: 643-653.

- CONN, C. W., A. L. LEWELLYN and J. L. MALLER, 2004 The DNA damage checkpoint in embryonic cell cycles is dependent on the DNA-to-cytoplasmic ratio. *Dev Cell* **7**: 275-281.
- COOK, K., R. GARTON, A. BROWN, M. WARD, J. DEAL *et al.*, 2010 Basal X chromosome segments present on Dp(1;Y)BSC chromosomes, pp.
- DAHANUKAR, A., J. A. WALKER and R. P. WHARTON, 1999 Smaug, a novel RNA-binding protein that operates a translational switch in *Drosophila*. *Mol Cell* **4**: 209-218.
- DAINES, B., H. WANG, L. WANG, Y. LI, Y. HAN *et al.*, 2011 The *Drosophila melanogaster* transcriptome by paired-end RNA sequencing. *Genome research* **21**: 315-324.
- DAVIDSON, E. H., 2001 *Genomic Regulatory Systems: In Development and Evolution*. Academic Press.
- DE RENZIS, S., O. ELEMENTO, S. TAVAZOIE and E. F. WIESCHAUS, 2007 Unmasking activation of the zygotic genome using chromosomal deletions in the *Drosophila* embryo. *PLoS Biol* **5**: e117.
- EDGAR, B., 1995 Diversification of cell cycle controls in developing embryos. *Curr Opin Cell Biol* **7**: 815-824.
- EDGAR, B. A., and S. A. DATAR, 1996 Zygotic degradation of two maternal Cdc25 mRNAs terminates *Drosophila*'s early cell cycle program. *Genes Dev* **10**: 1966-1977.
- EDGAR, B. A., C. P. KIEHLE and G. SCHUBIGER, 1986 Cell cycle control by the nucleo-cytoplasmic ratio in early *Drosophila* development. *Cell* **44**: 365-372.
- EDGAR, B. A., D. A. LEHMAN and P. H. O'FARRELL, 1994a Transcriptional regulation of string (*cdc25*): a link between developmental programming and the cell cycle. *Development* **120**: 3131-3143.
- EDGAR, B. A., and P. H. O'FARRELL, 1990 The three postblastoderm cell cycles of *Drosophila* embryogenesis are regulated in G2 by string. *Cell* **62**: 469-480.
- EDGAR, B. A., and G. SCHUBIGER, 1986 Parameters controlling transcriptional activation during early *Drosophila* development. *Cell* **44**: 871-877.
- EDGAR, B. A., F. SPRENGER, R. J. DURONIO, P. LEOPOLD and P. H. O'FARRELL, 1994b Distinct molecular mechanisms regulate cell cycle timing at successive stages of *Drosophila* embryogenesis. *Genes Dev* **8**: 440-452.
- ERICKSON, J. W., and T. W. CLINE, 1993 A bZIP protein, sisterless-a, collaborates with bHLH transcription factors early in *Drosophila* development to determine sex. *Genes Dev* **7**: 1688-1702.
- ERICKSON, J. W., and T. W. CLINE, 1998 Key aspects of the primary sex determination mechanism are conserved across the genus *Drosophila*. *Development* **125**:

- 3259-3268.
- FENG, S., S. E. JACOBSEN and W. REIK, 2010 Epigenetic Reprogramming in Plant and Animal Development. *Science* **330**: 622-627.
- FOE, V. E., 1989 Mitotic domains reveal early commitment of cells in *Drosophila* embryos. *Development* **107**: 1-22.
- GAWLINSKI, P., R. NIKOLAY, C. GOURSOT, S. LAWO, B. CHAURASIA *et al.*, 2007 The *Drosophila* mitotic inhibitor Fruhstart specifically binds to the hydrophobic patch of cyclins. *EMBO Rep* **8**: 490-496.
- GERHART, T. A., 1980 *In Biological Regulation and Development* Plenum Press, New York.
- GIRALDEZ, A. J., Y. MISHIMA, J. RIHEL, R. J. GROCOCK, S. VAN DONGEN *et al.*, 2006 Zebrafish MiR-430 Promotes Deadenylation and Clearance of Maternal mRNAs. *Science* **312**: 75-79.
- GREENLEAF, A. L., J. R. WEEKS, R. A. VOELKER, S. OHNISHI and B. DICKSON, 1980 Genetic and biochemical characterization of mutants at an RNA polymerase II locus in *Drosophila melanogaster*. *Cell* **21**: 785-792.
- GROSSHANS, J., H. A. MULLER and E. WIESCHAUS, 2003 Control of cleavage cycles in *Drosophila* embryos by fruhsart. *Dev Cell* **5**: 285-294.
- GROSSHANS, J., C. WENZL, H. M. HERZ, S. BARTOSZEWSKI, F. SCHNORRER *et al.*, 2005 RhoGEF2 and the formin Dia control the formation of the furrow canal by directed actin assembly during *Drosophila* cellularisation. *Development* **132**: 1009-1020.
- GROSSHANS, J., and E. WIESCHAUS, 2000 A genetic link between morphogenesis and cell division during formation of the ventral furrow in *Drosophila*. *Cell* **101**: 523-531.
- HAU, P. M., W. Y. SIU, N. WONG, P. B. S. LAI and R. Y. C. POON, 2006 Polyploidization increases the sensitivity to DNA-damaging agents in mammalian cells. *FEBS Letters* **580**: 4727-4736.
- KANE, D. A., and C. B. KIMMEL, 1993 The zebrafish midblastula transition. *Development* **119**: 447-456.
- KLÄMBT, C., J. R. JACOBS and C. S. GOODMAN, 1991 The midline of the *drosophila* central nervous system: A model for the genetic analysis of cell fate, cell migration, and growth cone guidance. *Cell* **64**: 801-815.
- KORZH, V., 2009 Before Maternal-Zygotic Transition? There Was Morphogenetic Function of Nuclei. *Zebrafish* **6**: 295-302.
- KUNERT, N., J. MARHOLD, J. STANKE, D. STACH and F. LYKO, 2003 A Dnmt2-like protein mediates DNA methylation in *Drosophila*. *Development* **130**: 5083-5090.

- LANIEL, M.-A., A. BÉLIVEAU and S. GUÉRIN, 2001 Electrophoretic Mobility Shift Assays for the Analysis of DNA-Protein Interactions, pp. 13-30 in *DNA-Protein Interactions: Principles and Protocols*, edited by T. MOSS. Humana Press, Totowa, New Jersey.
- LECUIT, T., R. SAMANTA and E. WIESCHAUS, 2002 slam encodes a developmental regulator of polarized membrane growth during cleavage of the *Drosophila* embryo. *Developmental cell* **2**: 425-436.
- LIANG, H.-L., C.-Y. NIEN, S.-B. FU, S. BUTCHER, N. KIROV *et al.*, 2011 Zelda coordinates gene regulatory networks in the early embryos., pp. in *Drosophila Conference*, San Diego.
- LIANG, H. L., C. Y. NIEN, H. Y. LIU, M. M. METZSTEIN, N. KIROV *et al.*, 2008 The zinc-finger protein Zelda is a key activator of the early zygotic genome in *Drosophila*. *Nature* **456**: 400-403.
- LU, X., J. DROCCO and E. F. WIESCHAUS, 2010 Cell cycle regulation via inter-nuclear communication during the early embryonic development of *Drosophila melanogaster*. *Cell Cycle* **9**: 2908-2910.
- LU, X., J. M. LI, O. ELEMENTO, S. TAVAZOIE and E. F. WIESCHAUS, 2009 Coupling of zygotic transcription to mitotic control at the *Drosophila* mid-blastula transition. *Development* **136**: 2101-2110.
- MCCLELAND, M. L., and P. H. O'FARRELL, 2008 RNAi of mitotic cyclins in *Drosophila* uncouples the nuclear and centrosome cycle. *Curr Biol* **18**: 245-254.
- NEWPORT, J., and M. KIRSCHNER, 1982a A major developmental transition in early *Xenopus* embryos: I. characterization and timing of cellular changes at the midblastula stage. *Cell* **30**: 675-686.
- NEWPORT, J., and M. KIRSCHNER, 1982b A major developmental transition in early *Xenopus* embryos: II. Control of the onset of transcription. *Cell* **30**: 687-696.
- NEWPORT, J. W., and M. W. KIRSCHNER, 1984 Regulation of the cell cycle during early *Xenopus* development. *Cell* **37**: 731-742.
- NIEN, C.-Y., H.-L. LIANG, T. GOCHA, S.-B. FU, S. BUTCHER *et al.*, 2011 Characterization of Zelda binding sites., pp. in *Drosophila Conference*, San Diego.
- PENG, A., A. L. LEWELLYN and J. L. MALLER, 2007 Undamaged DNA transmits and enhances DNA damage checkpoint signals in early embryos. *Mol Cell Biol* **27**: 6852-6862.
- POPODI, E., T. C. KAUFMAN, S. L. HOLTZMAN, S. PARK, J. W. CARLSON *et al.*, 2010 Small X duplications for the stock center collection, pp.
- POURQUIE, O., 1998 Clocks regulating developmental processes. *Curr Opin Neurobiol*

- 8:** 665-670.
- ROTT, N. N., and G. A. SHEVELEVA, 1968 Changes in the rate of cell divisions in the course of early development of diploid and haploid loach embryos. *J Embryol Exp Morphol* **20**: 141-150.
- ROUGET, C., C. PAPIN, A. BOUREUX, A. C. MEUNIER, B. FRANCO *et al.*, 2010 Maternal mRNA deadenylation and decay by the piRNA pathway in the early *Drosophila* embryo. *Nature* **467**: 1128-1132.
- RUSSELL, P., S. MORENO and S. I. REED, 1989 Conservation of mitotic controls in fission and budding yeasts. *Cell* **57**: 295-303.
- RUSSELL, P., and P. NURSE, 1986 *cdc25+* functions as an inducer in the mitotic control of fission yeast. *Cell* **45**: 145-153.
- RUSSELL, P., and P. NURSE, 1987a The mitotic inducer *nim1+* functions in a regulatory network of protein kinase homologs controlling the initiation of mitosis. *Cell* **49**: 569-576.
- RUSSELL, P., and P. NURSE, 1987b Negative regulation of mitosis by *wee1+*, a gene encoding a protein kinase homolog. *Cell* **49**: 559-567.
- SAI LAKSHMI, S., and S. AGRAWAL, 2008 piRNABank: a web resource on classified and clustered Piwi-interacting RNAs. *Nucleic Acids Res* **36**: D173-177.
- SAMBROOK, J., and D. W. RUSSELL, 2001 *Molecular Cloning: A Laboratory Manual*. Cold Spring Harbor Laboratory Press, Cold Spring Harbor.
- SCHUBIGER, G., and B. EDGAR, 1994 Using inhibitors to study embryogenesis. *Methods in cell biology* **44**: 697-713.
- SEMOTOK, J. L., H. LUO, R. L. COOPERSTOCK, A. KARAIKAKIS, H. K. VARI *et al.*, 2008 *Drosophila* Maternal Hsp83 mRNA Destabilization Is Directed by Multiple SMAUG Recognition Elements in the Open Reading Frame. *Mol. Cell. Biol.* **28**: 6757-6772.
- SHIBUTANI, S. T., A. F. DE LA CRUZ, V. TRAN, W. J. TURBYFILL, 3RD, T. REIS *et al.*, 2008 Intrinsic negative cell cycle regulation provided by PIP box- and Cul4Cdt2-mediated destruction of E2f1 during S phase. *Developmental cell* **15**: 890-900.
- SIBON, O. C., V. A. STEVENSON and W. E. THEURKAUF, 1997 DNA-replication checkpoint control at the *Drosophila* midblastula transition. *Nature* **388**: 93-97.
- SIEWEKE, M., 2000 Detection of transcription factor partners with a yeast one hybrid screen. *Methods Mol Biol* **130**: 59-77.
- SIGNORET J., L. J., 1971 Contribution a l'etude de la segmentation de l'oef d'axolotl. Definition de la transition blastuleenne. *Ann Embryol Morphogen* **4**: 113-123.
- SMIBERT, C. A., J. E. WILSON, K. KERR and P. M. MACDONALD, 1996 *smaug* protein

- represses translation of unlocalized nanos mRNA in the *Drosophila* embryo. *Genes Dev* **10**: 2600-2609.
- STANCHEVA, I., and R. R. MEEHAN, 2000 Transient depletion of xDnmt1 leads to premature gene activation in *Xenopus* embryos. *Genes Dev.* **14**: 313-327.
- STARK, A., J. BRENNECKE, N. BUSHATI, R. B. RUSSELL and S. M. COHEN, 2005 Animal MicroRNAs confer robustness to gene expression and have a significant impact on 3'UTR evolution. *Cell* **123**: 1133-1146.
- STARK, A., J. BRENNECKE, R. B. RUSSELL and S. M. COHEN, 2003 Identification of *Drosophila* MicroRNA targets. *PLoS Biol* **1**: E60.
- STRAUSFELD, U., J. C. LABBE, D. FESQUET, J. C. CAVADORE, A. PICARD *et al.*, 1991 Dephosphorylation and activation of a p34cdc2/cyclin B complex in vitro by human CDC25 protein. *Nature* **351**: 242-245.
- TADROS, W., A. L. GOLDMAN, T. BABAK, F. MENZIES, L. VARDY *et al.*, 2007a SMAUG is a major regulator of maternal mRNA destabilization in *Drosophila* and its translation is activated by the PAN GU kinase. *Dev Cell* **12**: 143-155.
- TADROS, W., and H. D. LIPSHITZ, 2009 The maternal-to-zygotic transition: a play in two acts. *Development* **136**: 3033-3042.
- TADROS, W., J. T. WESTWOOD and H. D. LIPSHITZ, 2007b The mother-to-child transition. *Dev Cell* **12**: 847-849.
- TEN BOSCH, J. R., J. A. BENAVIDES and T. W. CLINE, 2006 The TAGteam DNA motif controls the timing of *Drosophila* pre-blastoderm transcription. *Development* **133**: 1967-1977.
- TWEEDIE, S., M. ASHBURNER, K. FALLS, P. LEYLAND, P. MCQUILTON *et al.*, 2009 FlyBase: enhancing *Drosophila* Gene Ontology annotations. *Nucleic Acids Res* **37**: D555-559.
- UMEN, J. G., 2005 The elusive sizer. *Current opinion in cell biology* **17**: 435-441.
- VOGT, N., 2006 A genetic screen for novel factors involved in mRNA localization during *Drosophila* oogenesis, pp. Uni-Tübingen, Tübingen.
- VOGT, N., I. KOCH, H. SCHWARZ, F. SCHNORRER and C. NÜSSEIN-VOLHARD, 2006 The γ TuRC components Grip75 and Grip128 have an essential microtubule-anchoring function in the *Drosophila* germline. *Development* **133**: 3963-3972.
- YASUDA, G. K., J. BAKER and G. SCHUBIGER, 1991 Independent roles of centrosomes and DNA in organizing the *Drosophila* cytoskeleton. *Development* **111**: 379-391.
- YASUDA, G. K., and G. SCHUBIGER, 1992 Temporal regulation in the early embryo: is MBT too good to be true? *Trends Genet* **8**: 124-127.
- YASUDA, G. K., G. SCHUBIGER and B. T. WAKIMOTO, 1995 Genetic Characterization

of *ms(3)K81*, A Paternal Effect Gene of *Drosophila melanogaster*. *Genetics* **140**: 219-229.

List of Figures

List of Figures

Introduction

- Figure 1: Summary of the events during mid-blastula transition.
- Figure 2: The models of cell cycle during early *Drosophila* development
- Figure 3: N/C ratio controls number of cleavage cycles in embryos.
- Figure 4: the decision making of cell cycle stop is regional
- Figure 5: CDC 25 phosphatase activates the cyclin-CDK complex
- Figure 6: Degradation profiles of maternal transcripts during MZT
- Figure 7: The expression of *frs* as a readout of N/C ratio
- Figure 8: SMG may affect the ZGA by remove transcription repressor

Results

- Figure 9 : The summary of the motifs in 500bp upstream region of *frs* gene.
- Figure 10: The GFP reporter construct can represent the endogenous *frs* expression.
- Figure 11: The *prom 260* is the minimal genomic regulatory region for *frs* expression.
- Figure 12: Summary of the motif-substitution reporters.
- Figure 13: two motifs (-68--57) and (-174- -161) prevent the *frs* expression at cycle 13
- Figure 14: One DNA-protein interacting motif locates at -279bp to 211bp upstream of *frs*.
- Figure 15: The cold oligos competed to the shift in dose-dependent manner
- Figure 16: *X161* GLC embryos undergo one division less
- Figure 17: length of interphase and mitosis
- Figure 18: Centrosome cycle is not affected in *X161*
- Figure 19: The mitosis 14 occurred according to the mitotic domains
- Figure 20: *X161* GLC embryos contain normal set of chromosomes .
- Figure 21: Epistasis of *X161* and haploid mutants.
- Figure 22: The cellularization occurred immediately after last mitosis.
- Figure 23: Expression of *stg* and *tw*
- Figure 24: Expression of *frs* and *slam*
- Figure 25: *X161* requires zygotic gene expression
- Figure 26: Mapping of *X161* by meiotic recombination.
- Figure 27: The crossing-scheme of chromosome cleaning for *X161*
- Figure 28: *RPII215^{X161}* is a novel allele of *RNA polymerase II 215*
- Figure 29: Motif prediction of *X161* mutation site
- Figure 30: The dynamics of *RPII215* protein and transcripts
- Figure 31: the RNA-seq of *RPII 215* in *Drosophila*

Discussion

Figure 32: the genomic regulatory region of *frs*.

Figure 33: The models for phenotype of X161 mutant.

Figure 34: Summary of the known and predicted factors controlling the onset of ZGA

Figure 35: The role of zygotic gene activation during mid-blastula transition

List of Tables**Materials and Methods**

Table 1 : The Summary of SNP used in this study.

Results

Table 2: Summary of the number of cleavage cycles in different background

Table 3: The time length of nuclear division after cycle 10

Table 4: the complement test of original *X161* line with duplication kit

Table 5: the complement of the *X161^{ml}*, *FRT^{19A}* with duplication and deficiency lines.